DEPARTMENT OF
LIFE SCIENCES

NOVA SCHOOL OF
SCIENCE & TECHNOLOGY

JOANA LEANDRO FERNANDES
BSc in Biochemistry

METABOLIC DYSFUNCTION IN OBSTRUCTIVE SLEEP APNEA: IS THERE A ROLE FOR THE LIVER?

MASTER IN MOLECULAR GENETICS AND BIOMEDICINE
NOVA University Lisbon
March 2023

NOVA SCHOOL OF SCIENCE & TECHNOLOGY

DEPARTMENT OF LIFE SCIENCES

METABOLIC DYSFUNCTION IN OBSTRUCTIVE SLEEP APNEA: IS THERE A ROLE FOR THE LIVER?

JOANA LEANDRO FERNANDES

BSc in Biochemistry

Adviser: Sílvia Vilares Conde
Assistant Professor with habilitation, Faculdade de Ciências Médicas | Nova Medical School, Universidade Nova de Lisboa | NOVA University of Lisbon

Co-advisers: Paula Gonçalves
Associate Professor, NOVA Faculdade de Ciências e Tecnologia | Nova School of Science and Technology, Universidade Nova de Lisboa | NOVA University of Lisbon

Examination Committee:

Chair: Margarida Casal Ribeiro Castro Caldas Braga,
Assistant Professor, Faculdade de Ciências e Tecnologia | Nova School of Science and Technology, Universidade Nova de Lisboa | NOVA University of Lisbon

Rapporteurs: Inês Maria de Stoop Camões Teixeira Guerra Mollet,
Senior Researcher, Faculdade de Ciências e Tecnologia | Nova School of Science and Technology, Universidade Nova de Lisboa | NOVA University of Lisbon

Adviser: Sílvia Vilares Conde
Assistant Professor with habilitation, Faculdade de Ciências Médicas | Nova Medical School, Universidade Nova de Lisboa | NOVA University of Lisbon

MASTER IN MOLECULAR GENETICS AND BIOMEDICINE

NOVA University Lisbon
March 2023

METABOLIC DYSFUNCTION IN OBSTRUCTIVE SLEEP APNEA: IS THERE A ROLE FOR THE LIVER?

Part of the results in this thesis originated the following:

Oral Communications in national and international Conferences:

Joana L Fernandes, Martins FO, Melo BF, Sacramento JF, Olea E, Pietro-Loret J, Obeso A, Rocher A, Braga PC, Alves MG, Sequeira CO, Pereira SA, Conde SV. A disfunção mitocondrial e o stress oxidativo hepático estão associados à resistência à insulina na apneia obstrutiva do sono. 19º Congresso Português de Diabetes; Vilamoura, Portugal, 2023.

Joana L Fernandes, Martins FO, Melo BF, Sacramento JF, Olea E, Pietro-Loret J, Obeso A, Rocher A, Braga PC, Alves MG, Sequeira CO, Pereira SA, Conde SV. METABOLIC DYSFUNCTION IN OBSTRUCTIVE SLEEP APNEA: IS THERE A ROLE FOR THE LIVER?. 53ª Reunião da Sociedade Portuguesa de Farmacologia, Coimbra, Portugal, 2023.

Joana L Fernandes, Martins FO, Melo BF, Olea E, Pietro-Loret J, Obeso A, Rocher A, Sacramento JF, Conde SV. Insulin resistance in obstructive sleep apnea: Is there a role for mitochondrial dysfunction in the liver?. 58th EASD annual meeting, Stockholm, Sweden, 2022.

Joana L Fernandes, Martins FO, Melo BF, Sacramento JF, Olea E, Pietro-Loret J, Obeso A, Rocher A, Braga PC, Alves MG, Conde SV. Insulin resistance in obstructive sleep apnea: Is there a role for mitochondrial dysfunction in the liver?. Europhysiology 2022, Copenhagen, Denmark, 2022.

Joana L Fernandes, Martins FO, Melo BF, Olea E, Pietro-Loret J, Obeso A, Rocher A, Sacramento JF, Conde SV. Contribution of impaired hepatic mitochondrial bioenergetics to insulin resistance in Obstructive Sleep Apnea. ISAC XXI Meeting, Lisbon, Portugal, 2022.

Joana L Fernandes, Martins FO, Melo BF, Olea E, Pietro-Loret J, Obeso A, Rocher A, Sacramento JF, Conde SV. Resistência à insulina na apneia obstrutiva do sono: existe um papel para a disfunção mitocondrial no fígado?. 18º Congresso Português de Diabetes, Vilamoura, Portugal, 2022.

Joana L Fernandes, Martins FO, Melo BF, Olea E, Pietro-Loret J, Obeso A, Rocher A, Sacramento JF, Conde SV. INSULIN RESISTANCE IN OBSTRUCTIVE SLEEP APNEA: IS THERE A ROLE FOR DYSFUNCTIONAL MITOCHONDRIAL BIOENERGETICS IN THE LIVER?. 52ª Reunião da Sociedade Portuguesa de Farmacologia, Porto, Portugal, 2022.

Poster Communications in national and international Conferences:

Joana L Fernandes, Martins FO, Melo BF, Olea E, Pietro-Loret J, Obeso A, Rocher A, Sacramento JF, Conde SV. Insulin resistance in obstructive sleep apnea: is there a role for dysfunctional mitochondrial bioenergetics in the liver?. Annual International (Bio)Medical Students Meeting Research Competition, Lisboa, Portugal, 2022.

Awards:

Prémio Grupo Investigação Fundamental e Translacional (GIFT) da Sociedade Portuguesa de Diabetologia 2022: ''Is there a role for mitochondrial dysfunction and ROS in the link OSA-dysmetabolism?'', Fátima O. Martins; Marco G. Alves; Sílvia V. Conde; Pedro Oliveira; Joana Fernandes.

ACKNOWLEDGMENTS

Ao longo deste ano, várias pessoas apoiaram-me durante esta jornada quer a nível académico, quer a nível pessoal e tornaram possível a entrega deste trabalho, pelas quais estou muito grata.

Em primeiro lugar gostaria de agradecer à minha orientadora, Professora Doutora Sílvia Conde, pela oportunidade que me deu e me receber no seu laboratório. Muito obrigada por todos os ensinamentos que me deu ao longo deste ano e por todas as oportunidades concedidas que foram mais do que eu alguma vez pudesse imaginar. Muito obrigada por toda ajuda dentro e for a do laboratório, pelo conhecimento partilhado, por todas as conversas e paciência que teve comigo durante este tempo. Tudo fez com que crescesse a nível profissional e pessoal e, por isso, muito obrigada.

Gostaria também de agradecer à minha co-orientadora, Professora Doutora Paula Gonçalves, por toda ajuda e acompanhamento prestados durante a realização deste trabalho, especialmente nesta fase final.

Gostaria de agradecer a todos os membros do Neurometab lab por me terem recebido e acompanhado todos os dias durante este ano que passou.

Começo por agradecer à Fátima. Foste a primeira pessoa que conheci e acompanhaste-me desde então. Muito obrigada por tudo o que me ensinaste, por toda a ajuda dentro e fora do laboratório, por todas as boleias de carro, e por todas as conversas e paciência que tiveste comigo, especialmente nos dias mais stressantes em que me ajudaste a manter a calma. Foste uma verdadeira mentora.

Quero agradecer também à Joana Sacramento e à Bernardete por toda a ajuda que me deram durante a realização deste trabalho e por estarem sempre prontas para ajudar.

Gostava também de agradecer aos meus colegas de bancada, Adriana e Dinis pela boa disposição e pelos bons momentos que passámos juntos, dentro do laboratório e em todos os congressos por este mundo fora. Tornaram os meus dias mais divertidos! Um agradecimento especial à Esther. Durante os meses que estiveste em Portugal foste uma verdadeira companheira! Obrigada por todos os bons momentos e conversas e por me teres animado nos dias menos bons. Muchas gracias por todo minha linda!

Um agradecimento especial "às minhas meninas", Ana e Rita. Obrigada pela confiança que depositaram em mim nomeando-me vossa "mamã de laboratório" e por todo o companheirismo diário. Obrigada por todos os momentos que tivemos juntas, desde tardes desesperantes em frente ao Chemidoc a momentos de risadas intermináveis.

Gostava também de agradecer a todos os membros do laboratório de farmacologia renal, cardiovascular e metabólica pela ajuda que prestaram na realização de parte deste trabalho. Um especial agradecimento à Catarina por toda a ajuda e por me teres acompanhado. Obrigada António e Júnior pela boa companhia dentro e fora do laboratório.

Muito obrigada a todos os membros do laboratório do Professor Doutor Marco Alves, no instituto de ciências biomédicas Abel Salazar. Muito obrigada por terem recebido de braços abertos. Um obrigada especial à Patrícia por me ter acompanhado todos os dias durante a minha estadia no Porto.

Um agradecimento muito especial a todos os meus amigos que me acompanham e me têm visto crescer. Muito obrigada aos meus "amigos do mestrado", Tomás, Marta, Raul, Susana, Diana e Margarida que foram os meus fiéis companheiros durantes estes dois anos. Muito obrigada por todos momentos que passámos juntos, pelas jantaradas, por estarem lá sempre que precisei e por toda a motivação. De colegas a amigos pelos quais tenho um enorme carinho. Quero agradecer à Serena que esteve sempre pronta para me ouvir, que me apoia em tudo de forma incondicional e que festeja comigo todas as minhas vitórias e não me deixar desanimar com as minhas derrotas. Por último quero agradecer à Sofia que mesmo a milhares de quilómetros de distância nunca me deixou sentir só durante toda esta viagem. Obrigada pelas palavras de ânimo nos dias menos bons e por estares sempre presente, seja de onde for. És uma pessoa muito especial.

Um enorme agradecimento ao meu namorado, o Tiago. Obrigada por me teres acompanhado todos os dias, por nunca te cansares de me ouvir, por me nunca teres deixado desistir quando estava mais em baixo, por me teres dado força para continuar e por me colocares todos os dias um sorriso na cara. Um obrigada não chega para agradecer por toda a tua ajuda. Foste o meu rochedo.

Quero terminar fazendo um agradecimento do tamanho do mundo à minha família. À minha avó por todo o carinho e apoio em todos os momentos. E o meu maior agradecimento aos meus pais Carla e Ricardo. Sem vocês nada disto seria possível! Muito obrigada por me apoiarem em tudo o que faço, por todo o amor e dedicação, por me acompanharem todos os dias e me darem toda a liberdade para eu crescer. Acima de tudo obrigada por serem o meu apoio e por me darem a tranquilidade que preciso no meio das tempestades. Obrigada por tudo.

A todos vocês Muito Obrigada!

Abstract

The link between obstructive sleep apnea (OSA) and metabolic disorders is unquestionable. Despite different mechanisms have been proposed to explain this relationship, namely the sympathetic nervous system overactivation, alterations in adipokine levels, oxidative stress in white adipose tissue, none is consensual and do not completely clarify this relationship. The liver is a major organ in the maintenance of metabolic homeostasis and whose dysfunction is involved in several diseases, including metabolic diseases. Hence, we hypothesize that liver dysfunction is key in the development of metabolic dysfunction commonly associated with obstructive sleep apnea (OSA). Moreover, we aimed to explore the underlying mechanisms of this association within the liver.

Male Wistar Rats were divided into two groups: a control and an obese group fed with 60% lipid-enriched diet (HF diet) for 12 weeks. Half of the animals from each group were submitted to a severe chronic intermittent hypoxia (CIH) paradigm (40s, 5%O2/80s air, 8h/day), that mimics OSA, in the last 14 days. Liver samples were then collected and used for the evaluation of different parameters: lipid deposition, insulin signalling, glucose homeostasis, hypoxia, oxidative stress, antioxidant defenses, mitochondrial biogenesis and inflammation, using western blot, histological and fluorescent immunohistochemistry, HPLC and enzymatic assays.

Both CIH and HF diet led to insulin resistance and glucose intolerance, effects not aggravated in animals submitted to HF plus CIH. CIH aggravates hepatic lipid deposition in obese animals. Hypoxia-inducible factors levels were altered by these stimuli. CIH decreased the oxidative phosphorylation complexes in both groups and the levels of superoxide dismutase 1. HF diet reduced mitochondrial density and hepatic antioxidant capacity. CIH and HF diet produced alterations in cysteine-related thiols and pro-inflammatory markers.

The results obtained suggest that mitochondrial dysfunction and oxidative stress, leading to inflammation, may be significant factors contributing to the development of dysmetabolism associated with OSA.

Keywords: Obstructive sleep apnea, metabolic disorders, mitochondrial dysfunction, inflammation, oxidative stress.

Resumo

A relação entre a apneia obstrutiva do sono (SAOS) e as doenças metabólicas é inequívoca. Foram propostos diferentes mecanismos para explicar esta relação, nomeadamente sobreativação do sistema nervoso simpático, alterações nos níveis de adipocitocinas ou stress oxidativo no tecido adiposo, contudo nenhum é consensual ou esclarece completamente esta relação. O fígado é crucial na manutenção da homeostase metabólica e cuja disfunção está associada às doenças metabólicas. Assim, pressupomos que a disfunção hepática é fundamental no desenvolvimento do dismetabolismo associado à SAOS, tendo também como objetivo explorar os mecanismos subjacentes a esta associação.

Foram usados dois grupos de ratos divididos em grupo controlo e grupo submetido a uma dieta rica em lípidos (HF, 60% lípidos) durante 12 semanas. Metade dos animais de cada grupo foram submetidos a um paradigma de hipóxia crónica intermitente severo (HCI) (40s, 5%O2/80s ar, 8h/dia), que mimetiza a SAOS, nos últimos 14 dias. Foram recolhidas amostras de fígado para avaliação de diferentes parâmetros: esteatose hepática, sinalização da insulina, homeostase de glucose, hipóxia, stress oxidativo, defesas antioxidantes, biogénese mitocondrial e inflamação, através de w*estern blot*, imunohistoquímica histológica e fluorescente, HPLC e ensaios enzimáticos.

A HCI e a dieta HF provocaram insulino-resistência e intolerância à glucose, efeitos não agravados no modelo hipercalórica. A HCI agravou a esteatose hepática observada em animais obesos. Os níveis de fatores induzíveis por hipóxia foram alterados por estes estímulos. A HCI diminuiu os níveis dos complexos de fosforilação oxidativa e de superóxido dismutase 1 nos dois grupos. A dieta HF reduziu a densidade mitocondrial e a capacidade antioxidante hepática. Ambos os estímulos produziram alterações nos níveis de tióis e aumentaram os níveis de marcadores pró-inflamatórios.

Estes resultados sugerem que a disfunção mitocondrial e o stress oxidativo, que aumentam a inflamação, podem ser fatores significativos que contribuem para o desenvolvimento do dismetabolismo associado à SAOS.

Palavras chave: Apneia obstrutiva do sono, doenças metabólicas, disfunção mitocondrial, stress oxidativo, inflamação.

CONTENTS

1 INTRODUCTION 1

1.1 Sleep-Related Breathing Disorders 1

1.1.1 Obstructive sleep apnea (OSA) 1

1.2 OSA and metabolic disorders 3

1.2.1 OSA and Obesity 3

1.2.2 OSA and type 2 diabetes (T2D) 4

1.2.3 OSA and Metabolic Syndrome (MetS) 6

1.2.4 OSA and non-alcoholic fatty liver disease (NAFLD) 7

1.2.5 OSA and Insulin Resistance 9

1.2.5.1 OSA and hepatic insulin resistance 11

1.3 OSA and metabolic disorders: the possible links 12

1.3.1 Stabilization of hypoxia-inducible factors (HIFs) 13

1.3.2 Mitochondrial Dysfunction 18

1.3.3 Oxidative Stress, Antioxidant Defences and Inflammation 21

2 AIMS OF THE WORK 25

3 METHODS 27

3.1 Animal experiments and *in vivo* procedures 27

3.1.1 Assessment of Metabolic Parameters 28

3.2 Liver *Ex vivo* analysis 29

3.2.1 Assessment of protein levels from insulin signalling, glucose metabolism, mitochondrial biogenesis, antioxidant system and inflammation pathways....29
3.2.2 Histological and fluorescence immunolabelling analysis of the liver tissue....31
3.2.3 Assessment of mitochondrial complexes enzymatic activity....32
3.2.3.1 Measurement of complex I activity....33
3.2.3.2 Measurement of complex II activity....33
3.2.3.3 Assessment of citrate synthase activity....34
3.2.4 Determination of Intracellular ROS Content....34
3.2.5 Ferric reducing–antioxidant power (FRAP) assay....35
3.2.6 Quantification of Cysteine-Related Thiolome....35
3.2.7 Statistical Analysis....36
4 RESULTS....37
4.1 Effects of intermittent hypoxia and hypercaloric diet on insulin sensitivity and glucose tolerance....37
4.2 Effects of intermittent hypoxia and hypercaloric diet on liver tissue morphology....38
4.3 Effects of intermittent hypoxia and hypercaloric diet on hypoxia markers....39
4.4 Effects of intermittent hypoxia and hypercaloric diet on proteins involved in insulin signalling pathway....42
4.5 Effects of intermittent hypoxia and hypercaloric diet on proteins related to glucose metabolism....43
4.6 Effects of intermittent hypoxia and hypercaloric diet on mitochondrial biogenesis and activity....43
4.7 Effects of intermittent hypoxia and hypercaloric diet on ROS formation and antioxidant capacity....47
4.8 Effects of intermittent hypoxia and hypercaloric diet on pro-inflammatory markers51
5 DISCUSSION....53
5.1 Impact of CIH and HF diet on the metabolic phenotype....53
5.2 Impact of CIH and HF diet in Liver Tissue Hypoxia....55

5.3 Impact of CIH and HF diet on Oxidative Stress 56
5.4 Impact of CIH and HF diet on Mitochondrial Dysfunction 58
5.5 Impact of CIH and HF diet in Hepatic Inflammation 59
6 CONCLUSIONS AND FUTURE PERSPECTIVES 61
REFERENCES 63

LIST OF FIGURES

Figure 1.1 - Pathophysiology of hyperglycaemia in T2D. Once insulin resistance occurs, being then followed by β - cell dysfunction, insulin no longer can regulate the insulin-mediated mechanisms in the liver, adipose tissue and skeletal muscle. Thus blood glucose levels rise, leading to hyperglycaemia. Image taken from Zheng *et al.* [32]. 5
Figure 1.2 - Mechanisms linking OSA and T2D. The pathophysiologic mechanisms subsequent to this relationship are not elucidated but they are likely multifactorial. Nevertheless, different clinical studies and epidemiological studies demonstrate a strong association between these two disorders. Image adapted from Reutrakul *et al.* [33] 6
Figure 1.3 - The different mechanistic pathways linking OSA and NAFLD. OSA contributes to the development of insulin resistance, contributing to an increase of lipolysis. On the other hand CIH allows the stabilization of HIFs and decreases lipid β-oxidation in liver tissue. Ultimately all these alterations increase hepatic FFA, ROS production, promote mitochondrial dysfunction and the activation of pro-inflammatory pathways, leading to the onset and progression of NAFLD. Image adapted from Parikh *et al.* [51]. 9
Figure 1.4 - Insulin signalling. Insulin can activate different signalling pathways such as PI3K/AKT and MAPK. The insulin biding to IR promotes the activation of downstream proteins by its phosphorylation and leads to the activation of different processes such as cell growth and differentiation, glucose and lipid metabolism and vesicle trafficking. Image taken from Saltiel A.R [62]. 11
Figure 1.5 - Different features possibly involved in the pathophysiological mechanism linking OSA and metabolic diseases. Adapted from Martins *et al.* [56]. 13
Figure 1.6 - The regulation of HIF. Under normoxia, the HIF-α levels are regulated by PHD, which mark HIF-α subunits to ubiquitination, leading to their proteossomal degradation of HIF-α, and by FIH, which inhibit the recruitment of HIF-α co-activators, thereby inhibiting their

transcriptional activity. Once hypoxia occurs, PHD and FIH activity is diminished, which prevents HIF-α hydroxylation. As a result, HIF-α subunits stabilize, translocate to the nucleus and dimerize with HIF-β, activating the transcription of different target genes. Adapted from Gonzalez *et al.* [90]....14

Figure 1.7 The proposed HIF dependent mechanisms involved in WAT dysfunction. In obesity, along with other factors, the expansion of adipocytes results in a local hypoxia allowing HIF stabilization and transcriptional activity. HIF-1α mediates WAT fibrosis and the concomitant activation of inflammatory pathways. Conversely, HIF-2α appears to have a protective role against inflammation and fibrosis. Green and red arrows represent the activation and the inhibition of these pathways, respectively. Image adapted from Lefere *et al.* [80]....16

Figure 1.8 - The proposed HIF dependent mechanisms involved in liver dysfunction. The intake of hypercaloric food and CIH can thrive to a local hypoxia promoting the stabilization of HIF and the respective transcriptional activity. Hepatic *de novo* lipogenesis is upregulated by HIF-1α, which exacerbates FFA and TAG synthesis and leads to a state of hyperlipidemia, hepatic steatosis and liver injury. The decrease fatty acid β-oxidation, also mediated by HIF-1α, also contributes for the devolpment of this phenotype. HIF-2α also mediates the reduction of fatty acid β-oxidation and upregulates fatty acid uptake and synthesis. Both HIF-1α and HIF-2α mediate the increase of hepatic fibrosis and inflammation. Green and red arrows represent the activation and the inhibition of these pathways, respectively. Image adapted from Lefere *et al.* [80] 18

Figure 1.9- The process of oxidative phosphorylation. Inside the mitochondrial matrix, NADH derived from the TCA cycle is oxidized by NADH dehydrogenase (complex I, orange), allowing the formation of an electron pair that is transferred to ubiquinone (Q, light green). Ubiquinone is reduced to ubiquinol and transferred to succinate dehydrogenase (complex II, dark green), where it oxidizes again into ubiquinone. The complex II is responsible for the oxidation of $FADH_2$, also derived from the TCA cycle, and the electrons derived from this reaction are also transferred by ubiquinol to cytochrome c reductase (complex III, purple). Complex III performs as an electron shuttle to cytochrome c (Cyt c, brown) which then transfers the electrons to cytochrome c oxidase (complex IV, navy blue), the last electron acceptor of the ETC. Here, an oxygen atom is reduced by H^+ ions from the mitochondrial matrix to H_2O. The H+ ions released from the previous enzymatic reactions to the intermembrane space re-enter the mitochondrial matrix by ATP synthase (complex V, pink), catalysing the binding of a phosphate atom (Pi) to a ADP molecule, forming ATP. 20

Figure 3.1 — Schematic representation of the experimental design of the study. Male Wistar rats (12 weeks; 6-8 animals per group) were divided into a control (CTL), fed with a standard diet, and an obese group (HF), fed with a 60% lipid-enriched diet for 12 weeks. From weeks 10 to 12, half of the animals from both groups were submitted to a severe CIH protocol (CIH and HFIH) consisting of 30 CIH cycles/h, 8 h/day. During the CIH protocol, the remaining age-matched control or high-fat animals were in the same room and exposed to a normal air atmosphere, to experience similar conditions.....28
Figure 4.1 — Effects of chronic intermittent hypoxia (CIH) and high-fat diet on the metabolic parameters, insulin sensitivity (A) and glucose tolerance (B). Panel A shows the effect of CIH and diet on insulin sensitivity evaluated using HOMA-IR index. Panel B shows on the left the glucose excursion curves of the intra-peritoneal glucose tolerance test (ipGTT) and on the right the correspondent area under the curve (AUC). Animal groups: CTL- control; CIH – chronic intermittent hypoxia; HF – high-fat diet; HFIH – high-fat plus CIH; Data are presented as means ± SEM of 6-8 animals. One-way ANOVA with Turkey's multiple comparison tests, respectively: * $p < 0.05$, ** $p < 0.01$, *** $p < 0.001$ and **** $p < 0.0001$ compared with control animals. 38
Figure 4.2 — Effects of chronic intermittent hypoxia and high-fat diet on the morphology of liver tissue. Panels A, B, and C correspond to representative images of H&E staining from CTL, CIH, HF and HFIH animals, respectively. Visual analysis of H&E staining shows an increase in lipid deposition in the HF group, which is aggravated by exposure to chronic intermittent hypoxia. CTL- control; CIH – chronic intermittent hypoxia; HF – high-fat diet; HFIH – high-fat plus CIH. Scale bar 50 μm. 39
Figure 4.3 — Effects of chronic intermittent hypoxia (CIH) and high-fat (HF) diet on HIF-1α immunolabelling in the liver. A) Representative immunohistochemistry slices from liver labelled with HIF-1α and DAPI. Scale bar 50 μm. B) Mean fluorescence of HIF-1α normalized for the number of nuclei present in the liver slices of each animal. Animal groups: CTL- control; CIH – chronic intermittent hypoxia; HF – high-fat diet; HFIH – high-fat plus CIH; Data are presented as means ± SEM. One-way ANOVA with Turkey's multiple comparison tests, respectively: *** $p < 0.001$ compared with control animals; $$$$ $p < 0.0001$ compared with control animals submitted to the CIH protocol. 40
Figure 4.4 — Effect of chronic intermittent hypoxia (CIH) and high-fat (HF) diet on HIF-2α immunolabelling in the liver. A) Representative immunohistochemistry slices from liver labelled with HIF-2α and DAPI. Scale bar 50 μm. B) Mean fluorescence of HIF-2α normalized for the number of nucleus present per area of analysis. Animal groups: CTL- control; CIH – chronic intermittent hypoxia; HF – high-fat diet; HFIH – high-fat plus CIH. Data are presented

as means ± SEM. One-way ANOVA with Turkey's multiple comparison tests, respectively: ** p < 0.01 compared with control animals; $$$ p < 0.001 compared with control animals submitted to the CIH protocol.....41
Figure 4.5 — Effects of chronic intermittent hypoxia (CIH) and high-fat (HF) diet on the levels of proteins involved in insulin signalling in the liver. Panels A, B and C depicts the levels of Insulin Receptor (IR- 90 KDa), Protein Kinase B (AKT - 60 KDa) and Insulin Degrading Enzyme (IDE - 118 KDa), respectively. Proteins levels were normalized to the loading control β-actin (42 kDa). Top of the graphs show representative Western Blots for each protein studied. Animal groups: CTL- control; CIH – chronic intermittent hypoxia; HF – high-fat diet; HFIH – high-fat plus CIH. Data are presented as means ± SEM of 6-8 animals. One-way ANOVA with Turkey's multiple comparison tests, respectively: * p < 0.05 compared with control animals.....42
Figure 4.6 — Effects of chronic intermittent hypoxia (CIH) and high-fat (HF) diet on the levels of Glucose Transporter 2 (Glut2 - 60 KDa) in the liver. Protein levels were normalized to the loading control β-actin (42 kDa). Top of the graph show representative Western Blots for the protein studied. Animal groups: CTL- control; CIH – chronic intermittent hypoxia; HF – high-fat diet; HFIH – high-fat plus CIH. Data are presented as means ± SEM of 6-8 animals. One-way ANOVA with Turkey's multiple comparison tests, respectively: * p < 0.05 compared with control animals.....43
Figure 4.7 — Effects of chronic intermittent hypoxia (CIH) and high-fat (HF) diet on mitochondrial density immunolabelling in the liver. A — Representative immunohistochemistry slices from liver labelled with Mitotracker and DAPI. Scale bar 50 μm. B — Mean fluorescence of Mitotracker normalized for the number of nucleus present per area of analysis. Animal groups: CTL- control; CIH – chronic intermittent hypoxia; HF – high-fat diet; HFIH – high-fat plus CIH. Data are presented as means ± SEM. One-way ANOVA with Dunnett's multiple comparison tests, respectively: ** p < 0.01 compared with control animals; # p < 0.05 compared with obese animals. 45
Figure 4.8 — Effects of chronic intermittent hypoxia (CIH) and high-fat (HF) diet on the levels of oxidative phosphorylation complexes (OXPHOS) in the liver. The graph depicts the levels of Complex I (20 KDa), II (30 KDa), III (48 KDa), IV (40 KDa) and V (55 KDa). Proteins levels were normalized to the loading control Calnexin (90 KDa). Top of the graphs show representative Western Blots for each protein studied. Animal groups: CTL- control; HF – high-fat diet; CIH – chronic intermittent hypoxia; HFIH – high-fat plus CIH. Data are presented as means ± SEM of 6-8 animals. One-way ANOVA with Turkey's multiple comparison tests, respectively: * p <

0.05 and ** p < 0.01 compared with control animals; # p < 0.05, ## p < 0.01 and ### p < 0.001 compared with HF animals. 46
Figure 4.9 — Effects of chronic intermittent hypoxia (CIH) and high-fat (HF) diet on the activity of citrate synthase (A) Mitochondrial Complexes I (panel B) and II (panel C) activities. The enzymatic activity of each complex was normalized by Citrate Synthase activity. Animal groups: CTL- control; CIH – chronic intermittent hypoxia; HF – high-fat diet; HFIH – high-fat plus CIH. Data are presented as means ± SEM of 6-8 animals. One-way ANOVA with Turkey's multiple comparison tests, respectively: $ p < 0.05 compared with control animals submitted to CIH.46
Figure 4.10 — Effects of chronic intermittent hypoxia (CIH) and high-fat (HF) diet on ROS formation and antioxidant capacity. Panel A depicts the intracellular levels of Reactive Oxygen Species (ROS) in the liver by CM-H_2DCFDA labelling. Panel B presents the Ferric reducing-antioxidant power assay (FRAP), used to estimate the antioxidant potential of the tissue in each group. Panels C and D depicts the levels of Catalase (60 KDa) and Superoxide Dismutase 1 (SOD-1 - 23 KDa) respectively. Proteins levels were normalized to the loading control β-actin (42 kDa) and Calnexin (90 KDa). Top of the graphs show representative Western Blots for each protein studied. Animal groups: CTL- control; CIH – chronic intermittent hypoxia; HF – high-fat diet; HFIH – high-fat plus CIH. Data are presented as means ± SEM of 6-8 animals. One-way ANOVA with Turkey's multiple comparison tests and Dunnet's multiple comparison tests respectively: * p < 0.05 and ** p < 0.01 compared with control animals; # p < 0.05 and #### p < 0.0001 compared with obese animals; $ p < 0.05 and $$ p < 0.01 compared with control animals submitted to chronic intermittent hypoxia protocol.....49
Figure 4.11 — Effects of chronic intermittent hypoxia (CIH) and high-fat (HF) diet on the levels of Cysteine-related thiols in the liver. A — total Cysteine; B — free total cysteine; C — protein-bounded cysteine; D — total Cysteine-Glycine; E — free total Cysteine-Glycine; F — protein-bounded Cysteine-Glycine; G — total Glutathione; H — free total Glutathione; I — Glutathione. Animal groups: CTL- control; CIH – chronic intermittent hypoxia; HF – high-fat diet; HFIH – high-fat plus CIH. Data are presented as means ± SEM of 6-8 animals. One-way ANOVA with Turkey's multiple comparison tests, respectively: * p < 0.05 and ** p < 0.01 compared with control animals; $ p < 0.05 and $$ p < 0.01 compared with control animals submitted to the chronic intermittent hypoxia protocol.....50
Figure 4.12 — Effects of chronic intermittent hypoxia (CIH) and high-fat (HF) diet on the levels of inflammatory markers in the liver. Panels A, B, C, D, E and F depicts the levels of Arginase I (35 KDa), NF-κB (65 KDa), IL-6 Receptor (IL-6R - 80 KDa), IL-1 Receptor (IL-1R - 80 KDa), Tumour necrosis factor alpha (TNF-α - 17 KDa), and TNF-α Receptor (TNF-αR - 55 KDa), respectively.

Proteins levels were normalized to the loading control β-actin (42 kDa). Top of the graphs show representative Western Blots for each protein studied. Animal groups: CTL- control; CIH – chronic intermittent hypoxia; HF – high-fat diet; HFIH – high-fat plus CIH. Data are presented as means ± SEM of 6-8 animals. One-way ANOVA with Turkey's multiple comparison tests, respectively: * $p < 0.05$ and ** $p < 0.01$ compared with control animals; $ $p < 0.05$ compared with control animals submitted to the chronic intermittent hypoxia protocol. 52

List of Tables

Table 3.1— Primary antibodies used for the proteins of interest in the present study and their respective dilution factor, specie, and brand. 31

Table 5.1 - Summary table showing the impact of chronic intermittent hypoxia (CIH) and/or high-fat (HF) diet on metabolic status. Black symbols represent comparisons with the CTL group and red symbols represent comparisons with the HF group 54

Table 5.2 - Summary table showing the impact of chronic intermittent hypoxia (CIH) and/or high-fat (HF) diet on hepatic HIF levels. Black symbols represent comparisons with the CTL group and orange symbols represent comparisons with the CIH group. 56

Table 5.3 - Summary table showing the impact of chronic intermittent hypoxia (CIH) and/or high-fat (HF) diet on oxidative stress in liver tissue. Black symbols represent comparisons with the CTL group, orange symbols represent comparisons with the CIH group and red symbols represent comparisons with the HF group 58

Table 5.4 - Summary table showing the impact of chronic intermittent hypoxia (CIH) and/or high-fat (HF) diet on mitochondrial dysfunction in liver tissue. Black symbols represent comparisons with the CTL group and red symbols represent comparisons with the HF group 59

Table 5.5 - Summary table showing the impact of CIH and/or HF diet on the inflammatory status of liver tissue. Black symbols represent comparisons with the CTL group and orange symbols represent comparisons with the CIH group. 60

ACRONYMS

ADRP	Adipocyte differentiation-related protein
AHI	Apnea-hypopnea index
AKT	Protein kinase b
AUC	Area under the curve
BSA	Bovine serum albumin
CIH	Chronic intermittent hypoxia
CNS	Central nervous system
CPAP	Continuous positive air pressure
CREB	cAMP- responsive- element binding protein
CS	Citrate synthase
CTL	Control group
Cys	Cysteine
CysGly	Cysteine-glycine
Cyt C	Cytochrome C
DCPIP	2,6-dichlorophenolindo-phenol
DNTB	Dithio-bis-2-nitrobenzoic acid
ETC	Electric transport chain
FFA	Free fatty acids

FIH-1	Factor inhibiting HIF1
FOXO	Forkhead box
FRAP	Ferric reducing-antioxidant power
Glut2	Glucose transporter 2
GSH	Glutathione
H&E	Haematoxylin & eosin
HF diet	High fat diet
HF	High fat diet group
HFIH	High fat diet + chronic intermittent hypoxia group
HIF	Hypoxia inducible factor
HIF-1α	Hypoxia inducible factor 1 alpha
HIF-2α	Hypoxia inducible factor 2 alpha
HOMA-IR	Homeostasis model assessment
HRE	Hypoxia-responsive elements
IDE	Insulin degrading enzyme
IGF	Insulin-like growth factor
IL-1R	Interleukin-1 receptor
IL-6	Interleukin-6
IL-6R	Interleukin-6 receptor
IL-8	Interleukin-8
IpGTT	Intra-peritoneal glucose tolerance test
IR	Insulin receptor
IRS	Insulin receptor substrate
MAPK	Mitogen-activated protein kinase
MetS	Metabolic Syndrome
mTORC1	Mammalian target of rapamycin complex 1

NADPH	Nicotinamide adenine dinucleotide phosphate
NAFLD	Non-alcoholic fatty liver disease
NASH	NASH non-alcoholic steatohepatitis
NF- κB	Nuclear factor kappa B
Nrf-2	Nuclear factor E2-related factor 2
ODD	Oxygen-dependent degradation
OSA	Obstructive sleep apnea
OXPHOS	Oxidative phosphorylation complexes
PDK-1	Phosphoinositide-dependent kinase 1
PFA	Paraformaldehyde
PHD	Prolyl hydroxylase
PI3K	Phosphoinositide 3-kinase
PSG	Polysomnography
ROS	Reactive oxygen species
SBD-F	7-Fluorobenzofurazan-4-sulfonic acid ammonium salt
SDS-PAGE	Sodium dodecyl sulfate-polyacrylamide gel
SEM	Standard error of the mean
SF	Sleep fragmentation
SNS	Sympathetic nervous system
SOCS3	Suppressor of cytokine signalling 3
SOD	Superoxide dismutase
SOD-1	Superoxide dismutase one
SREBP	Sterol regulatory element binding protein
T2D	Type 2 diabetes
TAG	Triglycerides
TBS-T 0.1%	Tris buffer saline with 0.1% tween

TCA	Tricarboxylic acid
TCEP	Tris2-carboxyethyl phosphine hydrochloride
TNF-α	TNF-α Tumour necrosis factor-alpha
TNF-αR	TNF-αR tumour necrosis factor α receptor
TPTZ	2,4,6-tripyridyl-s-triazine
UPR	Unfolded protein response
US	United States of America
VHL	Hippel–Lindau-elongin BC-CUL2 protein complex
WAT	White adipose tissue
WHO	World health organization

1

INTRODUCTION

1.1 Sleep-Related Breathing Disorders

According to the American Academy of Sleep Medicine, sleep-related breathing disorders are a group of conditions defined by irregularities in respiration during sleep [1]. It is subdivided into four classes: obstructive sleep apnea syndromes, sleep-related hypoventilation disorders, central apnea syndromes, and sleep-related hypoxemia disorder [2].

1.1.1 Obstructive sleep apnea (OSA)

Obstructive sleep apnea (OSA) is the most common sleep-related breathing disorder, affecting nearly 1 billion adults aged 30-69, mostly men, with a higher prevalence in China (242 million), followed by India (81 million), the United States (78 million), and Brazil (74 million) [3], [4]. Besides the differences in prevalence between gender, other risk factors for OSA include ageing and obesity. As a result of the obesity global pandemic, OSA is becoming a major health issue [5], [6].

OSA is characterized by repetitive episodes of reduction (hypoapnea) or complete (apnea) cessation of the airflow due to the collapse of the pharyngeal airway during sleep [1]. These events promote a decrease in oxygen saturation and hypercapnia, which stimulate chemoreceptors, namely the carotid bodies, leading to the activation of sympathetic nervous system (SNS). This culminates in the activation of the central nervous system (CNS) to restore oxygen levels and suppress SNS [7], [8]. Chronic intermittent hypoxia (CIH) is the end result of

these constant apnea-hypoapnea cycles, and the continued respiratory-related arousals result in sleep fragmentation (SF) [8]. Consequently, the most common reported symptom of OSA is excessive sleepiness [9]. Other common symptoms include morning headache, fatigue, non-restorative sleep and regular awakenings during sleep time, especially when snoring [9], [10].

Patients with the described symptoms due to unknown causes are referred for polysomnography (PSG), the gold standard test for the diagnosis of OSA [11]. This procedure consists in the measurement and/or recording of several respiratory and sleep parameters, namely airflow, oximetry, respiratory effort, sleep stage and arousals and body movement. However, this test is highly expensive and promotes discomfort to the patient, so other techniques have been implemented, such as the home sleep apnea tests [9], [12]. Although specific and sensitive, this test is more limited than PSG and produces false negatives frequently, so a PSG it's still required to confirm the first result [13]. Also, some questionnaires such as the STOP-Bang questionnaire and the Berlin questionnaire, have been used as screening tools to identify patients with a high risk of OSA and refer them to a PSG [14], [15].

The number of apneas and hypopneas throughout each hour of the patient's sleep is also recorded in the PSG to determine the apnea-hypopnea index (AHI), a metric used to assess the severity of OSA [7]. OSA can be classified as mild (AHI= 5 - 15), moderate (AHI= 15 - 30) or severe (AHI≥30) [1].

Continuous positive airway pressure (CPAP) is the first line of treatment for OSA [16]. CPAP significantly reduces the AHI of patients, which results in more restorative sleep and decreased daytime sleepiness, culminating in a better quality of life. However, mainly due to the discomfort of sleeping with a mask, this option of treatment may not be viable [9], [17]. As alternatives, mandibular replacement devices can be used or a surgical procedure to wide the upper airway volume can be performed, but both options have less efficacy than CPAP, are more invasive and could have several complications [9]. Nonetheless, the beneficial effects of OSA treatments, especially CPAP, in the associated comorbidities of OSA are not consensual, so more studies are needed to infer this issue [18]–[20].

Over the years the link between OSA and its associated comorbidities - cardiovascular disease, metabolic disorders, neurological and pulmonary diseases - has been studied to understand the pathophysiological mechanisms behind these relations and to develop new forms of treatment. OSA, in particular CIH and SF, have been correlated with different metabolic disorders, including obesity, non-alcoholic fatty liver disease (NAFLD), metabolic syndrome (MetS) or type 2 diabetes (T2D), yet the mechanisms by which these diseases are related are not clear [20], [21].

1.2 OSA and metabolic disorders

1.2.1 OSA and Obesity

The World Health Organization (WHO) defines obesity as an excessive or abnormal accumulation of body fat to a point that becomes detrimental to health [22]. This disorder is also associated with a state of low-grade inflammation [23]. The prevalence of obesity has reached a pandemic proportion and it almost tripled since 1975 [24]. Furthermore, recent studies estimate that by 2030, 1 out of 2 adults in the US will be obese [23].

The principal cause of obesity is the resultant energy imbalance from a sedentary lifestyle and the overconsumption of high-energy foods rich in fat and sugar [24]. Other factors such as genetic predisposition and environmental factors also contribute to the increase of obesity [25].

Obesity is one of the principal risk factors for the development of different types of diseases, namely cardiometabolic disorders, such as T2D, hypertension or NAFLD, osteoarthritis, some types of cancer and, as stated above, OSA [22], [24]. The relation between OSA and obesity is bidirectional, since OSA leads to and aggravates obesity and, on the other hand, obesity, not only central obesity but also the fat deposition in the neck, contributes to the collapse of the pharyngeal airway during sleep and aggravation of OSA [20], [26]. Also, this relation is reinforced by the fact that OSA and obesity share common mechanisms such as oxidative stress and increased SNS activation [26].

1.2.2 OSA and type 2 diabetes (T2D)

Diabetes mellitus is a chronic metabolic disorder that arises from elevated blood glucose levels, as a result of impaired or insufficient production of insulin, or due to inefficient insulin use. In a long term, this state of hyperglycaemia can lead to damage of different tissues and organs, such as the eyes, kidneys, heart or nerves [27]. In accordance with the WHO and International Diabetes Federation, *diabetes mellitus* classification is composed of four classes: Type 1 Diabetes, T2D, Gestational Diabetes, and specialized forms of diabetes caused by a different origin [22], [27].

T2D is the most common type of diabetes. Last year, about 537 million adults aged between 20-79 years were living with diabetes and 90% of these cases were T2D [27]. The increased prevalence of this condition is brought on by population ageing as well as the obesity pandemic, which is driven by an increase in sedentary lifestyles and the intake of hypercaloric meals [28]. Other risk factors that can conduce to the development of T2D include family history, environmental and genetic factors [29].

T2D is preceded by a state of prediabetes, characterized by impaired glucose tolerance or impaired fasting glucose, both conditions where blood glucose concentrations are higher than a healthy state but below the diabetic threshold. These high blood glucose levels are driven by an insulin resistance condition [30]. The pancreatic β-cells are stimulated to produce and secrete increased concentrations of insulin, to overcome the elevated blood glucose levels due to impaired insulin sensitivity, and restore homeostasis [29], [30]. So, prediabetes constitutes a high-risk state for the development of T2D, yet this conversion is preventable with alterations in lifestyle [30].

As the disease progresses to T2D, the insulin-sensitive tissues became more resistant and as a result of long-term overstimulation, β-cells became dysfunctional, which ultimately results in failure and cell loss. So, a state of hyperglycaemia is established as a consequence of the decreased secretion of insulin [31]. The onset of a hyperglycemic state is related to the disruption of the metabolism of lipids, proteins, and carbohydrates [29] affecting many organs, including the liver, skeletal muscle, kidneys, brain, small intestine, and adipose tissue (fig. 1.1) [31], [32].

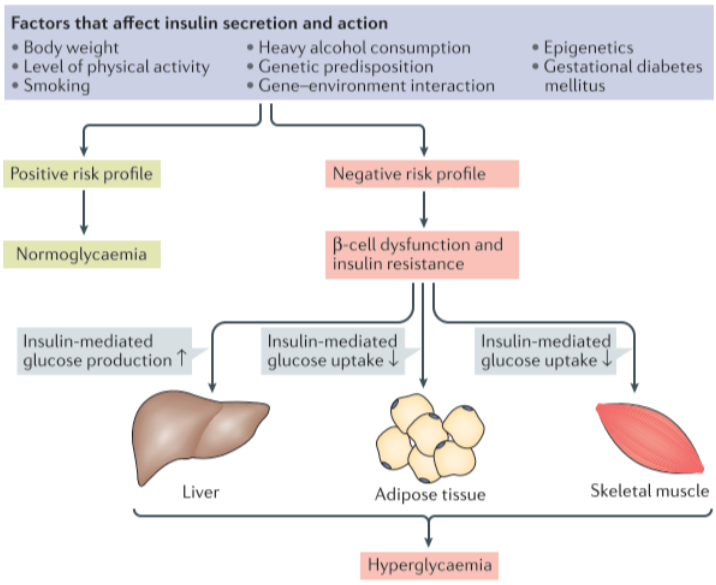

Figure 1.1 - Pathophysiology of hyperglycaemia in T2D. Once insulin resistance occurs, being then followed by β - cell dysfunction, insulin no longer can regulate the insulin-mediated mechanisms in the liver, adipose tissue and skeletal muscle. Thus blood glucose levels rise, leading to hyperglycaemia. Image taken from Zheng *et al.* [32].

The association between OSA and T2D have been demonstrated in different clinical and epidemiological studies. Recently, it has been demonstrated that at least 50% of T2D also have OSA, being this disorder extremely prevalent in obese patients [33]. Nevertheless, this association was also observed in non-obese patients, so this relationship can be independent of obesity [33]. It has also been demonstrated that the severity of OSA positively correlated with the degree of insulin resistance and glucose intolerance, two pathological conditions that increase the risk of developing T2D [21], [33]. Therefore, OSA is now considered an independent risk factor of T2D and there is a bidirectional relationship between these two disorders [20].

The pathophysiological mechanisms by which OSA and the impairment of glucose metabolism and T2D are connected are not fully elucidated (fig. 1.2). This relationship is likely multifactorial and is probably driven by the systemic inflammation, oxidative stress and

increased sympathetic activity promoted by CIH and SF, which lead to the dysfunction of pancreatic β-cells and insulin resistance and, for this reason, to the development of T2D [33], [34].

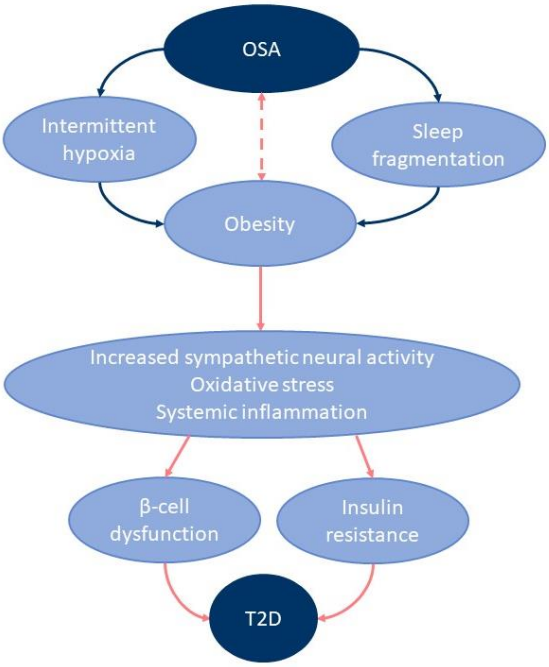

Figure 1.2 - Mechanisms linking OSA and T2D. The pathophysiologic mechanisms subsequent to this relationship are not elucidated but they are likely multifactorial. Nevertheless, different clinical studies and epidemiological studies demonstrate a strong association between these two disorders. Image adapted from Reutrakul *et al.* [33]

1.2.3 OSA and Metabolic Syndrome (MetS)

MetS, first defined in 1988 by Reaven and his colleagues, is a cluster of clinical conditions, comprising insulin resistance, impaired glucose metabolism, central obesity, atherogenic dyslipidemia and hypertension, that raise the risk of developing cardiovascular diseases and T2D [35]. Since then, different healthcare organizations proposed alternative definitions for MetS, all of which are based on the same parameters with slightly different cut-offs [36]. Like any other metabolic disorder, the increase of the western lifestyle, represented by physical inactivity and intake of unhealthy foods, contributes to the increase in the prevalence of MetS [37]. Also, MetS can be viewed as a self-perpetuating vicious cycle: its manifestation not only increases the risk of the aforementioned comorbidities but also leads to the progression of the previously established disorders, as the manifestation of these metabolic disorders (insulin

resistance, obesity, hypertension, etc.) raise the prevalence of MetS [38]. Taken together, MetS has emerged as the primary health risk of the modern era with a significant socioeconomic impact [36]. The global prevalence of MetS is influenced by different criteria, such as the criteria used to diagnose this disorder, age, geographic localization and sociodemographic factors [39]. It is estimated that 20-25% of adults worldwide have MetS, a number that continues to rise especially in people with advanced age [40]. This disease has been linked to several comorbidities such as NAFLD, prothrombotic and proinflammatory state and OSA.

Considering that obesity is an important factor contributing to OSA severity and one of the principal hallmarks of MetS, it follows that MetS is extremely prevalent in OSA patients, with a reported variable rate of up to 80% [41]. It was also demonstrated that OSA, more specifically CIH and SF, in both human and animal model studies led to a state of insulin resistance, glucose intolerance and elevated fasting glucose, conditions also present in MetS [20], [42], [43]. Taken together, there is a clear association between the CIH and SF present in OSA and metabolic syndrome and its core components, however, the mechanistic alterations connecting these disorders remain to be proven [20], [41], [44].

1.2.4 OSA and non-alcoholic fatty liver disease (NAFLD)

NAFLD is the most prevalent chronic liver disease affecting around 30% of the adult population, being more prevalent in man [45], [46]. Other factors that influence the prevalence of this disorder, include age and the presence of other pathologies such as OSA and/or endocrine dysfunctions [47].

NAFLD is a heterogeneous condition that encompasses a spectrum of liver tissue alterations with a variable degree of severity [48]. The first stage is hepatic steatosis, which manifests as the overaccumulation of triglycerides (TAG) in the hepatocytes in the form of lipid droplets. Additionally, there might or not be a low degree of hepatic tissue inflammation [48], [49]. With the progression of the disease, the increased deposition of lipids leads to a more severe state of steatosis referred to as non-alcoholic steatohepatitis (NASH), associated with inflammation, hepatocellular injury (hepatocyte ballooning) and fibrosis. Ultimately, NAFLD can lead to a state of cirrhosis, liver failure or hepatocarcinoma [50].

NAFLD pathogenesis is driven by adipose tissue dysfunction and hepatic *de-novo* lipogenesis. Due to overnutrition, the adipose tissue becomes dysfunctional and insulin resistant

[48]. As a result, lipolysis is dysregulated which raises the flow of free fatty acids (FFAs) to the liver through the bloodstream [48]. On the other hand, high sugar intake leads to an increase in hepatic *de-novo* lipogenesis, i.e., conversion of carbohydrates into FFAs [50]. This increase of flow and accumulation of FFAs, in turn, culminates in the deposition of TAG in the form of lipid droplets, and the production of lipotoxic metabolites, leading to an increase of oxidative stress, the activation of pro-inflammatory mechanisms and damage in the hepatocytes [51].

Altogether, there is a strong bidirectional relationship between the onset and progression of NAFLD and metabolic diseases, such as obesity and T2D, since the mechanisms underlying the development and progression of NAFLD increase the risk and/or severity of these conditions and vice-versa [20], [52]. Therefore, given the fact that OSA is related to the development and progression of the aforementioned diseases, as well as being independently associated with different pathological features of NAFLD, we can presuppose a relationship between OSA and NAFLD [20], [41].

In fact, different studies have shown that OSA, particularly CIH, is independently associated with NAFLD, having a potential role on its development and progression to NASH or liver fibrosis, contributing to histological alterations typical of NAFLD (lobular inflammation, steatosis, hepatocellular ballooning and fibrosis) and alterations in liver enzyme levels [51], [53]. Additionally, other studies have demonstrated that OSA patients have a higher incidence of NAFLD than patients without this disease, highlighting the need for OSA patients to undergo NAFLD screenings [21]. At a molecular level, different pathophysiological mechanisms were proposed to explain this link (fig. 1.3). Apart from CIH promoting a state of insulin resistance and glucose intolerance, contributing to the development of obesity [20], CIH increases mitochondrial dysfunction, triggers reactive oxygen species (ROS) production, which increases oxidative stress, promotes the release of inflammatory cytokines and adipose tissue inflammation, which culminates in a systemic inflammatory state, all factors that contribute for the progression of NAFLD and liver injury [51], [54], [55]. CIH-induced hypoxic state also activates hypoxia-inducible factors (HIFs), leading to an increase in the expression of genes involved in lipogenesis, profibrotic and inflammatory factors (fig. 1.3) [21]. In addition, CIH can also activate endoplasmatic reticulum stress pathways, namely unfolded protein response (UPR), which aggravates NAFLD [21].

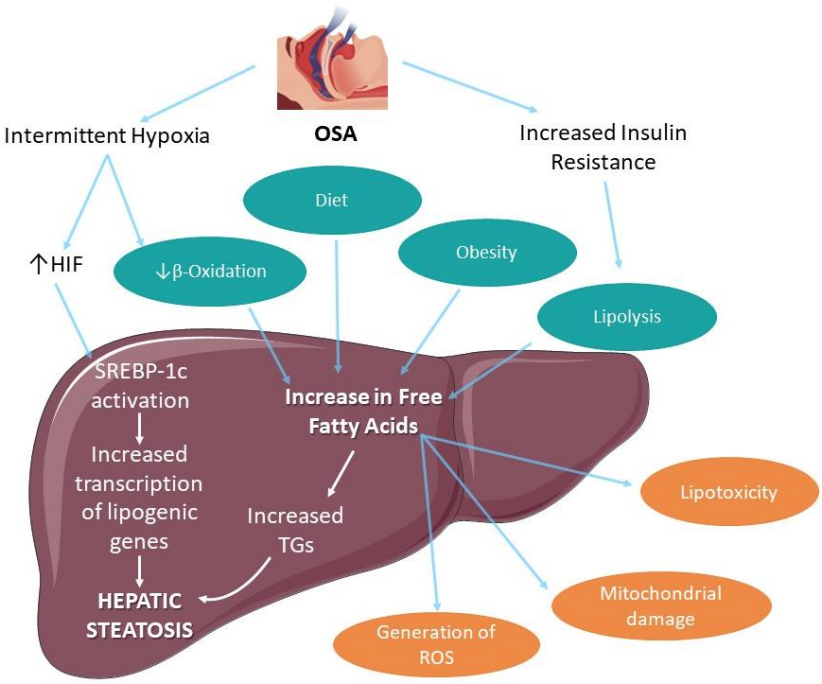

Figure 1.3 - The different mechanistic pathways linking OSA and NAFLD. OSA contributes to the development of insulin resistance, contributing to an increase of lipolysis. On the other hand CIH allows the stabilization of HIFs and decreases lipid β-oxidation in liver tissue. Ultimately all these alterations increase hepatic FFA, ROS production, promote mitochondrial dysfunction and the activation of pro-inflammatory pathways, leading to the onset and progression of NAFLD. Image adapted from Parikh *et al.* [51].

1.2.5 OSA and Insulin Resistance

Insulin resistance is a common hallmark for obesity and T2D and is also independently associated with OSA in both obese and non-obese subjects, as well as hyperinsulinemia and hyperglycaemia [20], [56]. In this condition, the insulin target tissues become less capable of responding to insulin, which inhibits its subsequent mediated response. As a result, the regulation of glucose and lipid metabolism is compromised [57].

Insulin is a 51 amino acids peptide hormone, formed by polypeptide chains A (21 amino acids) and B (30 amino acids) connected by disulphide bridges [58]. Insulin is the most important anabolic hormone having an imperative role in maintaining glucose homeostasis, cell growth and differentiation, thus this hormone has a pleiotropic effect on the different target tissues [59].

Insulin production and secretion mostly occur in the pancreas β-cells located in islets of Langerhans, and these processes are both regulated by circulating glucose levels [60]. After a meal, the increase in blood glucose triggers the biosynthesis and secretion of insulin in β-cells and decreases the release of glucagon from the pancreas' α-cells, another important hormone that stimulates catabolic pathways in insulin-sensitive tissues in order to increase blood glucose levels during a fasting state, thereby maintaining the basal levels of glucose needed to fulfil the body metabolic demand [60], [61].

Upon secretion, insulin is systemically distributed through the bloodstream and binds to the insulin receptors (IR) present in the target tissues' cell membranes, including the liver, adipose tissue and skeletal muscle (fig. 1.4) [60]. From a metabolic perspective, the binding of insulin to its receptor triggers a signalling cascade that culminates in the stimulation of the cellular uptake, storage, and synthesis of nutrients, while inhibiting catabolic pathways to prevent the degradation and release of nutrients to the bloodstream [59], [62]. As a result of insulin binding to IR, two distinct downstream signalling pathways can be activated: the phosphoinositide3-kinase (PI3K)/protein kinase B (Akt) pathway, which stimulates the cellular metabolic functions, and the mitogen-activated protein kinase (MAPK) pathway, which is principally responsible for coordinating the processes of cell growth, division, and differentiation (fig. 1.4) [58], [60].

IR is a glycoprotein that belongs to the same subfamily of tyrosine kinase receptors as the insulin-like growth factor (IGF)-I receptor [58]. It comprises two extracellular α subunits that bind to insulin and two transmembrane β subunits with a tyrosine-kinase domain in their intracellular region. This tetramer presents an $\alpha_2\beta_2$ configuration and a single disulphide bond links the two αβ dimers [62]. Upon insulin binding, α subunits stop the repression of the tyrosine kinase activity of the β-subunits, which transphosphorylates itself in different tyrosine residues, activating the IR [63]. Once active, the IR recruits several proteins to induce their phosphorylation and initiate a signalling cascade [60]. Within these, the proteins from insulin receptor substrate (IRS) family and Shc isoforms stand out as the ones that induce the PI3K/AKT and MAPK signalling pathways, respectively (fig. 1.4) [60], [62].

The consequently activated signalling cascades promote different processes such as cell growth and differentiation, glucose and lipid metabolism and vesicle trafficking [64]. The mediated phosphoinositide-dependent kinase 1 (PDK-1) activation of AKT is the most well-studied signalling cascade [60]. AKT stimulate the phosphorylation of different downstream proteins, which in turn activates a myriad of metabolic functions within the cell (fig. 1.4) [64].

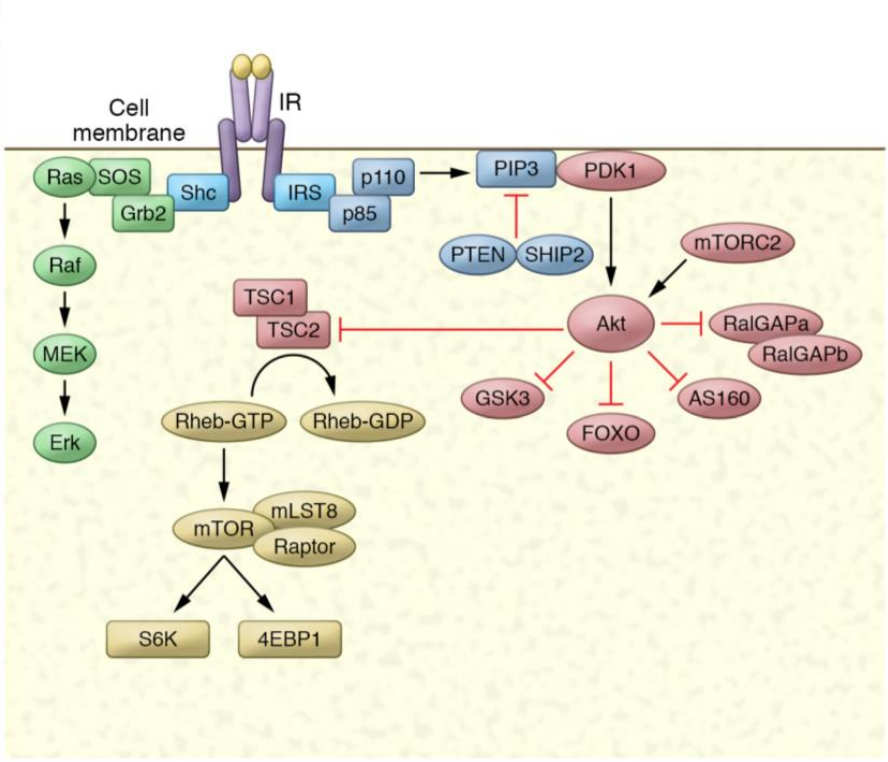

Figure 1.4 - Insulin signalling. Insulin can activate different signalling pathways such as PI3K/AKT and MAPK. The insulin biding to IR promotes the activation of downstream proteins by its phosphorylation and leads to the activation of different processes such as cell growth and differentiation, glucose and lipid metabolism and vesicle trafficking. Image taken from Saltiel A.R [62].

1.2.5.1 OSA and hepatic insulin resistance

One of the main action sites of insulin is the liver [60]. Following a meal, insulin levels in the bloodstream rise, signalling the liver to regulate hepatic lipid and glucose metabolism, allowing glucose to be transported from the blood into hepatocytes and converted into glycogen, fatty acids, and TAG [60]. Insulin increases glucose-utilizing activity by boosting hepatic glucose utilisation by glycolysis and glycogenesis while decreasing glucose production by quelling gluconeogenesis and glycogenolysis [65]. More specifically, through the PI3K / AKT pathway, it promotes the phosphorylation and respective inactivation of glycogen synthase kinase-3 (GSK-3), permitting the activation of glycogen synthase and subsequent glycogen synthesis [66]; phosphorylates the forkhead box (FOXO) transcription factors, namely FOXO1, inducing their nuclear exclusion and thus inhibits the expression of gluconeogenic genes [66]; leads to mammalian target of rapamycin complex 1 (mTORC1) activation, stimulating protein synthesis, and the activation of the downstream target sterol regulatory element binding (SREBP) proteins, which induces the expression of genes involved in lipogenesis [60], [62]. Moreover, indirect effects of insulin, such as the increased glucose uptake in muscle and

adipose tissue, the inhibition of lipolysis in white adipose tissue (WAT) and the activation of hypothalamic insulin signalling also influence the hepatic glucose production [67].

Different mechanisms lead to the development of insulin resistance in the liver. Insulin-mediated uptake and storage of glucose are impaired, so hepatic glucose production is not suppressed. Because of this, neither gluconeogenesis nor glycogenolysis is inhibited, hepatic glucose output is not reduced and hyperglycaemia occurs [68]. Furthermore, the increase of plasma FFA glycerol re-esterification in the liver resultant from adipose tissue insulin resistance, augments ectopic lipid deposition in the liver, which further contributes to hepatic insulin resistance [69], [70].

Overall, the development of hepatic insulin resistance, a common hallmark of almost all metabolic disorders, is also associated with OSA and it is an important factor in the OSA-dysmetabolism link.

1.3 OSA and metabolic disorders: the possible links

As stated throughout the previous sections, metabolic disorders and OSA are inextricably linked, in both obese and lean patients [71].

It has been proposed different molecular mechanisms to explain the relationship between these pathologies: deregulation of the hypothalamus-pituitary axis, overactivation of the SNS, inflammation of the adipose tissue, alterations in adipokine levels, stabilization of HIFs, mitochondrial dysfunction and generation of ROS and oxidative stress [20], [72], being the last three the main focus of these work (fig. 1.5). Nevertheless, this is poorly understood and the mechanism that links OSA to metabolic disorders is not clarified.

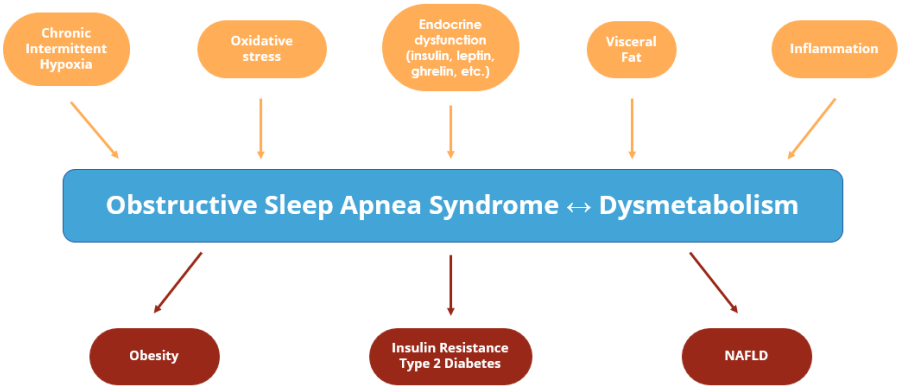

Figure 1.5 - Different features possibly involved in the pathophysiological mechanism linking OSA and metabolic diseases. Adapted from Martins *et al.* [56].

1.3.1 Stabilization of hypoxia-inducible factors (HIFs)

Since O_2 is a crucial element for the normal functioning of cells, several mechanisms were developed to detect variations in O_2 concentration and restore homeostasis [73]. HIFs are the principal regulators implicated in the hypoxic response. These transcription factors are heterodimers from the basic helix-loop-helix–PER-ARNT-SIM family, composed of a constitutively expressed β-subunit and an O_2-regulated α-subunit [74]. Currently, three α-subunits are known to be expressed in humans: HIF-1α, HIF-2α and HIF-3α, with HIF-1α and HIF-2α more well-characterized than HIF-3α, whose functions are yet unknown [75].

Under normoxia, different mechanisms regulate HIF-α subunits' cellular concentration and transcriptional activity [76]. Prolyl hydroxylases (PHD) are important oxygen sensors that lead to HIF-α degradation. Three isoforms of PHD are present in humans - PHD1, PHD2 and PHD3- being PHD2 the principal regulator of HIF-α stability [77]. These enzymes hydroxylate two proline residues in the oxygen-dependent degradation (ODD) domain of HIF-α subunits, allowing von Hippel–Lindau-elongin BC-CUL2 (VHL) protein complex recognition of these proteins (fig. 1.6A). Then, the VHL complex polyubiquitylates HIFs and marks them for proteasomal degradation fig. 1.6A [78], [79]. HIF asparaginyl hydroxylase or factor inhibiting HIF (FIH) is another important regulator of HIF-α subunits (fig. 1.6B). FIH catalyses the hydroxylation of an asparaginyl residue in the transactivation domain, located in the C-terminal of HIF-α subunits, which inhibits the recruitment of HIF-α coactivators p300 and cAMP-responsive-element binding protein (CREB) and, therefore, the HIF-α transcriptional activity (fig. 1.6B) [76], [78].

Conversely, in a hypoxic condition like CIH, both PHD and FIH activities are diminished. This results in the stabilization of HIF-α subunits and their respective translocation to the nucleus, where they dimerize with HIF-β forming the active form of these transcription factors (fig. 1.6C) [78]. The active complex then binds to hypoxia-responsive elements (HRE) from their target genes and activates their expression to increase oxygen delivery in the tissue and decrease O_2 consumption [80]. HIFs can directly activate over 1000 genes in response to hypoxia, which are involved in different processes such as angiogenesis, glucose and lipid metabolism, inflammation, erythropoiesis, tumorigenesis or extracellular matrix homeostasis [73], [77]. Nonetheless, the array of genes activated varies between tissues, and each isoform is responsible for inducing the expression of different types of genes [80], [81]. In the liver, HIF-1α promotes glycolysis, by regulating the expression of several glycolytic enzymes, and induces the expression of glucose transporters, while HIF-2α is crucial for the regulation of hepatic lipid metabolism and it's also responsible for the suppression of gluconeogenesis and the sensitization of insulin signalling [82], [83].

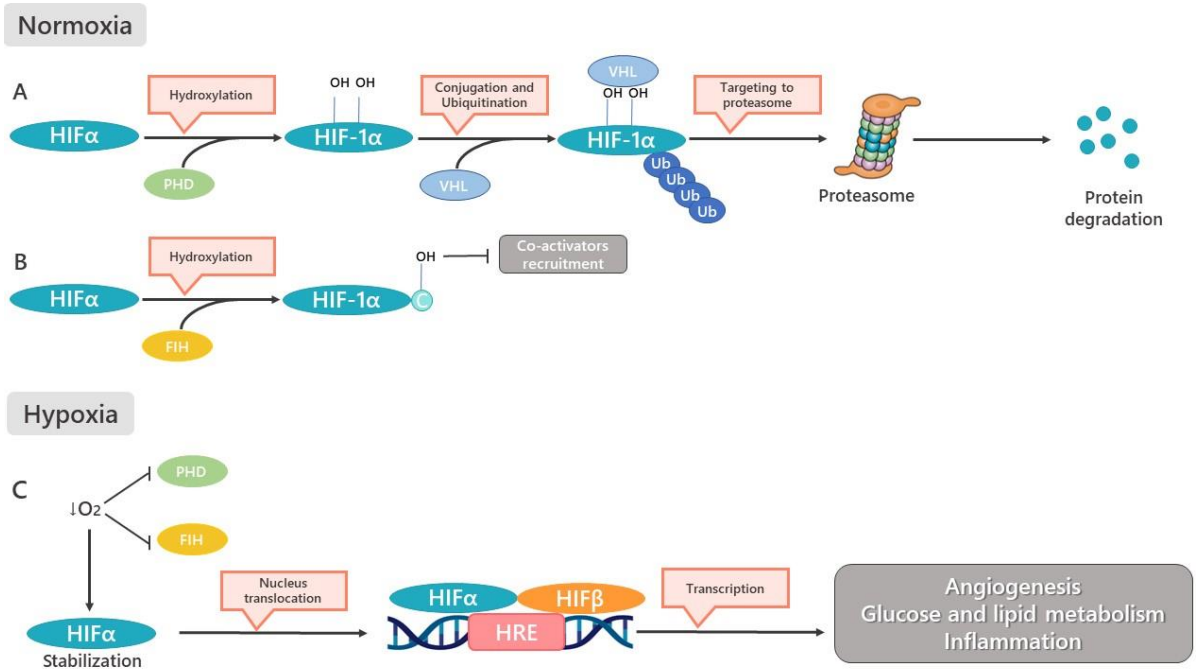

Figure 1.6 - The regulation of HIF. Under normoxia, the HIF-α levels are regulated by PHD, which mark HIF-α subunits to ubiquitination, leading to their proteossomal degradation of HIF-α, and by FIH, which inhibit the recruitment of HIF-α co-activators, thereby inhibiting their transcriptional activity. Once hypoxia occurs, PHD and FIH activity is diminished, which prevents HIF-α hydroxylation. As a result, HIF-α subunits stabilize, translocate to the nucleus and dimerize with HIF-β, activating the transcription of different target genes. Adapted from Gonzalez *et al.* [90]

Considering that HIFs are involved in the cells' metabolic reprogramming and are stabilized in a state of hypoxia, a plausible mechanism for the CIH-induced dysmetabolic phenotype is the stabilization of these transcription factors. As a matter of fact, different studies have been conducted to infer this issue.

Different cell culture studies show that under a hypoxic condition, HIF-1α increase glucose uptake by upregulating the expression of glucose transporters 1,3 and 4 and enhances glycolysis by inducing the expression of different glycolytic enzymes such as hexokinase 1 and 2, phosphoglycerate kinase 1, enolase 1 and pyruvate kinase M2 [75], [78]. Although some of the studies were performed using cancer cell lines [84], [85] (the expression of HIFs and its target genes is deeply connected to tumour growth and cancer progression), it is valid to assume that a similar phenomenon occurs in this case, since human patients with OSA present higher serum levels of HIF-1α [86], [87]. HIF-1α also promotes a shift towards a more anaerobic metabolism by increasing the expression of lactate dehydrogenase A, which elevates the production of lactate, and by elevating the levels of pyruvate dehydrogenase kinase 1, an enzyme that inhibits the enzymatic activity of the dehydrogenase complex, inhibiting the conversion of pyruvate to acetyl-CoA and, therefore, leads to the tricarboxylic cycle downregulation.

Despite its essential role in intracellular metabolic reprogramming in a state of hypoxia, HIF-1α function seems pleiotropic, taking part in different processes among tissues even in normoxic conditions. For pancreatic β-cells to operate properly, HIF-1α is required. According to a study by Cheng *et al.* [88], mice with specific HIF-1α deletion in β-cells developed glucose intolerance as a result of impaired glucose-mediated insulin secretion. Moreover, mice fed with an HF diet and administered an iron chelator to stabilize HIF-1α levels improved glucose tolerance [89]. This improvement was not seen in mice with HIF-1α deletion in β-cells, confirming the importance of HIF-1α in β-cell function [83], [89]. In contrast, in a state of hyperglycaemia, the levels of HIF-1α in β-cells reduce drastically and its transcriptional activity is reduced, which in turn blocks insulin secretion and further contributes to the increase of blood glucose levels, glucose intolerance and β-cells dysfunction [83]. In addition, in T2D patients the mRNA levels of HIF-1β are highly decreased [90]. Altogether, HIF signalling might have a role in the β-cell function and the induced inhibition of this pathway by glucose possibly contributes to the development and progression of T2D [83], [90].

Also, the expansion of adipocytes in WAT in conditions of obesity is not balanced by an adequate increase in angiogenesis, which results in insufficient oxygen delivery to the tissue. As a result, local hypoxia is induced, which enables HIFs stabilization [80]. In turn, the increase of HIFs expression and signalling promotes detrimental metabolic effects that lead to adipose

tissue dysfunction, insulin resistance and onset or progression of T2D (fig. 1.7) [75]. The increase in fatty acid metabolism and mitochondrial uncoupling, which both contribute to increased O_2 consumption, are other factors contributing to this localized hypoxia [80]. HIF-1α is the predominant isoform present in the adipose tissue and it is connected to the dysregulation of adipose tissue function [91]. On the other hand, HIF-2α expression seems to have a protective role against WAT inflammation and fibrosis [80]. HIF-1α upregulation can contribute to the increase in expression of inflammatory cytokines, namely interleukin-6 (IL-6), interleukin-8 (IL-8) and tumour necrosis factor α (TNF-α), and activates M1 macrophages, which further contributes to the secretion of inflammatory cytokines and tissue damage [80], [90]. The increase in HIF-1α also leads to WAT fibrosis by the increase of collagen deposition and cross-linking, which contributes to immune cell infiltration and, therefore, WAT inflammation [80]. Also, HIF-1α increases the expression of suppressor of cytokine signalling 3 (SOCS3) which leads to the inhibition of adiponectin expression [90], an adipokine crucial for glucose homeostasis and to preserve insulin sensitivity in WAT [21]. Collectively, HIF-1α stabilization and WAT hypoxia mediated by obesity dysregulate adipokine and inflammatory cytokines expression and secretion leading to WAT dysfunction, insulin resistance, glucose intolerance and the onset of T2D [21], [80], [90].

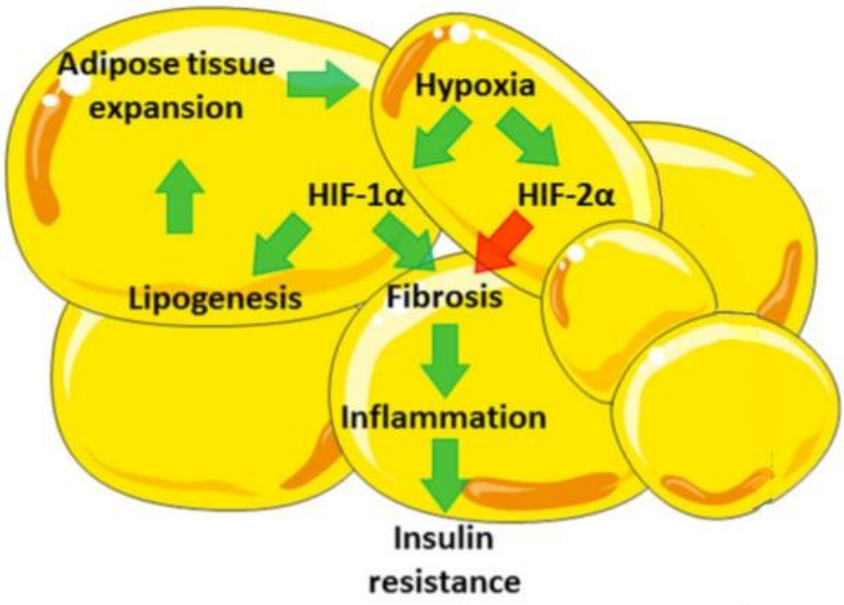

Figure 1.7 The proposed HIF dependent mechanisms involved in WAT dysfunction. In obesity, along with other factors, the expansion of adipocytes results in a local hypoxia allowing HIF stabilization and transcriptional activity. HIF-1α mediates WAT fibrosis and the concomitant activation of inflammatory pathways. Conversely, HIF-2α appears to have a protective role against inflammation and fibrosis. Green and red arrows represent the activation and the inhibition of these pathways, respectively. Image adapted from Lefere *et al.* [80]

Finally, different studies have reported that CIH plays a critical role in NAFLD onset and progression and it's the principal trigger for HIFs expression in the liver (fig. 1.8) [80]. Nevertheless, the intake of hypercaloric food itself can induce local hypoxia, driving HIFs expression [92]. Also, insulin resistance and dysregulated lipolysis, promote and aggravate hepatic steatosis, which also contributes to local tissue hypoxia and HIFs stabilization [80]. Since HIF-1α regulates genes involved in glucose and lipid metabolism, it is plausible to postulate that the development of NAFLD can be mediated by HIF-1α [51], [92]. Studies in mice models have demonstrated that SREBP-1c, a transcription factor crucial for the activation of hepatic *de novo* lipogenesis, and their respective downstream target genes, fatty acid synthase and acyl-CoA carboxylase, are upregulated in response to HIF-1α in hypoxia, which leads to an excessive FFA and TAG synthesis and, for this reason, to a state of hyperlipidemia and hepatic steatosis [51], [93]. Concomitantly, to decrease the O_2 consumption in liver tissue, fatty acid β-oxidation is inhibited by HIF-1α which increases the FFA concentration in the tissue which provokes fatty liver disease and tissue injury [51], [78]. In a protective manner, the expression of protein adipocyte differentiation-related protein (ADRP), which induces lipid droplet formation, also seems to be stimulated through a HIF-dependent mechanism [80]. Lysil oxidase expression and activity, an enzyme responsible for the cross-linking of collagen and elastin, is also stimulated by HIF-1α, which accelerates the development of hepatic fibrosis and the ensuing progression of NAFLD [51]. The increase in HIF-2α levels also contributes to the onset and development of NAFLD. HIF-2α also promotes a reduction in fatty acid β-oxidation and an increase in fatty acid uptake and synthesis. It also contributes to an increase in inflammation and fibrosis in the hepatic tissue, however, the mechanism that leads to this phenotype is not known [90].

In brief, the available literature shows that the adaptable mechanisms induced by HIFs in response to hypoxia are involved in the development of metabolic disorders, however, it can also be crucial for the correct organ function, so more studies are needed to uncover their role in the pathophysiology of metabolic disorders and their potential as therapeutic targets.

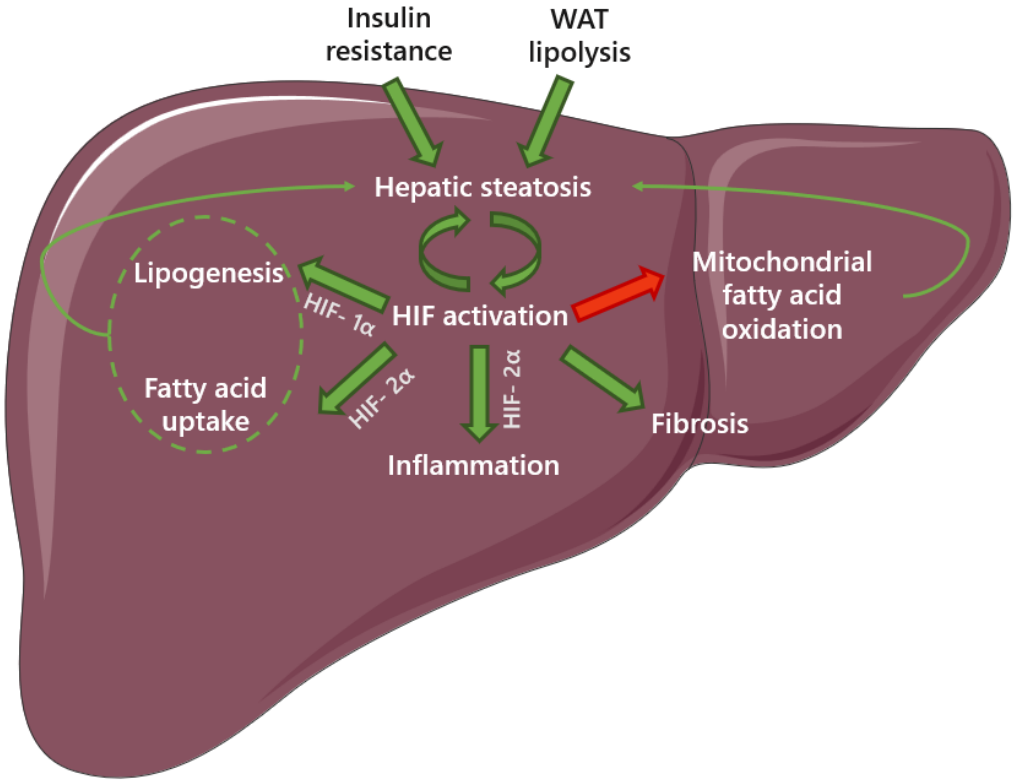

Figure 1.8 - The proposed HIF dependent mechanisms involved in liver dysfunction. The intake of hypercaloric food and CIH can thrive to a local hypoxia promoting the stabilization of HIF and the respective transcriptional activity. Hepatic *de novo* lipogenesis is upregulated by HIF-1α, which exacerbates FFA and TAG synthesis and leads to a state of hyperlipidemia, hepatic steatosis and liver injury. The decrease fatty acid β-oxidation, also mediated by HIF-1α, also contributes for the devolpment of this phenotype. HIF-2α also mediates the reduction of fatty acid β-oxidation and upregulates fatty acid uptake and synthesis. Both HIF-1α and HIF-2α mediate the increase of hepatic fibrosis and inflammation. Green and red arrows represent the activation and the inhibition of these pathways, respectively. Image adapted from Lefere *et al.* [80]

1.3.2 Mitochondrial Dysfunction

Among all cell organelles, mitochondria take the central stage as O_2 consumers, making them an appealing O_2 sensing system and fundamental in conditions of OSA-dysmetabolism link [94]–[96]. Mitochondria are cytoplasmic organelles responsible for generating chemical energy for the cell's biochemical reactions, which is provided through adenosine triphosphate (ATP) supply [96]. ATP synthesis is an aerobic process that occurs by oxidative phosphorylation through an electric transport chain (ETC), comprised of four protein complexes for electron transfer (I-IV) and one that aids in the production of ATP (complex V), which are located at the

mitochondrial matrix [95], [97]. It requires electron carriers as reducing components- NADH and $FADH_2$-which are formed during the tricarboxylic acid (TCA) cycle, a series of enzymatic reactions that also occurs in the mitochondria [95], [98].

The oxidative phosphorylation process starts with the oxidation of NADH to NAD^+ by the first complex (complex I), also known as NADH dehydrogenase (fig. 1.9) [99]. The entrance of the electron pair of NADH is supported by a prosthetic group, flavin mononucleotide, which is transferred throughout several iron-sulphur clusters and to ubiquinone, an oxidized form of the hydrophobic electron carrier coenzyme Q10. Ubiquinone is reduced to ubiquinol and transferred to complex II, where it oxidizes again into ubiquinone [99], [100]. Besides NAD^+ and ubiquinol, this enzymatic reaction produces H^+ ions that are released into the intermembrane space [94], [99].

The second process of oxidative phosphorylation is provided by complex II, referred to as succinate dehydrogenase (fig. 1.9) [96]. This enzyme is made up of iron-sulphur clusters and a bound cofactor called flavin adenine dinucleotide, responsible for the electron transfer from $FADH_2$ to ubiquinone [101]. In contrast with the latter stage, this enzymatic reaction does not produce H^+ ions because of the bypass of $FADH_2$ from complex I to complex II, thus not enough energy is released [99], [101]. The electrons from complexes I and II are then transferred to complex III by ubiquinol [99].

The third complex (complex III), also known as cytochrome c reductase (fig. 1.9), is mostly composed of many iron-sulphur clusters and cytochrome B and is responsible for the electron shuttle from ubiquinol to cytochrome c, followed by H^+ ion pumping into the intermembranous space [101].

The last complex involved in the electron transfer, complex IV, known as cytochrome c oxidase (fig. 1.9), is comprised by heme groups that sequester an oxygen atom into the complex with the simultaneous transfer of electrons from cytochrome c to the oxygen atom, that functions as the last electron acceptor [100]. Then, the oxygen molecule is reduced by the addition of H^+ ions from the mitochondria matrix to the oxygen atom, forming water (H_2O) [96], [101]. At the same time, this enzymatic reaction also releases H^+ ions into the intermembrane space [101].

The H^+ ions that have been released from previous enzymatic reactions are then reintroduced into the mitochondria matrix through the fifth complex (complex V), as known as ATP synthase (fig. 1.9) [95], [99]. ATP synthase contains several protein subunits, including a hydrophobic one responsible for the entrance of H^+ ions, and a hydrophilic one that acts as a catalytic

site, allowing the binding of an adenosine diphosphate (ADP) molecule to an inorganic phosphate (Pi) atom, producing ATP [99]–[101].

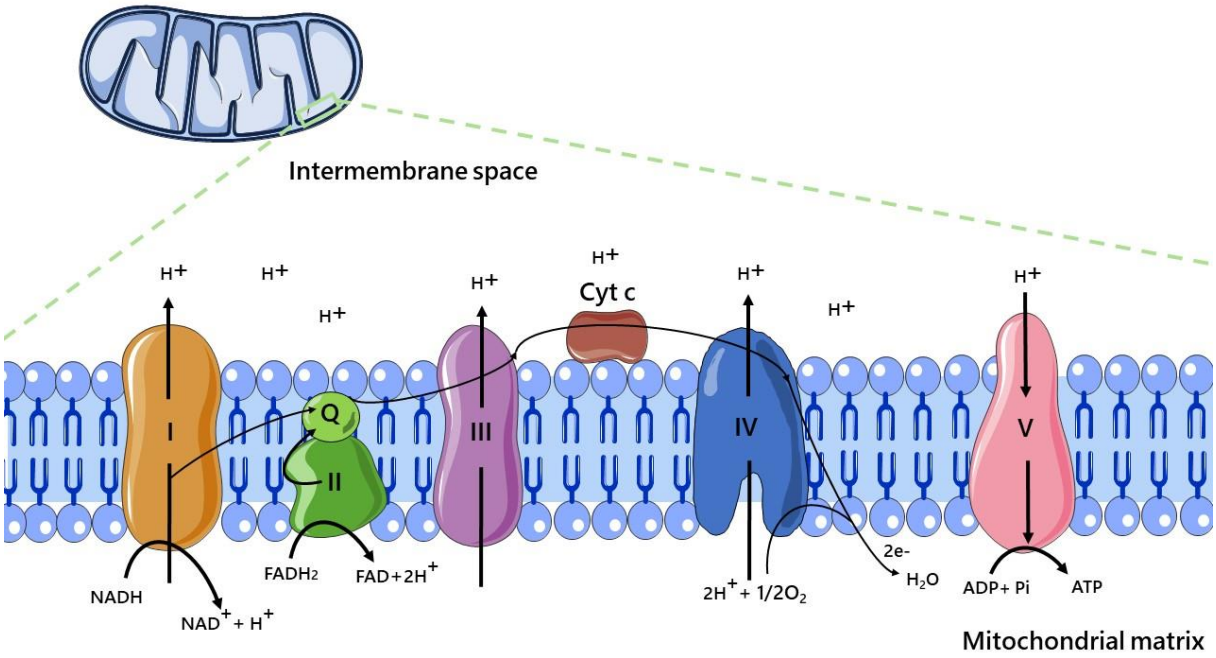

Figure 1.9- The process of oxidative phosphorylation. Inside the mitochondrial matrix, NADH derived from the TCA cycle is oxidized by NADH dehydrogenase (complex I, orange), allowing the formation of an electron pair that is transferred to ubiquinone (Q, light green). Ubiquinone is reduced to ubiquinol and transferred to succinate dehydrogenase (complex II, dark green), where it oxidizes again into ubiquinone. The complex II is responsible for the oxidation of $FADH_2$, also derived from the TCA cycle, and the electrons derived from this reaction are also transferred by ubiquinol to cytochrome c reductase (complex III, purple). Complex III performs as an electron shuttle to cytochrome c (Cyt c, brown) which then transfers the electrons to cytochrome c oxidase (complex IV, navy blue), the last electron acceptor of the ETC. Here, an oxygen atom is reduced by H^+ ions from the mitochondrial matrix to H_2O. The H+ ions released from the previous enzymatic reactions to the intermembrane space re-enter the mitochondrial matrix by ATP synthase (complex V, pink), catalysing the binding of a phosphate atom (Pi) to a ADP molecule, forming ATP.

Since the production of ATP by mitochondria is the largest O_2-consuming process within the cell, it can be anticipated that the variation in O_2 levels, as it occurs in the hypopnea-apnea episodes in OSA, will have an impact on ETC function. As stated, by a HIF-dependent mechanism the expression of lactate dehydrogenase A and pyruvate dehydrogenase kinase 1 is upregulated to inhibit the TCA cycle and, therefore, the ETC activity [78]. Under chronic hypoxia, ETC function is reduced by an HIF1-dependent induction of respiration reduction of the complex I, supressing ETC complex formation [102]. Also, CIH disrupts the assembling of complexes I, II and III iron-sulphur clusters through the expression of several microRNAs, compromising ETC expression and activity [103]. By decreasing the ETC activity, ROS production by

complex III is also reduced, which protects the cells' macromolecules from damage [78]. Hypoxia also triggers mitochondria fission to induce mitophagy, so mitochondrial ROS production is reduced and the cellular integrity is maintained [96]. However, other studies that are also in the context of liver disease, show that hypoxia upregulates the expression of genes involved in mitochondrial biogenesis and fusion, so more studies are needed to fully understand the mitochondrial response under hypoxic conditions [51], [104]. In summary, by one side mitochondrial activity is downregulated to reduce the production of mitochondrial ROS and their consequent deleterious effects that ultimately increase tissue inflammation and cell death, and by the other side IH also promotes hepatic mitochondrial fatty acid oxidation to produce ATP, which increases oxidative stress within the tissue and causes DNA damage which can progress to liver injury [104].

1.3.3 Oxidative Stress, Antioxidant Defences and Inflammation

Oxidative stress occurs when the balance between ROS and the body's antioxidant defence mechanisms is disrupted, resulting in an accumulation of ROS and subsequent damage to cells and tissues [105]. This can lead to a variety of health problems, including inflammation, ageing, and chronic diseases such as cardiometabolic disorders[72], [106]. In OSA, this alteration on the pro/antioxidant balance is brought on by the hypoxia/re-oxygenation cycles, which augment ROS formation and oxidative stress [72]. Patients with OSA show an increase in lipid peroxidation, a decrease in the antioxidant capacity and higher concentrations of ROS in circulating leukocytes than normal subjects, factors that can contribute to the development of metabolic conditions that are associated with OSA [72], [107]. These alterations are also observed in animal models [42]. Hence, oxidative stress may be a significant contributor to the establishment of the dysmetabolic state associated with this pathology.

An association between dysmetabolism and the CIH-mediated increase in oxidative stress was observed in mice WAT, as evidenced by higher ROS generation and changes in ETC activity, suggesting a potential role for WAT in the onset of this OSA-associated phenotype [108]. Despite this, other authors did not find any significant alterations in WAT oxidative stress in response to severe CIH [109]. Given that the animals were subjected to different time periods of CIH in these studies, with the former being longer than the latter, it is likely that oxidative stress in WAT does not immediately cause the dysmetabolic phenotype associated with OSA but rather develops as the disease progresses [56], [109].

Oxidative stress is thought to be also a cause of liver damage [106]. Due to an increase in the activation of pro-oxidant pathways, promoting ROS formation, and a decrease in the endogenous antioxidant mechanisms, both enzymatic and non-enzymatic, impede the scavenging of these free radical compounds which alter the cell normal function and ultimately lead to hepatic cells death [110], [111].

ROS can have an exogenous - hypoxia, alcohol consumption and smoking- or an endogenous source, being a product of pathways that requires O_2 consumption and are mostly produced in the mitochondria [112], [113]. The main ROS formed include superoxide anion, principally formed in ETC of mitochondria, hydroxyl radicals and hydrogen peroxide [110]. The production of these free radicals can also be mediated by extramitochondrial processes namely by xanthine oxidase, nicotinamide adenine dinucleotide phosphate (NADPH) oxidase and fatty acid β-oxidation [110]. In physiological conditions, ROS are often produced by mitochondria and have important signalling functions, however, with the disruption of the pro/antioxidant balance the consequent accumulation of ROS produces deleterious effects in cell function leading to a pathological state [94], [110].

The accumulation of ROS in the liver tissue, particularly superoxide anion and nitric oxide, has cytotoxic effects in the setting of liver disease. Higher levels of ROS are linked to an increase in lipid peroxidation, augmented activity of the free radical-producing enzymes, such as aldehyde oxidase and xanthine oxidase, the formation of toxic adducts as a result of ROS interactions with cellular macromolecules (DNA, proteins, and lipids) and promote alterations in antioxidant mechanisms. In turn, these alterations cause an increase in hepatic fibrosis, mitochondrial dysfunction, the activation of inflammatory pathways and, ultimately, cell death [111].

Antioxidant mechanisms have the role of decreasing ROS to restore tissue homeostasis and contain enzymatic and non-enzymatic components [113]. Regarding the enzymatic mechanisms, different enzymes catalyse ROS detoxification, such as superoxide dismutase (SOD), the first line of defence against mitochondrial ROS formation, as catalase, glutathione peroxidase and reductase, among others [114]. Non-enzymatic defences comprise different vitamins and glutathione, which react with ROS and accept electrons in their structure leading to their elimination or detoxification, and nuclear factor E2-related factor 2 (Nrf-2), a transcriptional factor activated by oxidative stress that upregulates the expression of antioxidant genes [113], [115]. For a more effective response, all these components are carefully distributed in the cells so that the response against the increased ROS is triggered more quickly [113].

Inflammation is concomitant to oxidative stress and mitochondrial dysfunction, so it can be a factor contributing to OSA/CIH-associated dysmetabolic phenotype. The increase in IL-6 and TNF-α plasma levels positively correlates with an increase in body mass index, which strengthens the link between OSA and obesity [116]. Moreover, an abnormal rise of cytokines is seen in OSA patients throughout nocturnal periods, which contributes to sleep dysregulation [56]. As stated throughout this document not only CIH and SF but also the onset and development of its associated metabolic comorbidities, all lead to a tissue-specific and systemic state of inflammation, characterized by the increased production and secretion of pro-inflammatory cytokines (IL-6 and TNF-α), the activation of inflammatory pathways as the nuclear factor kappa B (NF-κB) signalling and the induction of innate and adaptive immune responses, such macrophage M1 polarization [20], [117], [118]. Altogether these further contribute to the deleterious effects induced by CIH leading to metabolic dysfunction.

2

AIMS OF THE WORK

OSA and metabolic diseases, such as obesity, metabolic syndrome, T2D and NAFLD, are inextricably linked however, the subsequent mechanism of this relationship is yet to be clarified [20]. Different mechanisms were proposed to explain this relationship: oxidative stress and ROS production, inflammation, mitochondrial dysfunction, alterations in adipokines levels, overactivation of SNS, among others particularly on the adipose tissue with conflicting results [20]. Moreover, it is quite well described that other organs, like the liver, play a crucial role on metabolic homeostasis. Therefore, the principal aim of this work was to evaluate if liver dysfunction plays a role in the metabolic dysfunction associated with OSA and to explore the mechanisms behind this relationship. In addition, given the strong relationship between OSA and obesity, an animal model of obesity was also used to study if the interaction between CIH and obesity would worsen the induced dysmetabolic phenotype.

The specific aims are:

1. To evaluate the impact of CIH on liver insulin signalling and clearance and glucose homeostasis in control and obese animals;
2. To evaluate the impact of CIH on liver hypoxia in control and obese animals;
3. To explore the impact of CIH and the association between CIH and obesity on liver mitochondrial dysfunction, oxidative stress and inflammation.

3

METHODS

3.1 Animal experiments and *in vivo* procedures

Experiments were performed in male Wistar rats, 12 weeks aged, 6-8 animals per group, obtained from the vivarium of the Faculty of Medicine of the University of Valladolid, Spain. The animals were randomized and divided into two groups: a control group (CTL), fed with a standard control diet - 3.8 kcal/g with 10% kcal as fat (D12450B; Open Source Diets) - and an obese group (HF), fed with a high-fat diet (HF diet)- 5.2 kcal/g with 60% kcal as fat (D12492; Open Source Diets) - for 12 weeks. During the experimental period, the animals had food and water ad libitum and were kept under temperature and humidity control, with a regular light (08.00 – 20.00h) and dark (20.00h – 08.00) cycle.

In the last 2 weeks of diet, half of the animals from each group (CIH and HFIH, respectively) were submitted to a severe CIH protocol (fig 3.1). As described by Gonzalez-Martín *et al.*, to perform this protocol, the animals were housed in appropriate hermetic chambers (16 L, a maximum of four rats per chamber), with food and water ad libitum [119]. The chronic intermittent hypoxia protocol consisted in 30 cycles per hour of 40s exposure to 5% O_2, followed by 80s exposure to normal air atmosphere (21% O_2 and 79% N_2), for 8h per day, equivalent to an apnoea-hypopnoea index of 30. At the end of the protocol, the chambers were kept in a normal air atmosphere. The animals were submitted to this protocol during their period of inactivity (light phase of the cycle). During the CIH protocol, the remaining animals either from control or obese group were kept in the same room but were only exposed to a normal air atmosphere. Lastly, after 12 weeks of experimental period, the animals were sacrificed by an intracardiac overdose of sodium pentobarbital.

Laboratory care was carried out following the European Union Directive for Protection of Vertebrates Used for Experimental and Other Scientific Ends (2010/63/EU). Experimental protocols were approved by the NOVA Medical School, Faculdade de Ciências Médicas and Valladolid University Ethics Committee.

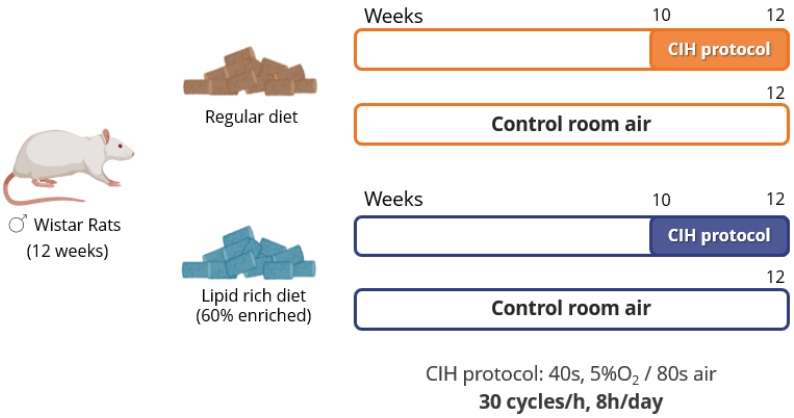

Figure 3.1 — Schematic representation of the experimental design of the study. Male Wistar rats (12 weeks; 6-8 animals per group) were divided into a control (CTL), fed with a standard diet, and an obese group (HF), fed with a 60% lipid-enriched diet for 12 weeks. From weeks 10 to 12, half of the animals from both groups were submitted to a severe CIH protocol (CIH and HFIH) consisting of 30 CIH cycles/h, 8 h/day. During the CIH protocol, the remaining age-matched control or high-fat animals were in the same room and exposed to a normal air atmosphere, to experience similar conditions.

3.1.1 Assessment of Metabolic Parameters

At the end of the CIH protocols, insulin sensitivity and glucose tolerance of the animals were assessed.

After an overnight fast (approximately 15-16 h), a blood sample was collected to measure the fasting glucose and insulin plasma levels as described in Olea *et al.* [42], which were used to calculate the insulin sensitivity of the animals with the homeostasis model assessment (HOMA-IR) index [fasting insulin (μU/mL) x fasting glucose (mM) / 22.5] [120].

To evaluate the glucose tolerance of the animals an intra-peritoneal glucose tolerance test (ipGTT) was performed. After overnight fasting, a glucose solution (2g/Kg in saline) was administrated in the animals by an I.p. injection, and glucose levels were monitored at 15, 30, 90, and 120 minutes by tail tipping. Basal glycemia was measured before the glucose administration, using the same method. All the measurements were performed with a glucose meter (Ascensia Breeze 2; Bayer).

3.2 Liver *Ex vivo* analysis

After 12 weeks of experimental period, the animals were sacrificed as described. Liver tissue samples were collected and placed in liquid nitrogen or in a 4% paraformaldehyde (PFA) solution. Samples were then stored at -80ºC or at 4ºC respectively.

3.2.1 Assessment of protein levels from insulin signalling, glucose metabolism, mitochondrial biogenesis, antioxidant system and inflammation pathways

The western blot technique was used to measure the levels of specific proteins in liver tissue extracts. Briefly, it consists in the separation of proteins according to their molecular weight, through gel electrophoresis. Afterwards, the separated proteins are transferred to a solid support membrane which is incubated with primary and secondary antibodies specific to the protein of interest. Finally, the protein of interest is detected through a chemiluminescence method.

Approximately 100 mg of liver tissue was homogenized in a lysis buffer (100 mM Tris-HCl pH=7.5, EGTA 0.2M, EDTA 50 mM, Triton X-100, Sucrose 0.27M, Na_3VO_4 0.1 M, NaF 100 mM, NaP_2O_7 10 mM and protease inhibitors (SigmaAldrich, St. Louis, MO, USA)). Homogenized tissues were then centrifuged at 15700 g for 20 minutes, 4°C, and the supernatants were collected and stored at -80ºC. Protein concentrations of the tissue extracts were measured by Micro-BCA Protein Assay Kit (Thermo Fisher Scientific; Waltham, MA, USA).

After, 20 µg of total protein samples from the homogenized liver tissue were combined with a loading buffer and were denatured in a dry bath for 5 minutes at 99°C or 10 minutes at 50°C (to measure oxidative phosphorylation complexes - OXPHOS). Afterwards, liver samples and the pre-stained molecular weight marker (Precision Plus ProteinTM Unstained Standards, Bio-Rad, Madrid, Spain) were separated by sodium dodecyl sulfate-polyacrylamide gel (SDS-PAGE) -10% separation gel and 4% concentration gel - in reductive conditions, and transferred to a nitrocellulose membrane (0.2 µM, Bio-Rad, Germany).

The membranes were blocked with 5% non-fat milk in Tris Buffer Saline with 0.1% Tween (TBS-T 0.1%) solution for 1.5 hours at room temperature to avoid nonspecific bounding,

washed with TBS-T 0.1% and then incubated with primary antibody overnight at 4°C. The used antibodies and the respective concentrations are described in table 1.

After the incubation with primary antibodies, the membranes were washed and incubated with respective secondary antibodies for 1.5 hours at room temperature. The secondary antibodies used were: goat anti-mouse (1:1000, Bio-Rad, Madrid, Spain), goat anti-rabbit (1:1000, Bio-Rad, Madrid, Spain) or mouse anti-goat (1:2000, Santa Cruz Biotechnology, Dallas, USA).

Next, the membranes underwent a second washing period and were revealed for the detection of the proteins of interest. A chemiluminescence detection method was carried out using a chemiluminescence reagent (ClarityTM Western ECL substrate, Bio-Rad, Madrid, Spain), according to the manufacturer's instructions. The chemiluminescence signal detection was performed in Chemidoc Molecular Imager (Chemidoc, Bio-Rad, Madrid, Spain) and quantified using the Image Lab software (Bio-Rad, Madrid, Spain).

To normalize the protein levels and proceed with the quantification of the proteins of interest the membranes were reprobed for loading proteins, namely: Calnexin (1:1000, goat, SicGen, Cantanhede, Portugal); β-actin (1:1000, goat, SicGen, Cantanhede, Portugal) in accordance with the molecular weights of the proteins of interest.

Table 3.1— Primary antibodies used for the proteins of interest in the present study and their respective dilution factor, specie, and brand.

Proteins	Primary Antibody
Insulin Receptor (IR) - 90 KDa	1:100, mouse, Santa Cruz Biotechnology, Dallas, USA
Protein Kinase B (AKT) - 60 KDa	1:1000, rabbit, Cell Signaling, Massachusetts, EUA
Insulin degrading enzyme (IDE) - 118 KDa	1:1000, rabbit, Abcam, Cambridge, UK
Glucose transporter 2 (Glut2) - 60 KDa	1:500, mouse, Santa Cruz Biotechnology, Dallas, USA
OXPHOS	1:500, mouse, MitoSciences, Eugene, OR, USA
Superoxide dismutase one (SOD-1) - 23 KDa	1:500, mouse, Santa Cruz Biotechnology, Dallas, USA
Catalase - 60 KDa	1:500, goat, SICGEN, Cantanhede, Portugal
Arginase I - 37 KDa	1:500, mouse, Santa Cruz Biotechnology, Dallas, USA
Interleukin-6 receptor (IL-6R) - 80 KDa	1:200, mouse, Santa Cruz Biotechnology, Dallas, USA
Interleukin-1 receptor (IL-1R) -80 KDa	1:100, mouse, Santa Cruz Biotechnology, Dallas, USA
TNF-α - 17 KDa	1:1000, goat, SicGen, Cantanhede, Portugal
TNF-α Receptor - 55 KDa	1:200, mouse, Santa Cruz Biotechnology, Dallas, USA
Nuclear factor kappa b (NF-κB) - 65 KDa	1:500, rabbit, Cell Signaling, Massachusetts, EUA

3.2.2 Histological and fluorescence immunolabelling analysis of the liver tissue

The previous PFA-fixed tissue was dehydrated in ethanol and embedded into paraffin. The paraffin tissue blocks were then cut into longitudinal slices of 8-10 µM thickness and transferred to slides either to perform haematoxylin & eosin (H&E) staining protocol for histology or to evaluate by fluorescent immunohistochemistry the levels of HIF-1α, HIF-2α and mitotracker, a mitochondrial density marker.

For the histological analysis, the stained slices were visualized in a Widefield Fluorescence Microscope Zeiss Z2 for the evaluation of fat deposition, ballooning, fibrosis, and necrosis in the livers.

For the immunohistochemistry protocol, the slides underwent a deparaffinization protocol and were rehydrated with ethanol and distilled water. After removing the paraffin from

the slides, antigen retrieval was carried out using 0.1M citrate buffer (pH=6.0) for 20 minutes, followed by 10 minutes in 0.1M glycine and 15 minutes of permeabilization with washing buffer (1% PBS, 0.1% Triton). Blockage of unspecific bounds was then performed using a 5% Bovine Serum Albumin (BSA) in washing buffer solution for 2 hours for the mitotracker assay or a 1% BSA, 1% goat serum in washing buffer solution for the evaluation of HIF-1α and HIF-2α levels. To evaluate HIF-1α and HIF-2α levels, the slides were incubated overnight, at 4ºC, with the respective primary antibody (anti-HIF-1α, 1:100, goat, SicGen, Cantanhede, Portugal; anti-HIF-2α, 1:100, mouse, Abcam, Cambridge, UK). The next day, the slices were submitted to 4 washing cycles, of 5 minutes each, with washing buffer and incubated with secondary antibody (donkey anti-goat Alexa Fluor 546, 1:5000, Abcam, Cambridge, UK for HIF-1α; and goat anti-mouse Alexa Fluor 550,1:5000, Abcam, Cambridge, UK for HIF-2α), together with 4',6-diamidino-2-phenylindole (DAPI) [1mg/mL], a nucleus cell marker, for 60 minutes, at room temperature protected from light. To conclude, the slides were washed as described, protected from light, and mounted with coverslips and Vectashield mounting medium.

To analyse the mitochondrial density, the slides were incubated with 15 nM mitotracker solution (Invitrogen™, Carlsbad, CA, USA; catalogue number: M7512), along with DAPI [1mg/ml], for 60 minutes at room temperature protected from light. The slides were then washed and mounted as previously described.

The slides were visualized under the microscope (Widefield Fluorescence Microscope Zeiss Z2) and fluorescence intensity of each slide was measured using ImageJ software [121]. These values were used to calculate the relative intensity for the area per nuclei number determined by DAPI staining.

3.2.3 Assessment of mitochondrial complexes enzymatic activity

Before performing the enzymatic assays, the mitochondria-rich fraction was isolated from liver tissue homogenates. In brief, using a glass-Teflon Potter Elvejhem 100 mg of liver tissue was homogenised in ice-cold potassium buffer (100 mM KH_2PO_4, 5 mM EDTA). The homogenate was transferred to an eppendorf, combined with an isolation buffer (250 mM Sucrose, 10 mM HEPES) in a 1:1 ratio and centrifuged at 800 g, for 15 minutes, 4°C. The supernatant was collected and again centrifuged at 12000 g for 15 minutes, 4°C. Lastly, the final supernatant, the mitochondria-free cytosolic fraction, was collected and stored at -20°C for further analysis. The pellet, corresponding to the mitochondria-rich fraction, was resuspended in an

appropriate buffer (100 mM Sucrose, 100 mM KCl, 2mM KH_2PO_4, 10 mM EDTA). The respective protein concentration was measured using the Pierce™ BCA Protein Assay Kit (Thermo Fisher Scientific; Waltham, MA, USA).

Mitochondria-rich fraction was then used to assess the activity of mitochondrial respiratory complexes I and II, and citrate synthase activity, as described in the next sections. All these protocols were performed at 37°C in, 96 well-plate.

3.2.3.1 Measurement of complex I activity

Complex I activity was evaluated by measuring the rate of NADH oxidation, which is the enzyme substrate. The correspondent volume of 10 µg from mitochondria-rich fraction was added to a potassium phosphate buffer (25 mM KH_2PO_4, 5mM $MgCl_2$, pH=7.5) supplemented with 100 mM KCN and 2 mM antimycin A, inhibitors of the complex IV and III, respectively, 38.75 mM decylubiquinone, an analogue of ubiquinone, and with or without a 500 µM rotenone solution, a specific inhibitor of complex I. To initiate the reaction, a 5mM NADH solution was added to the mix and the respective decrease of NADH fluorescence intensity was measured at 450 nm (λex = 366 nm) in 30s intervals for 20 minutes.

The difference in the rate of NADH oxidation in the presence and absence of rotenone was used to gauge the complex I activity, being the results expressed in relative fluorescence units (RFU), per minute, per milligram of protein.

3.2.3.2 Measurement of complex II activity

To evaluate complex II activity, the reduction rate of 2,6-dichlorophenolindo-phenol (DCPIP) was spectrophotometrically determined (ε = 20.7 $mM^{-1} \cdot cm^{-1}$). This mitochondrial complex promotes succinate oxidation, being DCIP the exogenous final acceptor of electrons from that reaction. As in the previous protocol, the correspondent volume of 10 µg from mitochondria-rich fraction was added to a potassium phosphate buffer (25 mM KH_2PO_4, pH=7.5) supplemented with 100 mM KCN, 2 mM antimycin A, 500 µM rotenone, 38.75 mM decylubiquinone. The reaction was performed in the presence or absence of 500 mM oxaloacetate solution in the mix, a complex II inhibitor, and initiated by adding a 100 mM succinate solution. The

time-dependent decrease of absorbance intensity at 600 nm was measured in 30s intervals for 20 minutes.

To determine the complex II activity, the difference in the DCIP reduction rate in the presence and absence of succinate was calculated, being the results expressed in concentration of reduced DCPIP, per minute, per milligram protein.

3.2.3.3 Assessment of citrate synthase activity

Citrate synthase (CS) activity was assessed spectrophotometrically by measuring 5,5-dithio-bis-2-nitrobenzoic acid (DNTB) reduction (ε = 13.6 mM^{-1}/cm^{-1}). To form the reaction mix, 10 µg from mitochondria-rich fraction lysate were added to a reaction buffer (200 mM Tris-HCl, 0.02% Triton X-100) supplemented with 10 mM DNTB and 100 mM oxaloacetate. The reaction was triggered by adding a 6.1 mM Acetyl-CoA to the reaction mix and the absorbance values at 412 nm were measured every 30s for 10 minutes.

The reduction rate of DNTB to 2-nitro-5-thiobenzoic acid (TNB) was used to calculate citrate synthase activity, and the result was expressed as millimoles of DNTB per minute per milligram of protein.

3.2.4 Determination of Intracellular ROS Content

To determine the ROS levels in the liver tissue, the fluorogenic dye CM-H_2DCFDA (C6827, Invitrogen™, Carlsbad, CA, USA) was used. The oxidation of this compound produces a fluorescent adduct, indicating ROS's presence.

Briefly, 100 mg of tissue was macerated in ice-cold Tris-HCl buffer (40 mM, pH=7.5). The homogenates were centrifuged at 1250 g for 10 minutes, 4°C, to remove cell debris, and the supernatants were collected. Afterwards, 100 µL of the homogenates were incubated with 1mL of 10 µM CM-H_2DCFDA solution for 40 minutes, at 37°C, protected from the light. Also, 100 µL of the homogenates were incubated with 1mL of Tris-HCl under the same conditions, as a control of the tissue autofluorescence. After this time, the fluorescence intensity of the samples and blanks was measured (λex = 495 nm and λem = 529 nm) using a Synergy™ H1 multi-mode microplate reader (Agilent, Santa Clara, CA, USA). Each sample was measured in duplicate, and the results are expressed as fluorescence intensity/mg protein. The protein

concentration was previously assessed using Pierce™ BCA Protein Assay Kit (Thermo Fisher Scientific; Waltham, MA, USA).

3.2.5 Ferric reducing–antioxidant power (FRAP) assay

The Ferric reducing-antioxidant power (FRAP) assay determines the antioxidant potential of the tissue by measuring its capability to reduce iron (III) to the ferrous form iron (II) in an acid medium. The colorimetric method was carried out using a modified method of Benzie & Strain [122].

Tissue homogenates were prepared as stated in section 1.2.4. Subsequently, FRAP reagent was prepared by combining acetate buffer 300mM, pH=3.6, 2,4,6-tripyridyl-s-triazine (TPTZ) 10 mM and $FeCl_3 \cdot 6H_2O$ 20 mM solutions in a 10:1:1 ratio.

To determine the antioxidant potential, the samples and FRAP reagent were mixed and the reduction of the Fe^{3+}–TPTZ complex to Fe^{2+}–TPTZ (blue coloured complex) was measured, by monitoring the alterations in absorbance at 595 nm. A blank of H_2O was used to correct the absorbance and a 1mM ascorbic acid solution was used as a positive control. The differences in the absorbance of the samples were then used to calculate the antioxidant potential values expressed as mmol of antioxidant potential/mg protein.

3.2.6 Quantification of Cysteine-Related Thiolome

The cysteine-related thiolome of liver tissue was obtained by quantifying the total and free total fractions of cysteine (Cys), cysteine-glycine (CysGly) and glutathione (GSH) with high-pressure liquid chromatography (HPLC) with fluorescence detection. Also, the protein-bound fraction of each moiety was calculated by subtracting the total free fraction from the total fraction.

At first, 50 mg of liver tissue in ice-cold phosphate buffer saline 1× (PBS1×) were sonicated at 50% intensity for 10 seconds. The samples were then centrifuged at 13000 g, for 5 minutes, 4°C and supernatant was collected for total and free total fractions measurements (initial volume = 50 µL).

To collect the total fraction, primarily, the sulfhydryl groups were reduced with Tris(2-carboxyethyl) phosphine hydrochloride (TCEP) solution (100 g/L, SigmaAldrich, St. Louis, MO, USA), followed by 30 minutes of incubation at room temperature. For protein precipitation, the samples were treated with a TCA solution (100 g/L, containing 1 mM EDTA), vortexed and centrifuged at 13000 g, 4°C for 10 minutes. To conclude, the sulfhydryl groups were derivatized by transferring 25 µL of the final supernatant to a new tube containing 1.55 M NaOH and $Na_2B_4O_7 \cdot 10H_2O$ (125 mM with 4 mM EDTA, pH 9.5) solutions, and incubated with 7-Fluorobenzofurazan-4-sulfonic acid ammonium salt (SBD-F) solution (1g/L, SigmaAldrich, St. Louis, MO, USA) for 1 hour, at 60°C, protected from the light.

For the total free fraction, the samples were first submitted to the protein precipitation protocol as described above. Subsequently, the resulting supernatant was collected and incubated with the TCEP solution in the same conditions described for the total fraction. Following this incubation, the same derivatization protocol was performed.

To separate the different thiol groups, a reversed-Phase C18 LiChroCART 250-4 column (LiChrospher 100 RP-18, 5 µm, VWR, Radnor, PA, USA) was used, in a column oven at 29°C on isocratic elution mode for 20 min, at a flow rate of 0.8 mL/min. The mobile phase was constituted by a 100 mM acetate buffer (pH 4.5) and methanol (99:1 (v/v)). The RF 10AXL fluorescence detector was used for the detection, setting the excitation and emission wavelengths to 385 and 515 nm, respectively.

3.2.7 Statistical Analysis

The analysis of data was performed using GraphPad Prism Software 8.1.1 (GraphPad Software Inc., San Diego, USA) and data was expressed as mean ± standard error of the mean (SEM). The significance of the results was calculated by the One-way Analysis Variance (ANOVA) with Turkey's or Dunnett's multiple comparison test. Differences were considered significant for $p \leq 0.05$. In immunohistochemical analysis, each point represents the average of two or three pictures from various locations in the liver tissue.

4

RESULTS

4.1 Effects of intermittent hypoxia and hypercaloric diet on insulin sensitivity and glucose tolerance

As expected, and previously described [42], [109], severe CIH and HF diet promoted alterations in insulin sensitivity and glucose tolerance, evaluated through the HOMA-IR index (fig.4.1A) and through the ipGTT (fig 4.2B), respectively.

Obesity increased insulin resistance, increasing the HOMA-IR index by 205.44% (CTL= 6.18±0.907; HF= 18.87±1.917) (Fig. 4.1A). Exposure to CIH protocol increased insulin resistance in both control and obese animals compared to the CTL group by 94.66% (CTL= 6.18±0.907; CIH= 12.02±1.649) and 130.21% (CTL= 6.18±0.907; HFIH= 14.22±2.365), respectively.

In figure 4.2B is depicted the effect of CIH and obesity on glucose excurse curves of the ipGTT (panel on the left) and corresponding areas under the curve (AUC) (panel on the right). Basal glycemia after 16 hours of fasting was slightly higher in the obesity group (CTL = 122.8 ± 13.90 mg/dL; HF =134.9 ±21.73 mg/dL) although this value did not reach statistical significance. CIH in both control and obese groups did not change fasting glycemia. From the glucose excursion curves and from the AUC values it is clear that obesity increased glucose intolerance showing a significant increase of 114.29% in the AUC compared to CTL group (CTL= 21285±2823 $mg.dL^{-1}$. min; HF= 45611±3906 $mg.dL^{-1}$. min). Note also, that the glucose excursion curves exhibited a higher glycemic peak at 15-30 min, denoting a higher insulin secretion to maintain normoglycemia and, that in contrast with control animals, the glycemia values do not recovered after 120 minutes post-injection, denoting an altered post-prandial management of glucose levels. CIH increased glucose intolerance in both controls and obese animals, promoting an increase in the AUC values of 40.66% (p-value= 0.43) and of 138.81%,

respectively (CTL= 21285±2823 mg.dL^{-1}. min; CIH = 29939 mg.dL^{-1}. min; HFIH= 50831±5046 mg.dL^{-1}. min).

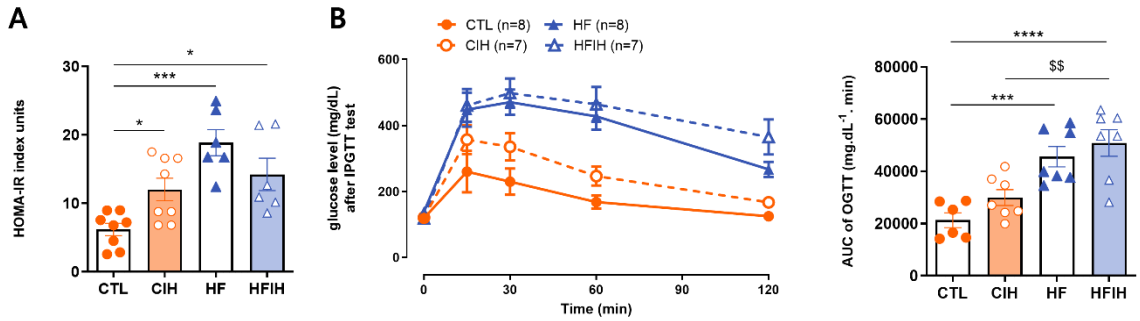

Figure 4.1 — Effects of chronic intermittent hypoxia (CIH) and high-fat diet on the metabolic parameters, insulin sensitivity (A) and glucose tolerance (B). Panel A shows the effect of CIH and diet on insulin sensitivity evaluated using HOMA-IR index. Panel B shows on the left the glucose excursion curves of the intra-peritoneal glucose tolerance test (ipGTT) and on the right the correspondent area under the curve (AUC). Animal groups: CTL- control; CIH – chronic intermittent hypoxia; HF – high-fat diet; HFIH – high-fat plus CIH; Data are presented as means ± SEM of 6-8 animals. One-way ANOVA with Turkey's multiple comparison tests, respectively: * $p < 0.05$, ** $p < 0.01$, *** $p < 0.001$ and **** $p < 0.0001$ compared with control animals.

4.2 Effects of intermittent hypoxia and hypercaloric diet on liver tissue morphology

Figure 4.2 shows the effect of CIH and of high-fat HF diet on lipid deposition and tissue morphology assessed through the staining of H&E staining. It is clear from the observation of figure 4.2B that CIH itself did not alter lipid deposition and tissue morphology in comparison with control animals (fig 4.2A). Furthermore, and as expected, the animals fed with a high-fat diet (fig.4.2C) exhibited an increased the number of lipid droplets in the liver, an effect that was exacerbated in obese animals submitted to CIH (fig.4.2D).

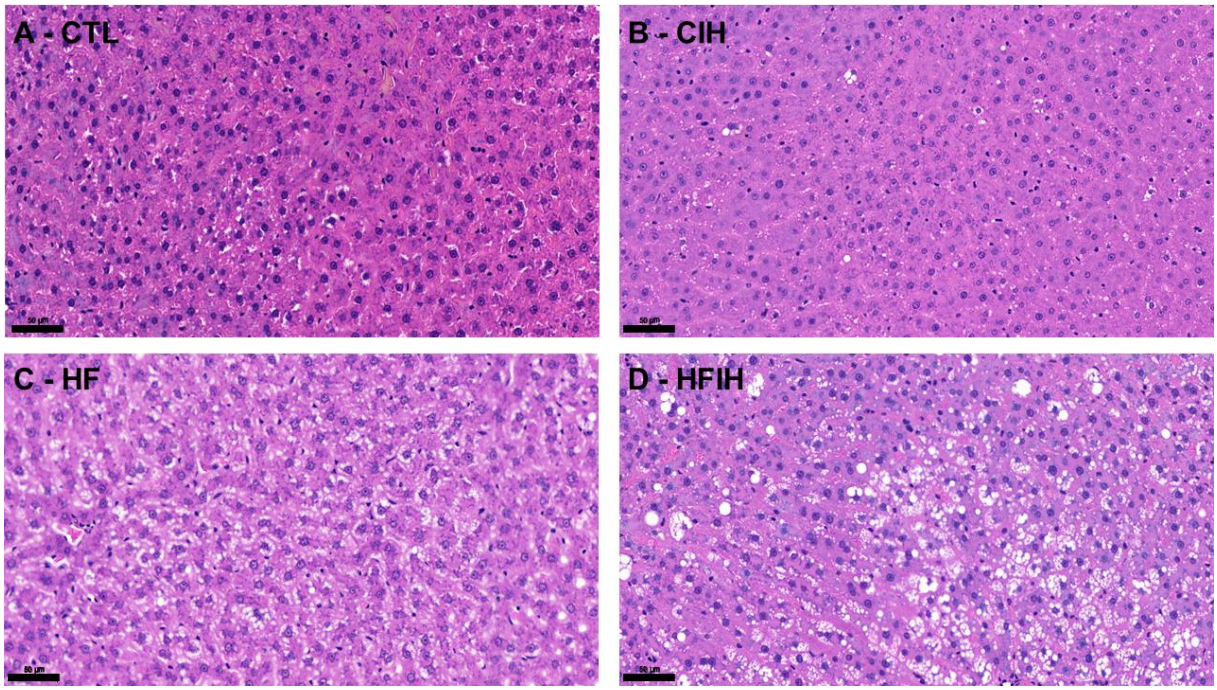

Figure 4.2 — Effects of chronic intermittent hypoxia and high-fat diet on the morphology of liver tissue. Panels A, B, and C correspond to representative images of H&E staining from CTL, CIH, HF and HFIH animals, respectively. Visual analysis of H&E staining shows an increase in lipid deposition in the HF group, which is aggravated by exposure to chronic intermittent hypoxia. CTL- control; CIH – chronic intermittent hypoxia; HF – high-fat diet; HFIH – high-fat plus CIH. Scale bar 50 μm.

4.3 Effects of intermittent hypoxia and hypercaloric diet on hypoxia markers

The effects of CIH and HF diet on the levels of two hypoxic markers, HIF-1α and HIF-2α, respectively, are displayed in figures 4.3 and 4.4. Representative immunohistochemistry images of each hypoxia marker are shown in figures 4.3A and 4.4A and figures 4.3B and 4.3B demonstrate the corresponding fluorescence intensity quantification.

Surprisingly HF diet consumption did not change the levels of HIF-1α in the liver. CIH increased HIF-1α levels in CTL animals by 22.16% (CTL =35.63±2.502%, CIH =57.48±1.795%), whereas it had a tendency to decrease in HFIH animals (HF= 35.02±3.445%, HFIH=24.67±2.806%; p-value= 0.06).

In contrast, 12 weeks of HF diet promoted a decrease of 9.42% in HIF-2α levels. CIH did not alter the levels of HIF-2α in both CIH and HFIH groups.

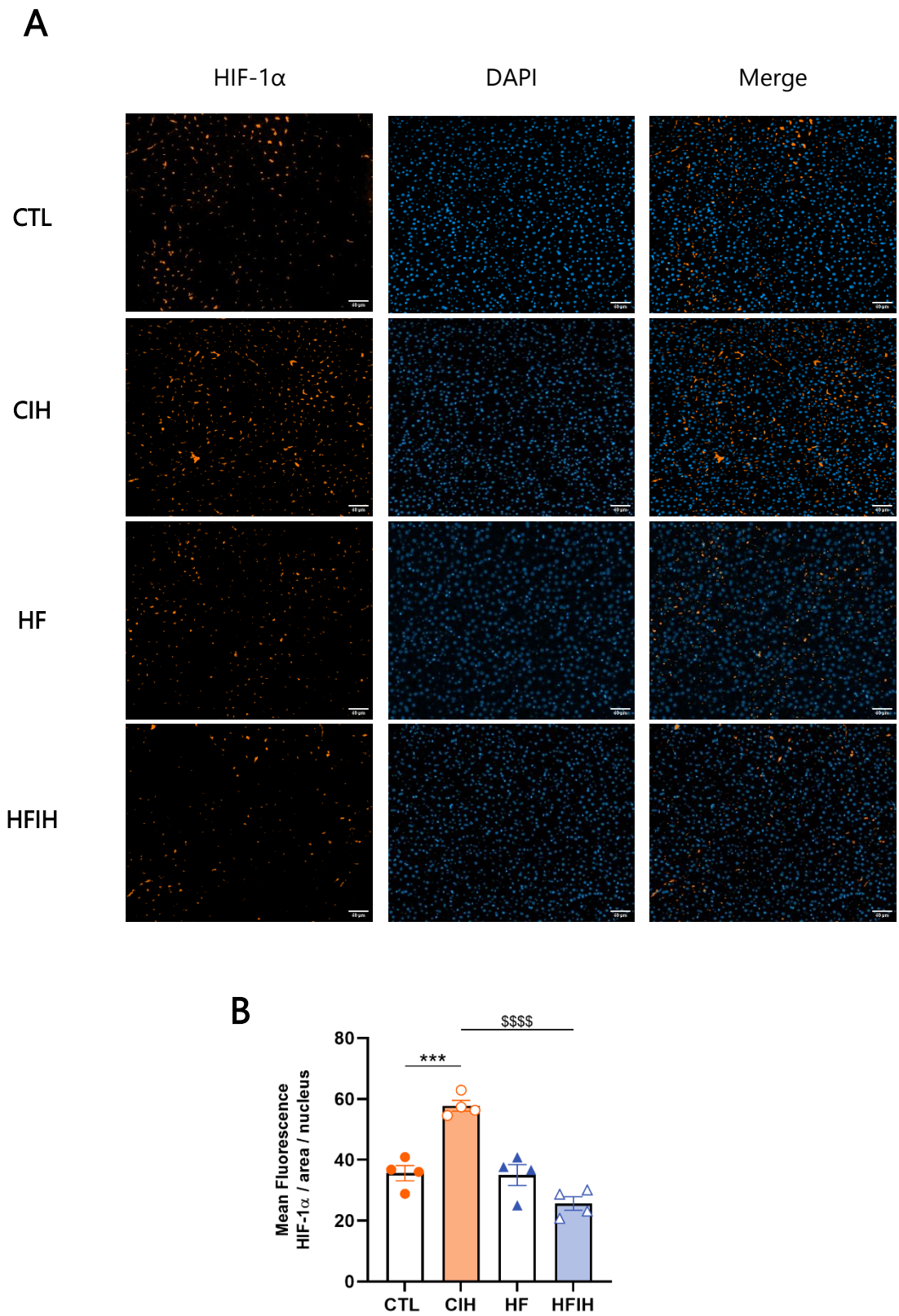

Figure 4.3 — Effects of chronic intermittent hypoxia (CIH) and high-fat (HF) diet on HIF-1α immunolabelling in the liver. A) Representative immunohistochemistry slices from liver labelled with HIF-1α and DAPI. Scale bar 50 µm. B) Mean fluorescence of HIF-1α normalized for the number of nuclei present in the liver slices of each animal. Animal groups: CTL- control; CIH – chronic intermittent hypoxia; HF – high-fat diet; HFIH – high-fat plus CIH; Data are presented as means ± SEM. One-way ANOVA with Turkey's multiple comparison tests, respectively: *** $p < 0.001$ compared with control animals; $$$$ $p < 0.0001$ compared with control animals submitted to the CIH protocol.

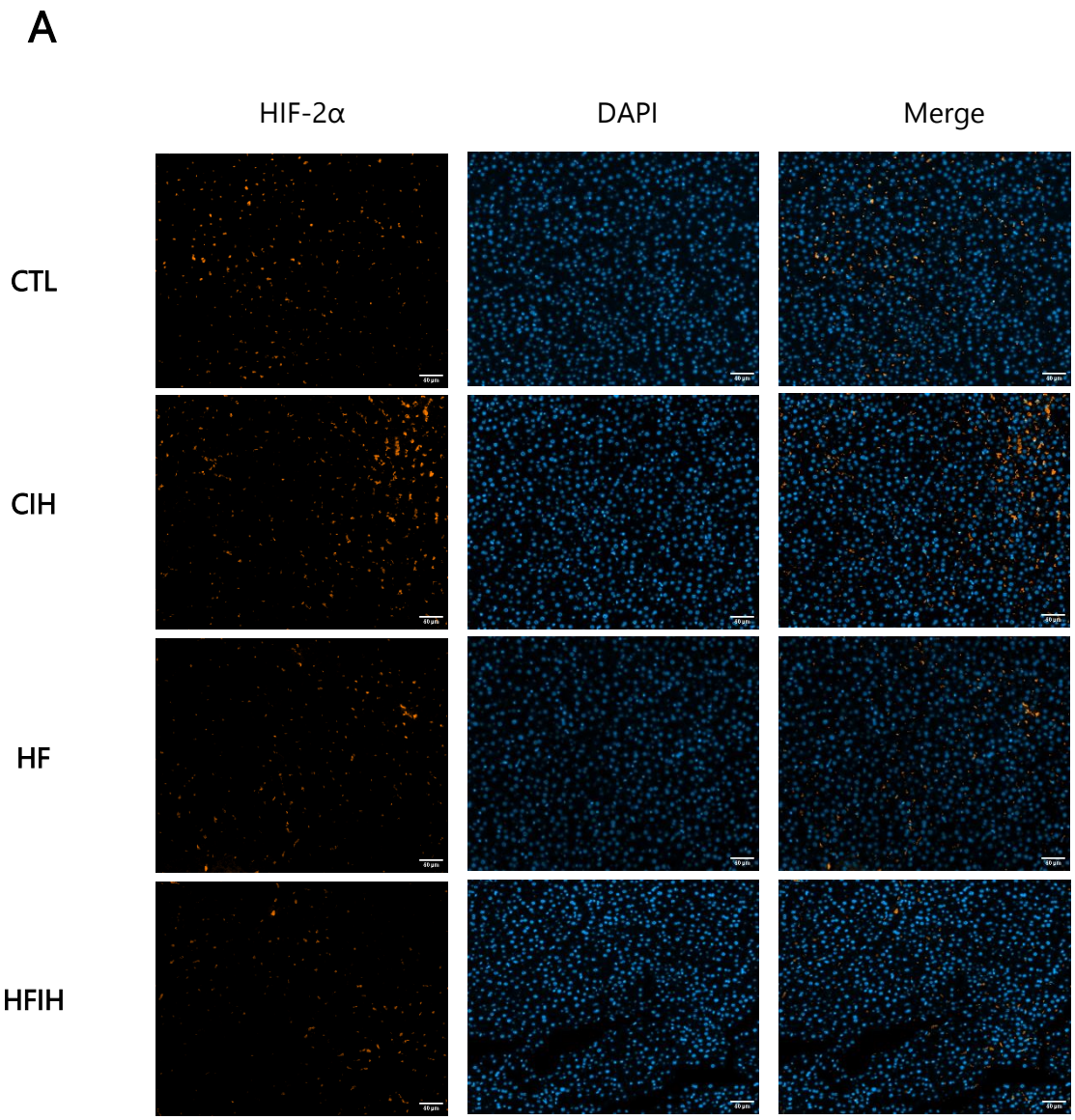

Figure 4.4 — Effect of chronic intermittent hypoxia (CIH) and high-fat (HF) diet on HIF-2α immunolabelling in the liver. A) Representative immunohistochemistry slices from liver labelled with HIF-2α and DAPI. Scale bar 50 µm. B) Mean fluorescence of HIF-2α normalized for the number of nucleus present per area of analysis. Animal groups: CTL- control; CIH – chronic intermittent hypoxia; HF – high-fat diet; HFIH – high-fat plus CIH. Data are presented as means ± SEM. One-way ANOVA with Turkey's multiple comparison tests, respectively: ** $p < 0.01$ compared with control animals; $$$ $p < 0.001$ compared with control animals submitted to the CIH protocol.

4.4 Effects of intermittent hypoxia and hypercaloric diet on proteins involved in insulin signalling pathway

Since CIH and HF diet both led to insulin resistance, we evaluated the levels of various proteins involved in insulin signalling in the liver, namely the IR (fig.4.5A), AKT (fig.4.5B), and IDE (fig.4.5C). The HF diet treatment promoted a significant increase in IR levels by 58.67% (CTL= 100±6.28%, HF= 158.7±23.42%), whereas CIH exposure did not alter the levels of the receptor in both groups.

Since IR phosphorylation, leads to the activation of AKT, which has a central role in the regulation of hepatic glucose and lipid metabolism [68] the levels of AKT were evaluated. No differences were observed between groups in AKT levels in response to CIH and HF diet (Fig. 4.5B).

To determine whether CIH or HF diet affected insulin clearance, the levels of IDE, the principal enzyme responsible for insulin degradation, were analysed. There were no statistical differences between the four groups.

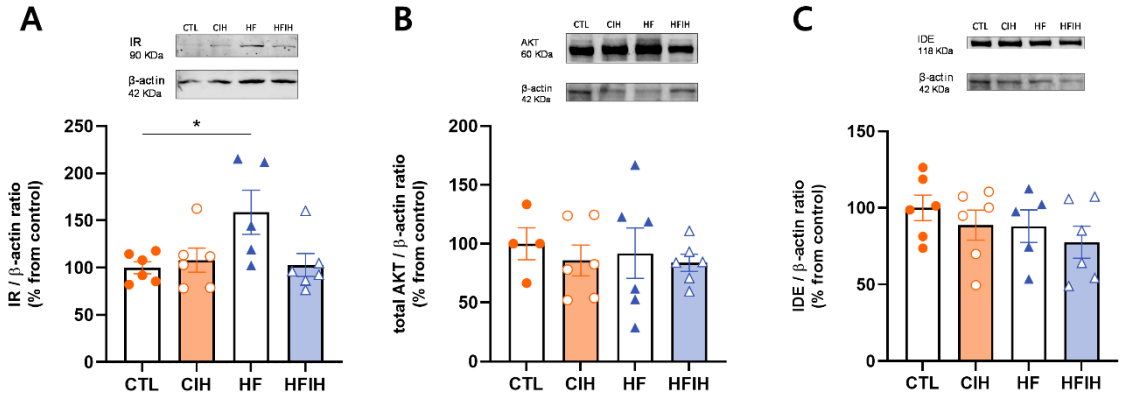

Figure 4.5 — Effects of chronic intermittent hypoxia (CIH) and high-fat (HF) diet on the levels of proteins involved in insulin signalling in the liver. Panels A, B and C depicts the levels of Insulin Receptor (IR- 90 KDa), Protein Kinase B (AKT - 60 KDa) and Insulin Degrading Enzyme (IDE - 118 KDa), respectively. Proteins levels were normalized to the loading control β-actin (42 kDa). Top of the graphs show representative Western Blots for each protein studied. Animal groups: CTL- control; CIH – chronic intermittent hypoxia; HF – high-fat diet; HFIH – high-fat plus CIH. Data are presented as means ± SEM of 6-8 animals. One-way ANOVA with Turkey's multiple comparison tests, respectively: * $p < 0.05$ compared with control animals.

4.5 Effects of intermittent hypoxia and hypercaloric diet on proteins related to glucose metabolism

We also evaluated the impact of CIH and HF diet on liver's Glut2 levels (fig.4.6), one of the major glucose transporters present in this organ, which is known to be altered in type 2 diabetes [123]. CIH increase Glut2 levels by 78.1% (CTL =100±4.01%, CIH =178±32.53%), while HFIH and HF groups had similar levels as the CTL group.

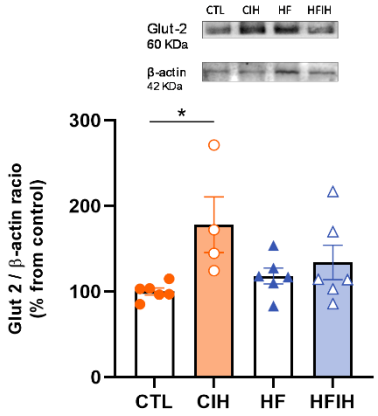

Figure 4.6 — Effects of chronic intermittent hypoxia (CIH) and high-fat (HF) diet on the levels of Glucose Transporter 2 (Glut2 - 60 KDa) in the liver. Protein levels were normalized to the loading control β-actin (42 kDa). Top of the graph show representative Western Blots for the protein studied. Animal groups: CTL- control; CIH – chronic intermittent hypoxia; HF – high-fat diet; HFIH – high-fat plus CIH. Data are presented as means ± SEM of 6-8 animals. One-way ANOVA with Turkey's multiple comparison tests, respectively: * $p < 0.05$ compared with control animals.

4.6 Effects of intermittent hypoxia and hypercaloric diet on mitochondrial biogenesis and activity

To determine whether CIH or HF diet impact mitochondrial biogenesis, we first examined the impact of these stimuli on liver mitochondrial density, as represented in figure 4.7. Figure 4.7A shows representative immunohistochemistry images for each group of animals and figure 4.7B the respective quantification of the mean fluorescence intensity normalized to the number

of nuclei. HF animals exhibited a significant decrease of 12.78% (CTL=37.69±2.337%, HF=24.91±0.841%) in mitochondrial density. CIH did not alter mitochondrial density either in control or in obese animals.

After this, to assess if mitochondrial function was influenced by these stimuli, the levels of OXPHOS complexes were measured in all groups (fig.4.8). In the HF group, complex I levels increased by 105.7% (CTL= 100±13.56, HF= 205.7±22.79%), and there was also tendency to increase in complexes II (0.14) and IV (0.55) . CIH decreased the levels of OXPHOS complexes I, II, III, IV and V by 61.33% (CTL= 100±13.56%, CIH= 38.68±12.04%), 60.75% (CTL= 100±17.67%, CIH= 39.25±10.49%), 47.73% (CTL= 100±28.72%, CIH=178±32.53%), 59.43% (CTL=100±12.46%, CIH=40.58±11.25%), 64.00% (CTL= 100±13.68%, CIH=36.00±7.96%) in control animals and 132.9% (HF=205.7±22.79%, HFIH=72.83±6.55%), 104.90% (HF=151.2±25.14%, HFIH=46.23±4.95%), 41.19% (HF=67.92±8.66%, HFIH=26.73±8.19%), 58.22% (HF=123.7±34.68%, HFIH=65.50±8.90%), 70.19% (HF=105.6±34.95%, HFIH=35.43±9.163%) in HF animals comparing to the respective group not submitted to CIH.

The enzymatic activity of CS and complexes I and II were also assessed, as represented in figures 4.9A, 4.9B and 4.9C, respectively. CS activity, an enzyme present in the citric acid cycle, was used to normalize the enzymatic activity of complexes I and II with the aim to rule out reputed alterations due to different mitochondrial content between the lysates from each group [124]. No differences were observed between the four groups in CS activity (fig.4.9A). The enzymatic activity of both complexes was increased by 142.42% (CTL= $1.96x10^5$±$6.41x10^4$ RFU, CIH= $1.93x10^6$±$8.40x10^5$ RFU) and 149.91% (CTL= 1130±318.4, CIH= 2823±1063 µM DCIP), respectively in complex I (fig.4.9B) and II (fig.4.9C), when control animals were exposed to CIH protocol. Furthermore, in the HFIH group, this trend did not occur in both complexes, and in complex II the enzymatic activity was lower than CTL group.

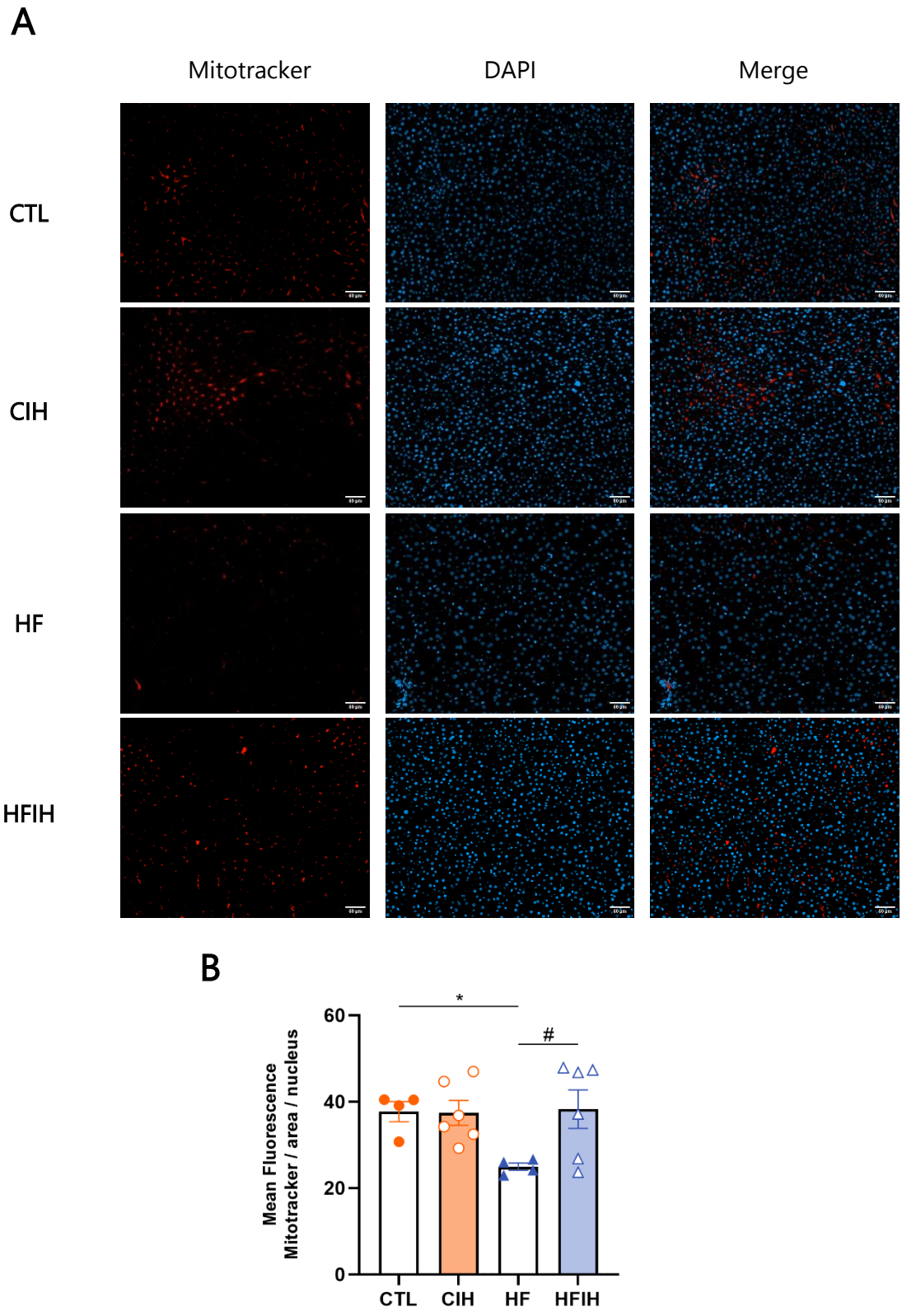

Figure 4.7 — Effects of chronic intermittent hypoxia (CIH) and high-fat (HF) diet on mitochondrial density immunolabelling in the liver. A — Representative immunohistochemistry slices from liver labelled with Mitotracker and DAPI. Scale bar 50 µm. B — Mean fluorescence of Mitotracker normalized for the number of nucleus present per area of analysis. Animal groups: CTL- control; CIH – chronic intermittent hypoxia; HF – high-fat diet; HFIH – high-fat plus CIH. Data are presented as means ± SEM. One-way ANOVA with Dunnett's multiple comparison tests, respectively: ** $p < 0.01$ compared with control animals; # $p < 0.05$ compared with obese animals.

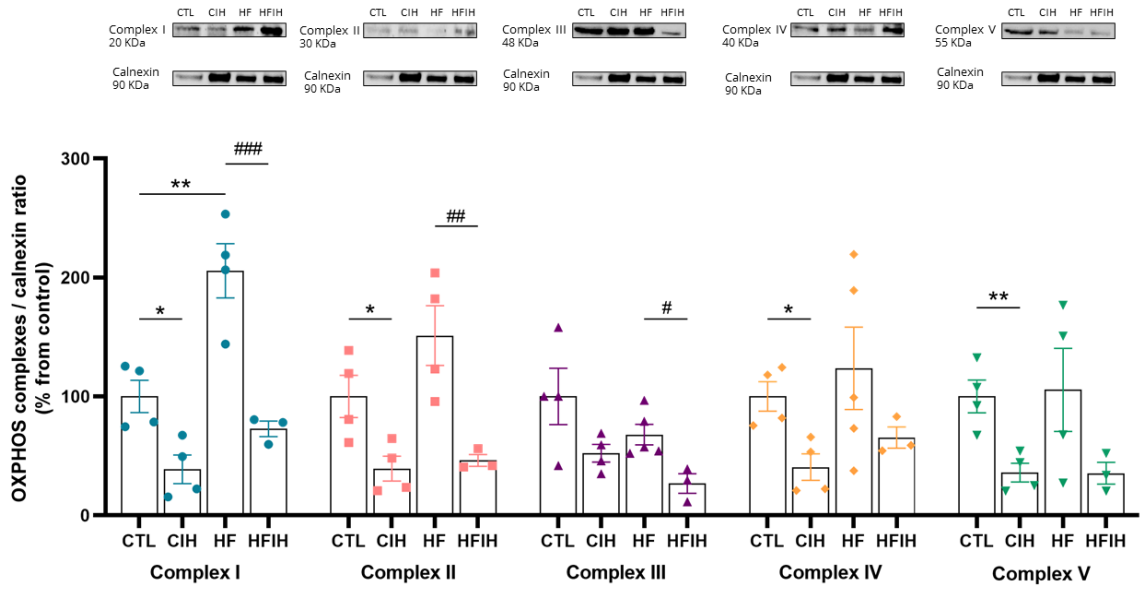

Figure 4.8 — Effects of chronic intermittent hypoxia (CIH) and high-fat (HF) diet on the levels of oxidative phosphorylation complexes (OXPHOS) in the liver. The graph depicts the levels of Complex I (20 KDa), II (30 KDa), III (48 KDa), IV (40 KDa) and V (55 KDa). Proteins levels were normalized to the loading control Calnexin (90 KDa). Top of the graphs show representative Western Blots for each protein studied. Animal groups: CTL- control; HF – high-fat diet; CIH – chronic intermittent hypoxia; HFIH – high-fat plus CIH. Data are presented as means ± SEM of 6-8 animals. One-way ANOVA with Turkey's multiple comparison tests, respectively: * $p < 0.05$ and ** $p < 0.01$ compared with control animals; # $p < 0.05$, ## $p < 0.01$ and ### $p < 0.001$ compared with HF animals.

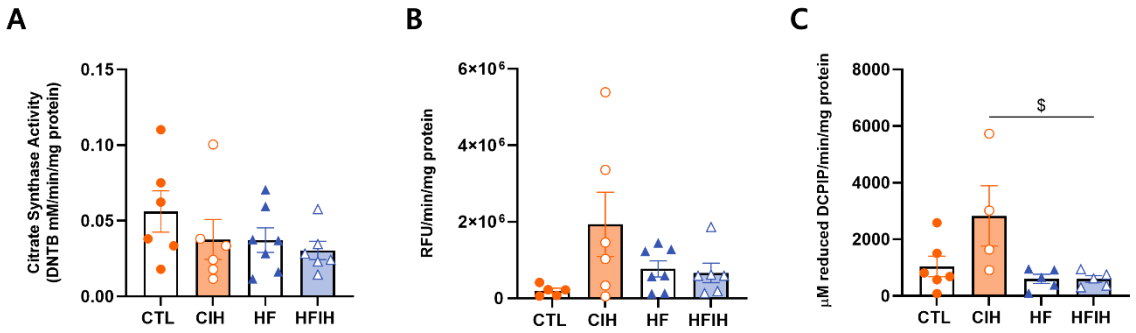

Figure 4.9 — Effects of chronic intermittent hypoxia (CIH) and high-fat (HF) diet on the activity of citrate synthase (A) Mitochondrial Complexes I (panel B) and II (panel C) activities. The enzymatic activity of each complex was normalized by Citrate Synthase activity. Animal groups: CTL- control; CIH – chronic intermittent hypoxia; HF – high-fat diet; HFIH – high-fat plus CIH. Data are presented as means ± SEM of 6-8 animals. One-way ANOVA with Turkey's multiple comparison tests, respectively: $ $p < 0.05$ compared with control animals submitted to CIH.

4.7 Effects of intermittent hypoxia and hypercaloric diet on ROS formation and antioxidant capacity

The labelling with CM-H_2DCFDA was carried out to measure the quantity of ROS in liver tissue, as represented in figure 4.10A. Surprisingly, the HF group presented a decrease of 52.02% (CTL= 2878±365.6, HF= 1381±86.11). This tendency was not modified by CIH, since HFIH group presented a decrease of 43.52% (CIH= 3773±264.0, HFIH= 2131±88.61). Nevertheless, in both groups exposed to CIH the fluorescence intensity was elevated by 31.10% (CTL= 2878±365.6, CIH= 3773±264.0) and 54.27% (HF= 1381±86.11), respectively in CTL and HF animals, showing an increase in ROS in response to hypoxia.

Considering this, we then determine if CIH or HF diet had impact on the tissue's antioxidant capacity. First, the liver's overall antioxidant capacity was estimated using the FRAP assay (fig.4.10B). HF diet decreased significantly the antioxidant capacity by 22.47% (CTL= 16.47±1.202, HF= 12.77±1.014). CIH did not modify the antioxidant capacity neither in controls nor in HF animals (CIH= 17.11±0.698, HFIH= 13.50±1.020).

To make further analysis on antioxidant capacity, the levels of catalase (fig.4.10C) and SOD-1 (fig.4.10D), two antioxidant enzymes were carried out using western blot and cysteine-related thiolome (fig.4.11) was quantified by HPLC. HF diet showed a tendency to increase catalase levels (CTL= 100±4.27%, HF=147.57±22.99%), however without reaching statistical significance (p-value= 0.06). CIH did not modified catalase levels neither in controls nor in HF animals. In relation to SOD-1, HF diet induced a reduction of 30.44% (CTL= 100±5.15%, HF= 69.56±10.20%). CIH lead to a profound reduction of 62.52% in the levels of SOD-1 (CTL= 100±5.15%, CIH= 37.48±10.79), yet the HFIH group did not present the same tendency as the SOD-1 levels were not modified in comparison with the HF group (HFIH= 76.34±9.77%).

CIH protocol produced a slight decrease in all Cys fractions (figs.4.11A, B and C) in CTL animals and only on protein-bounded fraction in HF animals. The HF diet induced a decrease of Cys in all fractions, specifically 30.34% (CTL= 5.580±0.789 μM, HF= 3.887±0214 μM; p-value= 0.060) in the total fraction, 26.79% (CTL= 4.789±0.558 μM, HF= 3.056±0.17 μM; p-value= 0.059) in the free total fraction, and 53.33% (CTL= 0.817±0.160 μM, HF= 0.382±0.085 μM; p-value= 0.044) in the protein-bound fraction. Furthermore, comparing both groups exposed to CIH, the obese animals presented a lower concentration of Cys in all fractions, especially in the protein-bound fraction.

Total and free total fractions of CysGly (figs.4.11D and E) had a significant decrease in the HF group of 15.05% (CTL= 0.111±0.003 μM, HF= 0.094±0.003 μM) and 26.05% (CTL= 0.038±0.003 μM, HF= 0.028±0.002 μM), respectively. Also, this tendency was not altered by intermittent hypoxia in the free total fraction, where the HFIH group presented a decrease of 21.46% (CIH=0.038±0.002 μM, HFIH= 0.030±0.002 μM). In the total fraction were not observed differences between these two groups. In the protein-bound fraction (fig.4.11F), there were no alterations between the four groups.

Regarding GSH levels (figs.4.11G, H and I), in CTL animals the chronic intermittent protocol led to an increase of this thiol in all fractions, although these were not significant. Between the HF groups, we only observed alterations in the protein-bound fraction, where the HFIH group exhibited a slight increase in the concentration of GSH.

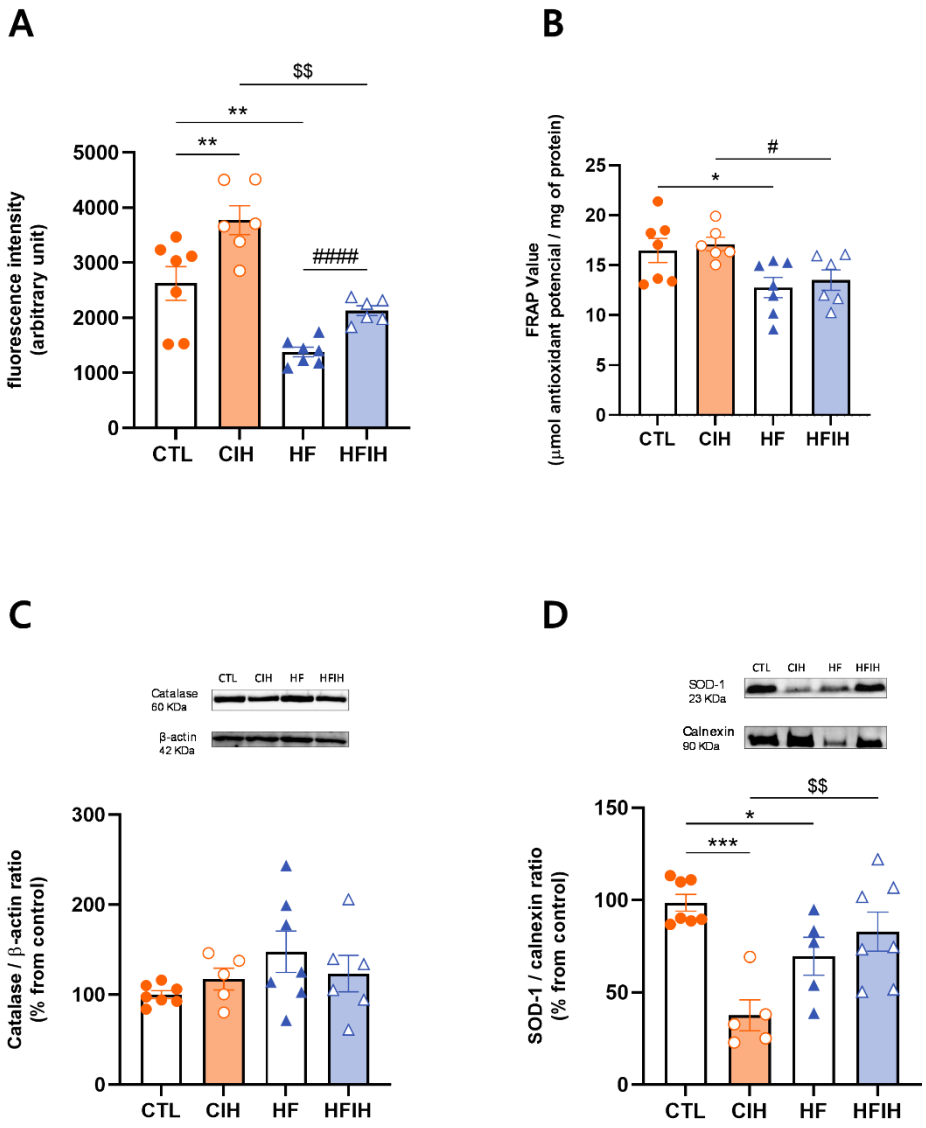

Figure 4.10 — Effects of chronic intermittent hypoxia (CIH) and high-fat (HF) diet on ROS formation and antioxidant capacity. Panel A depicts the intracellular levels of Reactive Oxygen Species (ROS) in the liver by CM-H_2DCFDA labelling. Panel B presents the Ferric reducing-antioxidant power assay (FRAP), used to estimate the antioxidant potential of the tissue in each group. Panels C and D depicts the levels of Catalase (60 KDa) and Superoxide Dismutase 1 (SOD-1 - 23 KDa) respectively. Proteins levels were normalized to the loading control β-actin (42 kDa) and Calnexin (90 KDa). Top of the graphs show representative Western Blots for each protein studied. Animal groups: CTL- control; CIH – chronic intermittent hypoxia; HF – high-fat diet; HFIH – high-fat plus CIH. Data are presented as means ± SEM of 6-8 animals. One-way ANOVA with Turkey's multiple comparison tests and Dunnet's multiple comparison tests respectively: * $p < 0.05$ and ** $p < 0.01$ compared with control animals; # $p < 0.05$ and #### $p < 0.0001$ compared with obese animals; $ $p < 0.05$ and $$ $p < 0.01$ compared with control animals submitted to chronic intermittent hypoxia protocol.

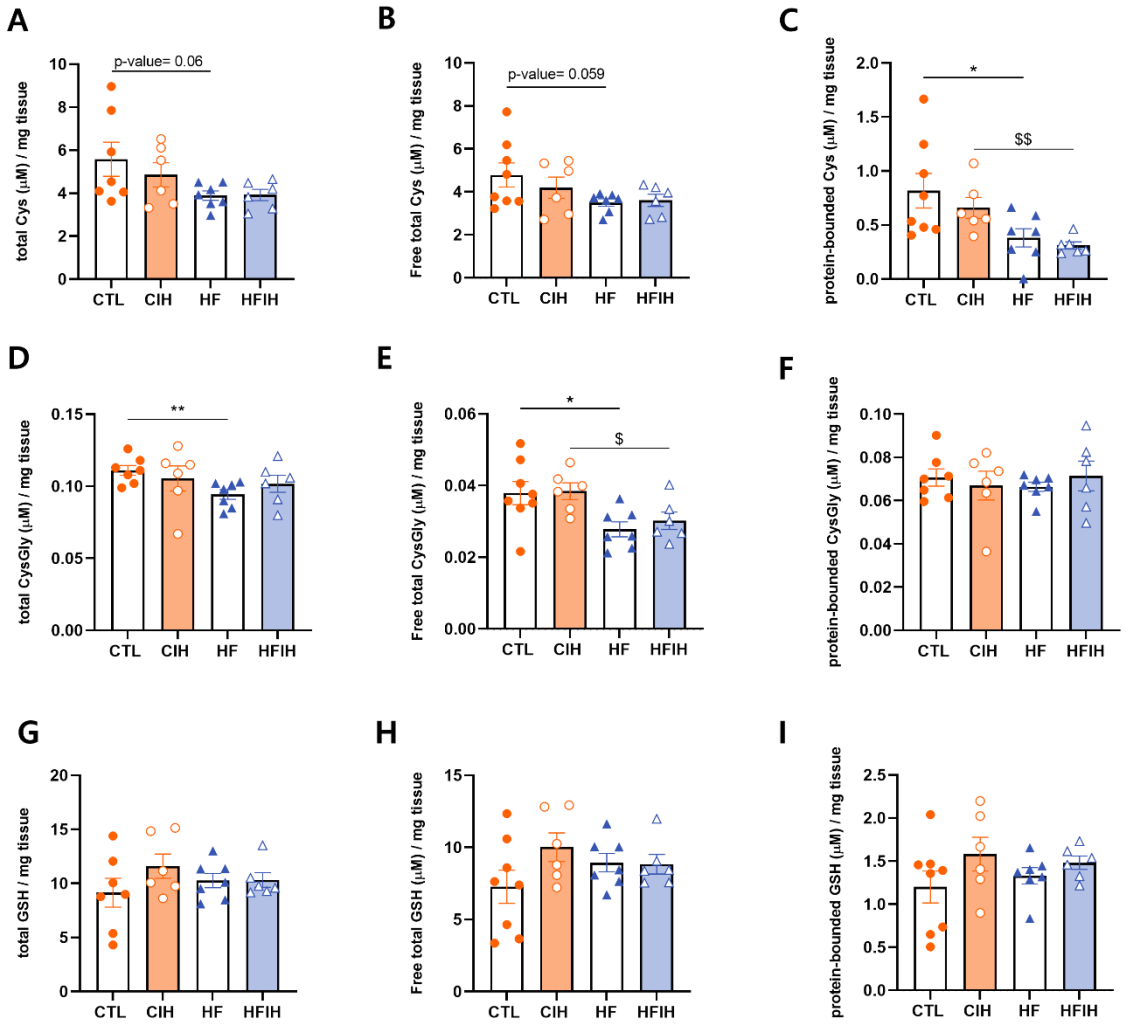

Figure 4.11 — Effects of chronic intermittent hypoxia (CIH) and high-fat (HF) diet on the levels of Cysteine-related thiols in the liver. A — total Cysteine; B — free total cysteine; C — protein-bounded cysteine; D — total Cysteine-Glycine; E — free total Cysteine-Glycine; F — protein-bounded Cysteine-Glycine; G — total Glutathione; H — free total Glutathione; I — Glutathione. Animal groups: CTL- control; CIH – chronic intermittent hypoxia; HF – high-fat diet; HFIH – high-fat plus CIH. Data are presented as means ± SEM of 6-8 animals. One-way ANOVA with Turkey's multiple comparison tests, respectively: * $p < 0.05$ and ** $p < 0.01$ compared with control animals; $ $p < 0.05$ and $$ $p < 0.01$ compared with control animals submitted to the chronic intermittent hypoxia protocol.

4.8 Effects of intermittent hypoxia and hypercaloric diet on pro-inflammatory markers

There is a clear association between insulin resistance and glucose intolerance and a low state of inflammation [20]. Herein we evaluated the effect of CIH and HF diet on some inflammatory markers: Arginase I, NF-κB, IL-6R, IL-1R, TNF-α and TNF-αR (figure 4.12). Neither hypoxia nor high-fat diet treatment altered the levels of Arginase I (fig.4.12A) NF-κB (fig.4.12B) and IL-6R (fig.4.12C).

IL-1R (fig.4.12D) was increased in CTL animals exposed to hypoxia by 22.33% (CTL= 100±3.80%, CIH= 122.3±8.60%), and by 32.65% (CTL= 100±3.80%, HF= 132.7±7.69%) due to high-fat diet consumption. In contrast, exposure to intermittent hypoxia in HF animals led to a slight decrease in IL-1R levels (HF= 132.7±7.69%, HFIH= 125.0±12.90%).

The levels of TNF-α (fig.4.12E) were increased by 45.20% (CTL= 100±7.193%, HF=145.2±13.81%) with the high-fat diet treatment. CIH did not alter this tendency since the HFIH animals presented a 53.30% increase in TNF-α levels (CIH= 87.76±9.334%, HFIH= 141.10±17.57%). Furthermore, CIH had no effect on the levels of this marker within the groups (CTL= 100±7.193%; CIH= 87.76±9.334%; HF=145.2±13.81%; HFIH= 141.10±17.57%).Lastly, only obese animals exposed to a hypoxic environment had altered TNF-αR levels (fig.4.12F), which exhibited a non-significant increase.

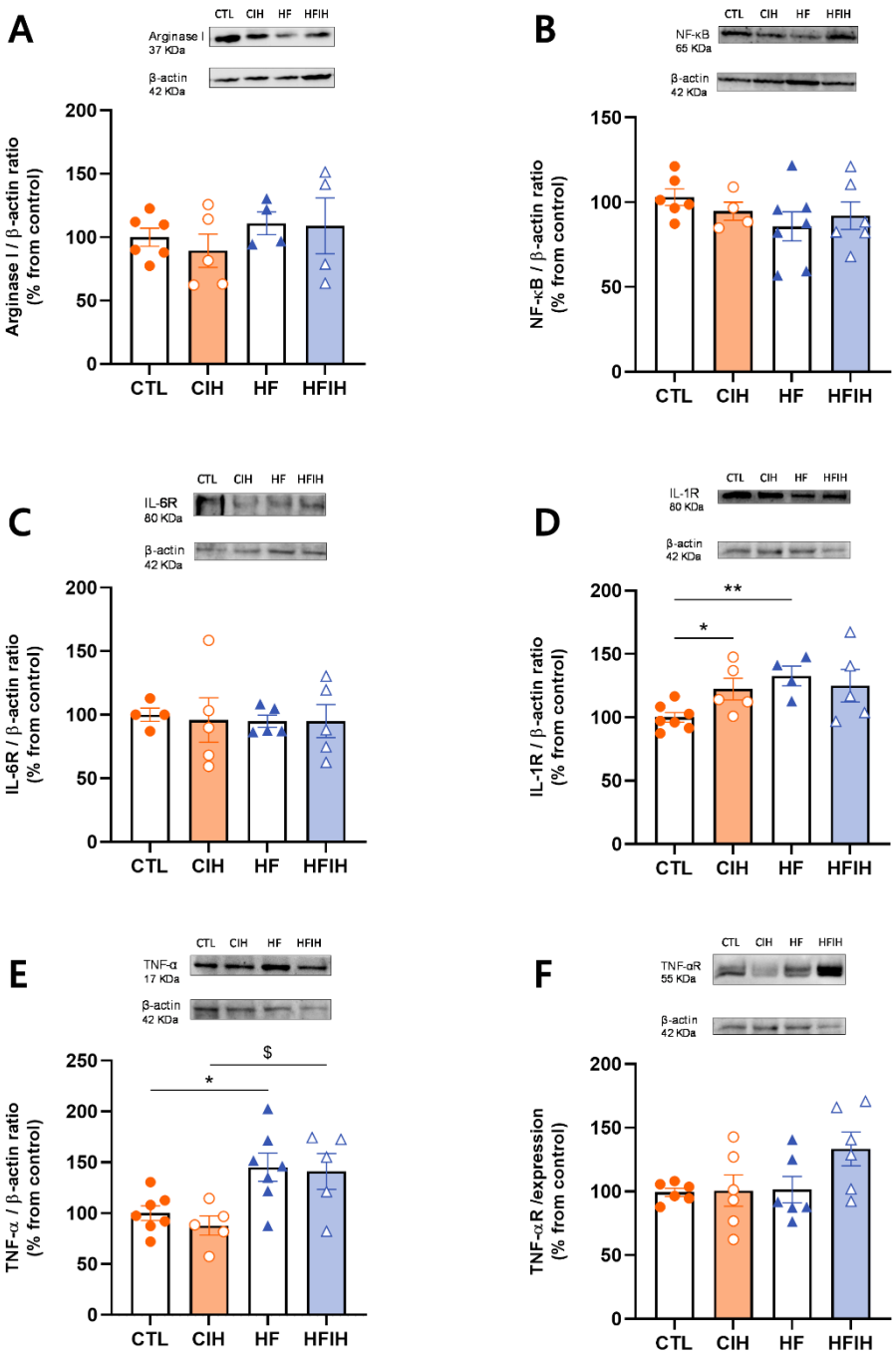

Figure 4.12 — Effects of chronic intermittent hypoxia (CIH) and high-fat (HF) diet on the levels of inflammatory markers in the liver. Panels A, B, C, D, E and F depicts the levels of Arginase I (35 KDa), NF-κB (65 KDa), IL-6 Receptor (IL-6R - 80 KDa), IL-1 Receptor (IL-1R - 80 KDa), Tumour necrosis factor alpha (TNF-α - 17 KDa), and TNF-α Receptor (TNF-αR - 55 KDa), respectively. Proteins levels were normalized to the loading control β-actin (42 kDa). Top of the graphs show representative Western Blots for each protein studied. Animal groups: CTL- control; CIH – chronic intermittent hypoxia; HF – high-fat diet; HFIH – high-fat plus CIH. Data are presented as means ± SEM of 6-8 animals. One-way ANOVA with Turkey's multiple comparison tests, respectively: * $p < 0.05$ and ** $p < 0.01$ compared with control animals; $ $p < 0.05$ compared with control animals submitted to the chronic intermittent hypoxia protocol.

5

DISCUSSION

In the present study, we showed that both hypoxia and HF diet induce insulin resistance and glucose intolerance. We also showed that hypoxia aggravates lipid deposition in the liver tissue of obese animals, and affects differently HIF-1α and HIF-2α levels. Moreover, we showed that CIH and HF diet alter mitochondrial bioenergetics, with intake of HF diet decreasing the mitochondrial density in the liver tissue and CIH leading to a decrease of all OXPHOS complexes levels in both control and obese animals. CIH also tends to increase the enzymatic activity of complexes I and II in the CIH group. Additionally, we found that surprisingly HF diet decreased the levels of ROS in liver tissue, but also decreased the overall liver tissue antioxidant capacity and produced an alteration in the free total fractions of both Cys and CysGly. Hypoxia decreased the levels of SOD-1 and alters in different ways the levels of cysteine-related thiols in the liver. Lastly, CIH affects inflammatory markers in different ways in control and obese rats. Altogether these results indicate that mitochondrial dysfunction and oxidative stress, and the consequent inflammation, are involved in the genesis of CIH-induced dysmetabolism.

5.1 Impact of CIH and HF diet on the metabolic phenotype

Herein, we showed that as expected, the glycemic control, measured *in vivo* by the HOMA-IR and the ipGTT test, is impacted by both CIH and HF diet [109]. HF feeding protocol caused an increase in body weight, as previously shown by Martins and colleagues [109]. Also

as expected, the CIH protocol herein used was also effective in altering glucose homeostasis, promoting both insulin resistance and glucose intolerance [42], [125] (table 5.1).

Table 5.1 - Summary table showing the impact of chronic intermittent hypoxia (CIH) and/or high-fat (HF) diet on metabolic status. Black symbols represent comparisons with the CTL group and red symbols represent comparisons with the HF group

		CIH	HF	HFIH
In vivo	HOMA-IR	↑	↑↑	↑
	IpGTT	=	↑	↑
Ex vivo	IR	=	↑	=
	AKT	=	=	=
	IDE	=	=	=
	Glut 2	↑	=	=
	H&E staining	=	↑	↑↑

Regarding insulin sensitivity, the exposure to severe CIH induced a systemic state of insulin resistance, as shown by an increase in the HOMA-IR index (Figure 4.1A). This is in accordance with the results obtained previously in both animal [42] and human studies [126], [127]. In the HF group, as well as expected, we also observed insulin resistance [128]. Despite this, in the HF animals exposed to CIH (HFIH group), although they also exhibit insulin resistance, this value seems to be a bit smaller probably due to the increase in lipid metabolism induced by CIH and the consequent decrease in adipocyte size, as demonstrated by Martins *et al.* [109], which might improve the animals' insulin sensitivity.

As expected, with the intake of hypercaloric diets and the consequent development of obesity, the animals became glucose intolerant [129], a state that was not worsened by CIH. In addition, based on the values of glycemia for CIH, HF and HFIH groups we can conclude that our experimental model produces a state of prediabetes [42], [130] (Figure 4.1B).

Hepatic steatosis is a state that is associated with obesity and T2D and that was recently associated with OSA [20]. Herein, we showed that hepatic steatosis was increased in the animals fed with the HF diet which is in agreement with the literature [50], [51], and that the exposition to CIH aggravated this phenotype, also as demonstrated in human patients with OSA and obesity [55], [131]. However, CIH itself did not seem to alter hepatic lipid deposition, a result that goes against previous studies with the same or a similar protocol of CIH [42], [93].

In this work, we only performed a qualitative evaluation by visualizing the histological staining of the liver tissue structures, with this evaluation being less robust than the quantitative analysis used in the studies described. Therefore, in our evaluation approach it would be more challenging to detect small changes like those shown in Olea *et al.* [42]. On the other hand, the small number of analysed animals might also have prevented us from reaching to a more meaningful conclusion.

We also evaluated Glut2, the main hepatic glucose transporter in rodents and humans, which was increased by CIH. This is in accordance with the results obtained by different authors [43], [132] where this increase in Glut2 was described to be a compensatory mechanism for the increase in insulin resistance. We also showed that the levels of IR were only increased in obese animals. According to James *et al.* [133], hepatic insulin resistance can be overcome by an increase in insulin secretion. So, the increase of IR levels might be another mechanism activated in conditions of hepatic insulin resistance to augment insulin signalling cascade, which is also affected in a state of insulin resistance. Additionally, since we only measure the total form of IR the ratio between phosphorylated and total forms cannot be calculated and, for this reason, we cannot evaluate the activation of this signalling cascade. Trying to evaluate the effect of insulin in tissues we assessed the insulin clearance, by analysing the levels of IDE, which were not affected by CIH. In the work of Minchenko *et al.* [134], they observed a decrease in the levels of IDE in response to hypoxia. However, this was a model of sustained hypoxia and a cancerous cell line, a type of cell model known to have high rates of glucose use, therefore, a decrease in insulin clearance will promote an increase in insulin availability to promote the use of glucose by these cells.

5.2 Impact of CIH and HF diet in Liver Tissue Hypoxia

Hypoxia is one the major factors contributing to liver and adipose tissue dysfunction in metabolic diseases. Herein we indirectly evaluated hepatic hypoxia by measuring the levels of the hypoxic markers HIF-1α and HIF-2α in this tissue (table 5.2). The levels of HIF-1α were increased in the CIH animals, as previously observed in another study from our group [43]. It was previously described that HIF-1α promotes glycolysis and regulates the expression of glucose transporters in the liver [82], [135]. Therefore, as in the work of Sacramento and colleagues we can speculate that the increase in Glut2 transporters herein observed is due to the

upregulation of hepatic HIF-1α signalling. However, the levels of this hypoxic marker were decreased in the HFIH. Different studies describe the role of HIF-1α in the development of NAFLD [51], [90], and experiments using NAFLD mice models show an increase of HIF-1α levels in the hepatic tissue [136], [137]. Since our animal model is not a true model of NAFLD, we can conclude that, probably, a more severe state of hepatic steatosis and the onset of fatty liver disease are required for the increase of HIF-1α levels. HIF-2α levels were decreased in the HF animals and this tendency was not altered by CIH protocol. Different studies report that hyperglycaemia inhibits the expression and activity of HIFs in different tissues even in conditions of hypoxia, namely pancreatic β-cells and the retina [88], and that HIF-2α is usually activated slower and for longer time [138]. In addition, it should be noted that, even under physiological conditions, the levels of HIF vary between liver regions, being upregulated in perivenous areas where the O_2 concentrations are lower [51], [139]. Therefore, this should be taken into consideration since we cannot determine if the analysed slices were all from similar regions among the four groups.

Table 5.2 - Summary table showing the impact of chronic intermittent hypoxia (CIH) and/or high-fat (HF) diet on hepatic HIF levels. Black symbols represent comparisons with the CTL group and orange symbols represent comparisons with the CIH group.

	CIH	HF	HFIH
HIF - 1α	↑	=	↓
HIF - 2α	=	↓	↓

5.3 Impact of CIH and HF diet on Oxidative Stress

To infer the hepatic oxidative status and the mediated alterations in the antioxidant defences of this tissue, different techniques were performed. The principal alterations are depicted in table 5.3.

The decrease in FRAP values seen herein, accompanied by a decrease on SOD-1 levels of HF and HFIH animals are indicative of oxidative damage which is in agreement with the available literature [42], [140]. Nevertheless, in contrary to the results obtained by Olea *et al.* [42], and Quintero *et al.* [141], we observe a decrease in SOD-1 levels in control animals exposed to CIH. Previous works related with airways exposure to hypoxia and effects on SOD

activity have shown the same result than the one found in the present thesis and speculate that the decrease with hypoxia is consistent with but not unequivocally establish an important role for SOD in protecting against cellular O_2 toxicity [142].

Moreover, the levels of glutathione, the principal non-enzymatic antioxidant defence, were not altered by CIH, which is in agreement with the study of Quintero *et al.* [141]. Also, HF diet produced an alteration in the free total fractions of both Cys and CysGly, precursors of glutathione. Altogether, this might be indicative of the upregulation of the synthesis of glutathione in conditions of HF diet associated with CIH to prevent the respective reduction under the induced states of cellular stress.

Overall, these results indicate an increase in oxidative stress, especially in response to hypercaloric diets, as would be expected. Despite this, these animal groups present diminished fluorescence intensity in the CM-H_2DCFDA, which presumably indicates a lower ROS concentration. CM-H_2DCFDA assay is an indirect method of ROS concentration, evaluating the development of a fluorescent adduct mediated by the reaction between this molecule and intracellular thiols, which are partially diminished in both HF and HFIH animals as shown in table 5.3, which might explain the obtained results.

Table 5.3 - Summary table showing the impact of chronic intermittent hypoxia (CIH) and/or high-fat (HF) diet on oxidative stress in liver tissue. Black symbols represent comparisons with the CTL group, orange symbols represent comparisons with the CIH group and red symbols represent comparisons with the HF group

		CIH	HF	HFIH
CM-H_2DCFDA		↑	↓	↓ / ↑
FRAP assay		=	↓	↓
Catalase		=	=	=
SOD-1		↓↓	↓	↓
Cys	Total	=	↓	=
	Free total	=	↓	=
	protein-bound	=	↓	↓
Cys-Gly	Total	=	↓	=
	Free total	=	↓	↓
	protein-bound	=	=	=
GSH	Total	=	=	=
	Free total	=	=	=
	protein-bound	=	=	=

5.4 Impact of CIH and HF diet on Mitochondrial Dysfunction

Mitochondrial dysfunction is related to the occurrence and development of various chronic liver diseases, including metabolic diseases. Herein we showed that the number of mitochondria in the liver tissue is reduced in response to the HF diet, manifested as a decrease in mitotracker levels. Also, the levels of OXPHOS are reduced in both groups exposed to hypoxia (table 5.4). In addition, we also show that the enzymatic activity of complexes I and II has a tendency to increase in the CIH group (table 5.4).

Chen *et al.* [143] also observed a reduction of mitochondria number in the genioglossus, the largest upper airway dilator muscle whose function is altered in patients with OSA [143]. Also, the increase of FFA, consequent to the increase in hepatic steatosis observed in the HF group, can be contributing to mitochondrial damage and, therefore, to the reduction of mitochondria levels [51]. It is also described that hypoxia induces mitophagy to reduce

mitochondrial ROS production, however, we did not observe any alterations. Since CIH drastically reduced the levels of OXPHOS, probably a compensatory mechanism was activated to prevent this decrease. The decrease of OXPHOS levels in conditions of hypoxia is indicative of mitochondrial damage, probably induced by ROS. This result is in agreement with the available literature [103], [144]. However, it should also be noted that exactly the opposite is also observed by other authors [104]. Regarding the enzymatic activity of the complexes, it is described a reduction of Complex I and II activity under hypoxic conditions [96], [102]. However, these results were obtained in models of sustained hypoxia, so our CIH paradigm might produce the activation by different mechanisms or to compensate for the decrease in the complexes levels and mitochondrial function.

Table 5.4 - Summary table showing the impact of chronic intermittent hypoxia (CIH) and/or high-fat (HF) diet on mitochondrial dysfunction in liver tissue. Black symbols represent comparisons with the CTL group and red symbols represent comparisons with the HF group

		CIH	HF	HFIH
	Mitotracker	=	↓	=
Protein Levels	Complex I	↓	↑↑	↓↓
	Complex II	↓	=	↓↓
	Complex III	=	=	↓
	Complex IV	↓	=	=
	Complex V	↓↓	=	=
Enzymatic activity	Complex I	↑	=	=
	Complex II	↑	=	=

5.5 Impact of CIH and HF diet in Hepatic Inflammation

A low grade of inflammation is known to run with obesity and metabolic dysfunction and liver inflammation is known to have a major role in the genesis and setting of NAFLD [20], [51]. To evaluate the hepatic inflammatory status, the levels of different pro-inflammatory proteins and receptors were evaluated (Table 5.5). Herein, the observed increase in the levels of IL-1R, TNF-αR and TNF-α confirms the inflammatory state within the tissue. The available literature

also describes an increase in the levels of IL-6 [117], however, herein CIH does not seem to produce alterations in the hepatic levels of the receptor for this cytokine. Moreover, we did not find any alteration in arginase I levels, suggesting that the increase in hepatic inflammation is not manifested by changes in this enzyme. Arginase I is expressed in different blood cells such as Kupfer cells and neutrophils, being expressed constitutively in the latter [145]. Arginase I is up-regulated in response to inflammation in Kupfer cells however, in the liver tissue, it is not known if this would trigger higher levels of this marker [146]. It is also described the activation of NF-κB in response to CIH [42], [117]. In this study, we measured the levels of this protein on total tissue lysates, instead of analysing just the nuclear levels of NF-κB, so we could evaluate the impact of our stimuli in the activation of this signalling pathway. Since the different members of NF-κB are continuously expressed and then sequestered in the cytoplasm [147], this is a plausible explanation for the absence of differences between the different groups analysed.

Table 5.5 - Summary table showing the impact of CIH and/or HF diet on the inflammatory status of liver tissue. Black symbols represent comparisons with the CTL group and orange symbols represent comparisons with the CIH group.

	CIH	HF	HFIH
Arginase I	=	=	=
NF-κB	=	=	=
IL-6R	=	=	=
IL-1R	↑	↑	=
TNF-α	=	↑	↑
TNF-αR	=	=	↑

6

Conclusions and Future Perspectives

The relationship between metabolic diseases and OSA is undeniable, however the subsequent mechanism(s) that link them is yet to be clarified. With the increase in prevalence of these disorders, deciphering the mechanisms underlying this relationship are crucial to, ultimately, discover new potential therapeutic targets and develop new therapies to allow the improvement of the metabolic burden of OSA patients.

In the present work, we demonstrated that:

1. CIH promotes the development of insulin resistance and glucose intolerance in lean and obese animal models, which strengthens the already established link between OSA and dysmetabolism.
2. CIH augments the hepatic lipid deposition in a state of obesity, a typical characteristic observed in patients with NAFLD and OSA.
3. CIH is capable to decrease the levels of OXPHOS, tend to increase the enzymatic activity of complexes I and II, possibly as a compensatory mechanism, while HF diet consumption diminishes hepatic mitochondrial density and antioxidant status, which does not seem to be worsened by CIH.
4. Both stimuli mediate inflammation development in this organ. Additionally, these mechanisms can be activated or inhibited by HIF signaling.

Altogether, these results further confirm the link between OSA and dysmetabolism and suggest that mitochondrial dysfunction and oxidative stress, along with the consequent onset of inflammation, might be key factors contributing to the development of this CIH-induced dysmetabolic phenotype.

Nevertheless, a lot of questions remain to be answered and further investigation is needed to discover the exact mechanism leading to this phenotype. It would be interesting to evaluate the ratios between total and phosphorylated forms of AKT and IR to infer the impact of obesity and CIH in insulin signalling pathway. It would also be important to evaluate the levels of enzymes involved in the glycogenesis, gluconeogenesis and glycogenolysis to assess hepatic glucose production and output in our conditions. Since we already evaluated the levels of antioxidant enzymes and OXPHOS complexes, the next step would be to evaluate the impact of CIH and HF diet consumption in the activity of SOD-1, Catalase and the remaining complexes from the ETC. Finally, since lipid peroxidation is a crucial contributor for the development of oxidative stress and inflammation in fatty liver disease, it would be important to infer this issue by evaluating the levels of malonaldehyde.

REFERENCES

[1] M. J. Sateia, "International classification of sleep disorders-third edition highlights and modifications," *Chest*, vol. 146, no. 5, pp. 1387–1394, Nov. 2014, doi: 10.1378/chest.14-0970.

[2] Y. Adir, M. Humbert, and A. Chaouat, "Sleep-related breathing disorders and pulmonary hypertension," *European Respiratory Journal*, vol. 57, no. 1, Jan. 2021, doi: 10.1183/13993003.02258-2020.

[3] A. v. Benjafield *et al.*, "Estimation of the global prevalence and burden of obstructive sleep apnoea: a literature-based analysis," *Lancet Respir Med*, vol. 7, no. 8, pp. 687–698, Aug. 2019, doi: 10.1016/S2213-2600(19)30198-5.

[4] I. Fietze *et al.*, "Prevalence and association analysis of obstructive sleep apnea with gender and age differences – Results of SHIP-Trend," *J Sleep Res*, vol. 28, no. 5, 2019, doi: 10.1111/jsr.12770.

[5] C. v. Senaratna *et al.*, "Prevalence of obstructive sleep apnea in the general population: A systematic review," *Sleep Med Rev*, vol. 34, pp. 70–81, Aug. 2017, doi: 10.1016/J.SMRV.2016.07.002.

[6] L. F. Drager, S. M. Togeiro, V. Y. Polotsky, and G. Lorenzi-Filho, "Obstructive Sleep Apnea: A Cardiometabolic Risk in Obesity and the Metabolic Syndrome," *J Am Coll Cardiol*, vol. 62, no. 7, p. 569, Aug. 2013, doi: 10.1016/J.JACC.2013.05.045.

[7] A. S. Jordan, D. G. McSharry, and A. Malhotra, "Adult obstructive sleep apnoea," *The Lancet*, vol. 383, no. 9918. Elsevier B.V., pp. 736–747, 2014. doi: 10.1016/S0140-6736(13)60734-5.

[8] P. Lévy *et al.*, "Obstructive sleep apnoea syndrome," *Nat Rev Dis Primers*, vol. 1, Jun. 2015, doi: 10.1038/nrdp.2015.15.

[9] D. J. Gottlieb and N. M. Punjabi, "Diagnosis and Management of Obstructive Sleep Apnea: A Review," *JAMA - Journal of the American Medical Association*, vol. 323, no. 14, pp. 1380–1400, Apr. 2020, doi: 10.1001/jama.2020.3514.

[10] S. Savini *et al.*, "Assessment of obstructive sleep apnoea (OSA) in children: An update," *Acta Otorhinolaryngologica Italica*, vol. 39, no. 5. Pacini Editore S.p.A., pp. 289–297, Oct. 01, 2019. doi: 10.14639/0392-100X-N0262.

[11] C. R. Laratta, N. T. Ayas, M. Povitz, and S. R. Pendharkar, "Diagnosis and treatment of obstructive sleep apnea in adults," *CMAJ*, vol. 189, no. 48, pp. E1481–E1488, Dec. 2017, doi: 10.1503/CMAJ.170296/-/DC1.

[12] V. K. Kapur *et al.*, "Clinical Practice Guideline for Diagnostic Testing for Adult Obstructive Sleep Apnea: An American Academy of Sleep Medicine Clinical Practice Guideline," *J Clin Sleep Med*, vol. 13, no. 3, pp. 479–504, 2017, doi: 10.5664/JCSM.6506.

[13] M. R. Zeidler, V. Santiago, J. M. Dzierzewski, M. N. Mitchell, S. Santiago, and J. L. Martin, "Predictors of Obstructive Sleep Apnea on Polysomnography after a Technically Inadequate or Normal Home Sleep Test," *Journal of Clinical Sleep Medicine*, vol. 11, no. 11, pp. 1313–1318, Nov. 2015, doi: 10.5664/JCSM.5194.

[14] N. C. Netzer, R. A. Stoohs, C. M. Netzer, K. Clark, and K. P. Strohl, "Using the Berlin Questionnaire to identify patients at risk for the sleep apnea syndrome," *Ann Intern Med*, vol. 131, no. 7, pp. 485–491, Oct. 1999, doi: 10.7326/0003-4819-131-7-199910050-00002.

[15] M. Nagappa *et al.*, "Validation of the STOP-Bang Questionnaire as a Screening Tool for Obstructive Sleep Apnea among Different Populations: A Systematic Review and Meta-Analysis," *PLoS One*, vol. 10, no. 12, Dec. 2015, doi: 10.1371/JOURNAL.PONE.0143697.

[16] P. Pavwoski and A. V. Shelgikar, "Treatment options for obstructive sleep apnea," *Neurol Clin Pract*, vol. 7, no. 1, p. 77, Feb. 2017, doi: 10.1212/CPJ.0000000000000320.

[17] V. Lavanya, D. Ganapathy, and R. M. Visalakshi, "In the clinic. Obstructive sleep apnea," *Ann Intern Med*, vol. 161, no. 9, pp. 1471–1474, Jul. 2014, doi: 10.7326/0003-4819-161-9-201411040-01005.

[18] M. S. M. Ip, K. S. L. Lam, C. M. Ho, K. W. T. Tsang, and W. Lam, "Serum leptin and vascular risk factors in obstructive sleep apnea," *Chest*, vol. 118, no. 3, pp. 580–586, Sep. 2000, doi: 10.1378/chest.118.3.580.

[19] A. R. Babu, J. Herdegen, L. Fogelfeld, S. Shott, and T. Mazzone, "Type 2 Diabetes, Glycemic Control, and Continuous Positive Airway Pressure in Obstructive Sleep Apnea," *Arch Intern Med*, vol. 165, no. 4, pp. 447–452, Feb. 2005, doi: 10.1001/ARCHINTE.165.4.447.

[20] I. Almendros, Ö. K. Basoglu, S. V. Conde, C. Liguori, and T. Saaresranta, "Metabolic dysfunction in OSA: Is there something new under the sun?," *Journal of Sleep Research*, vol. 31, no. 1. John Wiley and Sons Inc, Feb. 01, 2022. doi: 10.1111/jsr.13418.

[21] M. Li, X. Li, and Y. Lu, "Obstructive Sleep Apnea Syndrome and Metabolic Diseases," */endo Endocrinology*, vol. 159, no. 7, pp. 2670–2675, 2018, doi: 10.1210/en.2018-00248.

[22] "World Health Organization (WHO)." https://www.who.int/ (accessed Nov. 05, 2022).

[23] J. C. Purdy and J. J. Shatzel, "The hematologic consequences of obesity," *Eur J Haematol*, vol. 106, no. 3, pp. 306–319, Mar. 2021, doi: 10.1111/EJH.13560.

[24] M. Blüher, "Obesity: global epidemiology and pathogenesis," *Nature Reviews Endocrinology 2019 15:5*, vol. 15, no. 5, pp. 288–298, Feb. 2019, doi: 10.1038/s41574-019-0176-8.

[25] Y. C. Chooi, C. Ding, and F. Magkos, "The epidemiology of obesity," *Metabolism*, vol. 92, pp. 6–10, Mar. 2019, doi: 10.1016/j.metabol.2018.09.005.

[26] M. R. Bonsignore, W. T. McNicholas, J. M. Montserrat, and J. Eckel, "Adipose tissue in obesity and obstructive sleep apnoea," *Eur Respir J*, vol. 39, no. 3, pp. 746–767, Mar. 2012, doi: 10.1183/09031936.00047010.

[27] "IDF Diabetes Atlas 10th edition," 2021, Accessed: Dec. 04, 2022. [Online]. Available: www.diabetesatlas.org

[28] U. Galicia-Garcia *et al.*, "Pathophysiology of type 2 diabetes mellitus," *International Journal of Molecular Sciences*, vol. 21, no. 17. MDPI AG, pp. 1–34, Sep. 01, 2020. doi: 10.3390/ijms21176275.

[29] R. A. DeFronzo *et al.*, "Type 2 diabetes mellitus," *Nat Rev Dis Primers*, vol. 1, Jul. 2015, doi: 10.1038/nrdp.2015.19.

[30] A. G. Tabák, C. Herder, W. Rathmann, E. J. Brunner, and M. Kivimäki, "Prediabetes: A high-risk state for developing diabetes," *Lancet*, vol. 379, no. 9833, p. 2279, Jun. 2012, doi: 10.1016/S0140-6736(12)60283-9.

[31] S. Chatterjee, K. Khunti, and M. J. Davies, "Type 2 diabetes," *The Lancet*, vol. 389, no. 10085. Lancet Publishing Group, pp. 2239–2251, Jun. 03, 2017. doi: 10.1016/S0140-6736(17)30058-2.

[32] Y. Zheng, S. H. Ley, and F. B. Hu, "Global aetiology and epidemiology of type 2 diabetes mellitus and its complications," *Nat Rev Endocrinol*, vol. 14, no. 2, pp. 88–98, 2018, doi: 10.1038/NRENDO.2017.151.

[33] S. Reutrakul and B. Mokhlesi, "Obstructive Sleep Apnea and Diabetes: A State of the Art Review," *Chest*, vol. 152, no. 5, pp. 1070–1086, Nov. 2017, doi: 10.1016/J.CHEST.2017.05.009.

[34] N. A. Dewan, F. J. Nieto, and V. K. Somers, "Intermittent hypoxemia and OSA: Implications for comorbidities," *Chest*, vol. 147, no. 1, pp. 266–274, Jan. 2015, doi: 10.1378/chest.14-0500.

[35] G. Fahed *et al.*, "Metabolic Syndrome: Updates on Pathophysiology and Management in 2021," *International Journal of Molecular Sciences 2022, Vol. 23, Page 786*, vol. 23, no. 2, p. 786, Jan. 2022, doi: 10.3390/IJMS23020786.

[36] M. G. Saklayen, "The Global Epidemic of the Metabolic Syndrome," *Current Hypertension Reports*, vol. 20, no. 2. Current Medicine Group LLC 1, Feb. 01, 2018. doi: 10.1007/s11906-018-0812-z.

[37] R. H. Eckel, S. M. Grundy, and P. Z. Zimmet, "The metabolic syndrome," *Lancet*, vol. 365, no. 9468, pp. 1415–1428, Apr. 2005, doi: 10.1016/S0140-6736(05)66378-7.

[38] J. P. Girod and D. J. Brotman, "The metabolic syndrome as a vicious cycle: does obesity beget obesity?," *Med Hypotheses*, vol. 60, no. 4, pp. 584–589, Apr. 2003, doi: 10.1016/S0306-9877(03)00053-7.

[39] A. J. Cameron, J. E. Shaw, and P. Z. Zimmet, "The metabolic syndrome: Prevalence in worldwide populations," *Endocrinol Metab Clin North Am*, vol. 33, no. 2, pp. 351–375, Jun. 2004, doi: 10.1016/j.ecl.2004.03.005.

[40] P. B. Nolan, G. Carrick-Ranson, J. W. Stinear, S. A. Reading, and L. C. Dalleck, "Prevalence of metabolic syndrome and metabolic syndrome components in young adults: A pooled analysis," *Prev Med Rep*, vol. 7, pp. 211–215, Sep. 2017, doi: 10.1016/J.PMEDR.2017.07.004.

[41] M. R. Bonsignore, A. L. Borel, E. Machan, and R. Grunstein, "Sleep apnoea and metabolic dysfunction," *European Respiratory Review*, vol. 22, no. 129. pp. 353–364, Oct. 01, 2013. doi: 10.1183/09059180.00003413.

[42] E. Olea *et al.*, "Intermittent hypoxia and diet-induced obesity: effects on oxidative status, sympathetic tone, plasma glucose and insulin levels, and arterial pressure," *J Appl Physiol*, vol. 117, pp. 706–719, 2014, doi: 10.1152/japplphysiol.00454.2014.-Obstructive.

[43] J. F. Sacramento *et al.*, "Insulin resistance is associated with tissue-specific regulation of HIF-1α and HIF-2α during mild chronic intermittent hypoxia," *Respir Physiol Neurobiol*, vol. 228, pp. 30–38, Jul. 2016, doi: 10.1016/j.resp.2016.03.007.

[44] S. V. Conde *et al.*, "Carotid body, insulin and metabolic diseases: Unravelling the links," *Front Physiol*, vol. 5, no. OCT, p. 418, Oct. 2014, doi: 10.3389/FPHYS.2014.00418/TEXT.

[45] K. Riazi *et al.*, "The prevalence and incidence of NAFLD worldwide: a systematic review and meta-analysis," *Lancet Gastroenterol Hepatol*, vol. 7, no. 9, pp. 851–861, Sep. 2022, doi: 10.1016/S2468-1253(22)00165-0.

[46] Z. Younossi *et al.*, "Global burden of NAFLD and NASH: trends, predictions, risk factors and prevention," *Nature Reviews Gastroenterology & Hepatology 2017 15:1*, vol. 15, no. 1, pp. 11–20, Sep. 2017, doi: 10.1038/nrgastro.2017.109.

[47] B. J. Perumpail, M. A. Khan, E. R. Yoo, G. Cholankeril, D. Kim, and A. Ahmed, "Clinical epidemiology and disease burden of nonalcoholic fatty liver disease," *World J Gastroenterol*, vol. 23, no. 47, p. 8263, Dec. 2017, doi: 10.3748/WJG.V23.I47.8263.

[48] E. E. Powell, V. W. S. Wong, and M. Rinella, "Non-alcoholic fatty liver disease," *The Lancet*, vol. 397, no. 10290, pp. 2212–2224, Jun. 2021, doi: 10.1016/S0140-6736(20)32511-3.

[49] J. C. Cohen, J. D. Horton, and H. H. Hobbs, "Human Fatty Liver Disease: Old Questions and New Insights," *Science*, vol. 332, no. 6037, p. 1519, Jun. 2011, doi: 10.1126/SCIENCE.1204265.

[50] S. L. Friedman, B. A. Neuschwander-Tetri, M. Rinella, and A. J. Sanyal, "Mechanisms of NAFLD development and therapeutic strategies," *Nature Medicine 2018 24:7*, vol. 24, no. 7, pp. 908–922, Jul. 2018, doi: 10.1038/s41591-018-0104-9.

[51] M. P. Parikh, N. M. Gupta, and A. J. McCullough, "Obstructive Sleep Apnea and the Liver," *Clinics in Liver Disease*, vol. 23, no. 2. W.B. Saunders, pp. 363–382, May 01, 2019. doi: 10.1016/j.cld.2019.01.001.

[52] L. Montesi, A. Mazzotti, S. Moscatiello, G. Forlani, and G. Marchesini, "Insulin resistance: Mechanism and implications for carcinogenesis and hepatocellular carcinoma in NASH," *Hepatol Int*, vol. 7, no. 2, pp. S814–S822, Dec. 2013, doi: 10.1007/S12072-013-9451-2/METRICS.

[53] S. Jin, S. Jiang, and A. Hu, "Association between obstructive sleep apnea and non-alcoholic fatty liver disease: a systematic review and meta-analysis," *Sleep and Breathing*, vol. 22, no. 3, pp. 841–851, Sep. 2018, doi: 10.1007/S11325-018-1625-7/FIGURES/5.

[54] Y. Ji, Y. Liang, J. C. W. Mak, and M. S. M. Ip, "Obstructive sleep apnea, intermittent hypoxia and non-alcoholic fatty liver disease," *Sleep Med*, vol. 95, pp. 16–28, Jul. 2022, doi: 10.1016/J.SLEEP.2022.04.006.

[55] O. A. Mesarwi, R. Loomba, and A. Malhotra, "Obstructive Sleep Apnea, Hypoxia, and Nonalcoholic Fatty Liver Disease," *Am J Respir Crit Care Med*, vol. 199, no. 7, pp. 830–841, Apr. 2019, doi: 10.1164/RCCM.201806-1109TR.

[56] F. O. Martins and S. V. Conde, "Gender Differences in the Context of Obstructive Sleep Apnea and Metabolic Diseases," *Front Physiol*, vol. 12, Dec. 2021, doi: 10.3389/fphys.2021.792633.

[57] M. Wolosowicz, S. Prokopiuk, and T. W. Kaminski, "Recent Advances in the Treatment of Insulin Resistance Targeting Molecular and Metabolic Pathways: Fighting a Losing Battle?," *Medicina (Lithuania)*, vol. 58, no. 4, Apr. 2022, doi: 10.3390/medicina58040472.

[58] N. Rachdaoui, "Insulin: The friend and the foe in the development of type 2 diabetes mellitus," *International Journal of Molecular Sciences*, vol. 21, no. 5. MDPI AG, pp. 1–21, Mar. 01, 2020. doi: 10.3390/IJMS21051770.

[59] A. R. Saltiel and C. R. Kahn, "Insulin signalling and the regulation of glucose and lipid metabolism," *Nature*, vol. 414, no. 6865, pp. 799–806, Dec. 2001, doi: 10.1038/414799A.

[60] M. S. Rahman *et al.*, "Role of insulin in health and disease: An update," *International Journal of Molecular Sciences*, vol. 22, no. 12. MDPI, Jun. 02, 2021. doi: 10.3390/ijms22126403.

[61] R. A. DeFronzo, "Pathogenesis of type 2 diabetes mellitus," *Medical Clinics of North America*, vol. 88, no. 4, pp. 787–835, Jul. 2004, doi: 10.1016/j.mcna.2004.04.013.

[62] A. R. Saltiel, "Insulin signaling in health and disease," *Journal of Clinical Investigation*, vol. 131, no. 1, Jan. 2021, doi: 10.1172/JCI142241.

[63] J. M. Lizcano and D. R. Alessi, "The insulin signalling pathway," *Curr Biol*, vol. 12, no. 7, Apr. 2002, doi: 10.1016/S0960-9822(02)00777-7.

[64] B. D. Hopkins, M. D. Goncalves, and L. C. Cantley, "Insulin–PI3K signalling: an evolutionarily insulated metabolic driver of cancer," *Nature Reviews Endocrinology*, vol. 16, no. 5. Nature Research, pp. 276–283, May 01, 2020. doi: 10.1038/s41574-020-0329-9.

[65] H. Kim, D. Zhang, Z. Song, X. Tong, and K. Zhang, "Analysis of Insulin Resistance in Nonalcoholic Steatohepatitis," *Methods in Molecular Biology*, vol. 2455, pp. 233–241, 2022, doi: 10.1007/978-1-0716-2128-8_18.

[66] T. M. Batista, N. Haider, and C. R. Kahn, "Defining the underlying defect in insulin action in type 2 diabetes," *Diabetologia*, vol. 64, no. 5. Springer Science and Business Media Deutschland GmbH, pp. 994–1006, May 01, 2021. doi: 10.1007/s00125-021-05415-5.

[67] A. R. Saltiel and J. E. Pessin, *Mechanisms of insulin action*, 1st ed. Springer New York, 2007. doi: 10.1007/978-0-387-72204-7/COVER.

[68] P. M. Titchenell, M. A. Lazar, and M. J. Birnbaum, "Unraveling the Regulation of Hepatic Metabolism by Insulin," *Trends Endocrinol Metab*, vol. 28, no. 7, p. 497, Jul. 2017, doi: 10.1016/J.TEM.2017.03.003.

[69] M. J. Watt, P. M. Miotto, W. De Nardo, and M. K. Montgomery, "The Liver as an Endocrine Organ-Linking NAFLD and Insulin Resistance," *Endocr Rev*, vol. 40, no. 5, pp. 1367–1393, May 2019, doi: 10.1210/ER.2019-00034.

[70] M. C. Petersen and G. I. Shulman, "Mechanisms of Insulin Action and Insulin Resistance," *Physiol Rev*, vol. 98, no. 4, pp. 2133–2223, Oct. 2018, doi: 10.1152/PHYSREV.00063.2017.

[71] C. Gündüz *et al.*, "Obstructive sleep apnoea independently predicts lipid levels: Data from the European Sleep Apnea Database," *Respirology*, vol. 23, no. 12, pp. 1180–1189, Dec. 2018, doi: 10.1111/RESP.13372.

[72] C. Arnaud, T. Bochaton, J. L. Pépin, and E. Belaidi, "Obstructive sleep apnoea and cardiovascular consequences: Pathophysiological mechanisms," *Arch Cardiovasc Dis*, vol. 113, no. 5, pp. 350–358, May 2020, doi: 10.1016/J.ACVD.2020.01.003.

[73] P. I. Aaronson and A. Rocher, "Oxygen Sensing: Physiology and Pathophysiology," *Antioxidants 2022, Vol. 11, Page 1018*, vol. 11, no. 5, p. 1018, May 2022, doi: 10.3390/ANTIOX11051018.

[74] G. L. Wang, B. H. Jiang, E. A. Rue, and G. L. Semenza, "Hypoxia-inducible factor 1 is a basic-helix-loop-helix-PAS heterodimer regulated by cellular O2 tension.," *Proceedings of the National Academy of Sciences*, vol. 92, no. 12, pp. 5510–5514, Jun. 1995, doi: 10.1073/PNAS.92.12.5510.

[75] A. Gabryelska, F. F. Karuga, B. Szmyd, and P. Białasiewicz, "HIF-1α as a Mediator of Insulin Resistance, T2DM, and Its Complications: Potential Links With Obstructive Sleep Apnea," *Front Physiol*, vol. 11, p. 1035, Sep. 2020, doi: 10.3389/FPHYS.2020.01035/BIBTEX.

[76] G. L. Semenza, "Oxygen sensing, hypoxia-inducible factors, and disease pathophysiology," *Annual Review of Pathology: Mechanisms of Disease*, vol. 9, pp. 47–71, 2014, doi: 10.1146/annurev-pathol-012513-104720.

[77] P. Koivunen, R. Serpi, and E. Y. Dimova, "Hypoxia-inducible factor prolyl 4-hydroxylase inhibition in cardiometabolic diseases," *Pharmacological Research*, vol. 114. Academic Press, pp. 265–273, Dec. 01, 2016. doi: 10.1016/j.phrs.2016.11.003.

[78] P. Lee, N. S. Chandel, and M. C. Simon, "Cellular adaptation to hypoxia through hypoxia inducible factors and beyond," *Nature Reviews Molecular Cell Biology*, vol. 21, no. 5. Nature Research, pp. 268–283, May 01, 2020. doi: 10.1038/s41580-020-0227-y.

[79] G. L. Semenza, "Hypoxia-Inducible Factors in Physiology and Medicine," *Cell*, vol. 148, no. 3, pp. 399–408, Feb. 2012, doi: 10.1016/J.CELL.2012.01.021.

[80] S. Lefere, C. Van Steenkiste, X. Verhelst, H. Van Vlierberghe, L. Devisscher, and A. Geerts, "Hypoxia-regulated mechanisms in the pathogenesis of obesity and non-alcoholic fatty liver disease," *Cellular and Molecular Life Sciences*, vol. 73, no. 18, pp. 3419–3431, Sep. 2016, doi: 10.1007/s00018-016-2222-1.

[81] A. Loboda, A. Jozkowicz, and J. Dulak, "HIF-1 versus HIF-2 — Is one more important than the other?," *Vascul Pharmacol*, vol. 56, no. 5–6, pp. 245–251, May 2012, doi: 10.1016/J.VPH.2012.02.006.

[82] E. B. Rankin *et al.*, "Hypoxia-Inducible Factor 2 Regulates Hepatic Lipid Metabolism," *Mol Cell Biol*, vol. 29, no. 16, pp. 4527–4538, Aug. 2009, doi: 10.1128/MCB.00200-09/SUPPL_FILE/200LEGS.ZIP.

[83] J. E. Gunton, "Hypoxia-inducible factors and diabetes," *J Clin Invest*, vol. 130, no. 10, p. 5063, Sep. 2020, doi: 10.1172/JCI137556.

[84] M. S. Nakazawa, B. Keith, and M. C. Simon, "Oxygen availability and metabolic adaptations," *Nat Rev Cancer*, vol. 16, no. 10, pp. 663–673, Sep. 2016, doi: 10.1038/NRC.2016.84.

[85] H. Xie and M. C. Simon, "Oxygen availability and metabolic reprogramming in cancer," *J Biol Chem*, vol. 292, no. 41, pp. 16825–16832, Oct. 2017, doi: 10.1074/JBC.R117.799973.

[86] A. Gabryelska, B. Szmyd, M. Panek, J. Szemraj, P. Kuna, and P. Białasiewicz, "Serum hypoxia–inducible factor–1α protein level as a diagnostic marker of obstructive sleep apnea," *Pol Arch Intern Med*, vol. 130, no. 2, pp. 158–160, Feb. 2020, doi: 10.20452/PAMW.15104.

[87] D. Lu, N. Li, X. Yao, and L. Zhou, "Potential inflammatory markers in obstructive sleep apnea-hypopnea syndrome," *Biomolecules and Biomedicine*, vol. 17, no. 1, pp. 47–53, Feb. 2017, doi: 10.17305/bjbms.2016.1579.

[88] K. Cheng *et al.*, "Hypoxia-inducible factor-1α regulates β cell function in mouse and human islets," *J Clin Invest*, vol. 120, no. 6, pp. 2171–2183, Jun. 2010, doi: 10.1172/JCI35846.

[89] R. A. Stokes *et al.*, "Hypoxia-inducible factor-1α (HIF-1α) potentiates β-cell survival after islet transplantation of human and mouse islets," *Cell Transplant*, vol. 22, no. 2, pp. 259–266, Feb. 2013, doi: 10.3727/096368912X647180/ASSET/IMAGES/LARGE/10.3727_096368912X647180-FIG2.JPEG.

[90] F. J. Gonzalez, C. Xie, and C. Jiang, "The role of hypoxia-inducible factors in metabolic diseases," *Nature Reviews Endocrinology 2018 15:1*, vol. 15, no. 1, pp. 21–32, Oct. 2018, doi: 10.1038/s41574-018-0096-z.

[91] Y. S. Lee *et al.*, "Increased adipocyte O2 consumption triggers HIF-1α, causing inflammation and insulin resistance in obesity," *Cell*, vol. 157, no. 6, pp. 1339–1352, Jun. 2014, doi: 10.1016/J.CELL.2014.05.012.

[92] A. Gileles-Hillel, L. Kheirandish-Gozal, and D. Gozal, "Biological plausibility linking sleep apnoea and metabolic dysfunction," *Nat Rev Endocrinol*, vol. 12, no. 5, pp. 290–298, May 2016, doi: 10.1038/nrendo.2016.22.

[93] J. Li *et al.*, "Intermittent Hypoxia Induces Hyperlipidemia in Lean Mice," *Circ Res*, vol. 97, no. 7, pp. 698–706, Sep. 2005, doi: 10.1161/01.RES.0000183879.60089.A9.

[94] G. B. Waypa, K. A. Smith, and P. T. Schumacker, "O2 sensing, mitochondria and ROS signaling: The fog is lifting," *Mol Aspects Med*, vol. 47–48, pp. 76–89, Feb. 2016, doi: 10.1016/j.mam.2016.01.002.

[95] C. Auger, A. Alhasawi, M. Contavadoo, and V. D. Appanna, "Dysfunctional mitochondrial bioenergetics and the pathogenesis of hepatic disorders," *Front Cell Dev Biol*, vol. 3, no. JUN, Jun. 2015, doi: 10.3389/fcell.2015.00040.

[96] D. C. Fuhrmann and B. Brüne, "Mitochondrial composition and function under the control of hypoxia," *Redox Biol*, vol. 12, pp. 208–215, Aug. 2017, doi: 10.1016/j.redox.2017.02.012.

[97] J. Lemire, R. Mailloux, S. Puiseux-Dao, and V. D. Appanna, "Aluminum-induced defective mitochondrial metabolism perturbs cytoskeletal dynamics in human astrocytoma cells," *J Neurosci Res*, vol. 87, no. 6, pp. 1474–1483, May 2009, doi: 10.1002/JNR.21965.

[98] J. Lemire, R. Mailloux, R. Darwich, C. Auger, and V. D. Appanna, "The disruption of L-carnitine metabolism by aluminum toxicity and oxidative stress promotes dyslipidemia in human astrocytic and hepatic cells," *Toxicol Lett*, vol. 203, no. 3, pp. 219–226, Jun. 2011, doi: 10.1016/J.TOXLET.2011.03.019.

[99] O. A. Deshpande and S. S. Mohiuddin, "Biochemistry, Oxidative Phosphorylation - StatPearls - NCBI Bookshelf," Aug. 01, 2022. https://www.ncbi.nlm.nih.gov/books/NBK553192/ (accessed Dec. 06, 2022).

[100] J. A. Letts and L. A. Sazanov, "Clarifying the supercomplex: the higher-order organization of the mitochondrial electron transport chain," *Nature Structural & Molecular Biology 2017 24:10*, vol. 24, no. 10, pp. 800–808, Oct. 2017, doi: 10.1038/nsmb.3460.

[101] H. Lodish *et al.*, *Molecular Cell Biology*, 7th edition. Macmillan higher education, 2013.

[102] D. Tello *et al.*, "Induction of the mitochondrial NDUFA4L2 protein by HIF-1α decreases oxygen consumption by inhibiting Complex I activity," *Cell Metab*, vol. 14, no. 6, pp. 768–779, Dec. 2011, doi: 10.1016/J.CMET.2011.10.008.

[103] S. Y. Chan, Y. Y. Zhang, C. Hemann, C. E. Mahoney, J. L. Zweier, and J. Loscalzo, "MicroRNA-210 controls mitochondrial metabolism during hypoxia by repressing the iron-sulfur cluster assembly proteins ISCU1/2," *Cell Metab*, vol. 10, no. 4, pp. 273–284, Oct. 2009, doi: 10.1016/J.CMET.2009.08.015.

[104] J. Gaucher *et al.*, "Intermittent Hypoxia Rewires the Liver Transcriptome and Fires up Fatty Acids Usage for Mitochondrial Respiration," *Front Med (Lausanne)*, vol. 9, p. 257, Feb. 2022, doi: 10.3389/FMED.2022.829979/BIBTEX.

[105] H. Cichoz-Lach and A. Michalak, "Oxidative stress as a crucial factor in liver diseases," *World J Gastroenterol*, vol. 20, no. 25, pp. 8082–8091, 2014, doi: 10.3748/WJG.V20.I25.8082.

[106] R. Rezzani and C. Franco, "Liver, oxidative stress and metabolic syndromes," *Nutrients*, vol. 13, no. 2. MDPI AG, pp. 1–4, Feb. 01, 2021. doi: 10.3390/nu13020301.

[107] K. Ramar and S. M. Caples, "Vascular changes, cardiovascular disease and obstructive sleep apnea," *Future Cardiol*, vol. 7, no. 2, pp. 241–249, Mar. 2011, doi: 10.2217/FCA.10.123.

[108] A. Gileles-Hillel *et al.*, "Prolonged Exposures to Intermittent Hypoxia Promote Visceral White Adipose Tissue Inflammation in a Murine Model of Severe Sleep Apnea: Effect of Normoxic Recovery," *Sleep*, vol. 40, no. 3, Mar. 2017, doi: 10.1093/SLEEP/ZSW074.

[109] F. O. Martins *et al.*, "Chronic intermittent hypoxia induces early-stage metabolic dysfunction independently of adipose tissue deregulation," *Antioxidants*, vol. 10, no. 8, Aug. 2021, doi: 10.3390/antiox10081233.

[110] L. Lavie, "Oxidative stress in obstructive sleep apnea and intermittent hypoxia--revisited--the bad ugly and good: implications to the heart and brain," *Sleep Med Rev*, vol. 20, pp. 27–45, Apr. 2015, doi: 10.1016/J.SMRV.2014.07.003.

[111] H. A. Hassan, "Oxidative Stress as a Crucial Factor in Liver Associated Disorders: Potential Therapeutic Effect of Antioxidants," *The Liver: Oxidative Stress and Dietary Antioxidants*, pp. 121–130, Jan. 2018, doi: 10.1016/B978-0-12-803951-9.00011-2.

[112] M. P. Murphy, "How mitochondria produce reactive oxygen species," *Biochem J*, vol. 417, no. 1, pp. 1–13, Jan. 2009, doi: 10.1042/BJ20081386.

[113] L. Conde de la Rosa, L. Goicoechea, S. Torres, C. Garcia-Ruiz, and J. C. Fernandez-Checa, "Role of Oxidative Stress in Liver Disorders," *Livers*, vol. 2, no. 4, pp. 283–314, Oct. 2022, doi: 10.3390/LIVERS2040023/S1.

[114] R. Pamplona and D. Costantini, "Molecular and structural antioxidant defenses against oxidative stress in animals," *Am J Physiol Regul Integr Comp Physiol*, vol. 301, no. 4, Oct. 2011, doi: 10.1152/AJPREGU.00034.2011.

[115] J. D. Hayes and A. T. Dinkova-Kostova, "The Nrf2 regulatory network provides an interface between redox and intermediary metabolism," *Trends Biochem Sci*, vol. 39, no. 4, pp. 199–218, 2014, doi: 10.1016/J.TIBS.2014.02.002.

[116] A. N. Vgontzas, E. O. Bixler, and G. P. Chrousos, "Metabolic disturbances in obesity versus sleep apnoea: the importance of visceral obesity and insulin resistance," *J Intern Med*, vol. 254, no. 1, pp. 32–44, Jul. 2003, doi: 10.1046/J.1365-2796.2003.01177.X.

[117] A. M. Murphy *et al.*, "Intermittent hypoxia in obstructive sleep apnoea mediates insulin resistance through adipose tissue inflammation," *European Respiratory Journal*, vol. 49, no. 4, Apr. 2017, doi: 10.1183/13993003.01731-2016.

[118] E. P. Cummins, C. E. Keogh, D. Crean, and C. T. Taylor, "The role of HIF in immunity and inflammation," *Mol Aspects Med*, vol. 47–48, pp. 24–34, Feb. 2016, doi: 10.1016/J.MAM.2015.12.004.

[119] M. C. Gonzalez-Martín *et al.*, "Carotid body function and ventilatory responses in intermittent hypoxia. evidence for anomalous brainstem integration of arterial chemoreceptor input," *J Cell Physiol*, vol. 226, no. 8, pp. 1961–1969, Aug. 2011, doi: 10.1002/jcp.22528.

[120] D. R. Matthews, J. P. Hosker, A. S. Rudenski, B. A. Naylor, D. F. Treacher, and R. C. Turner, "Homeostasis model assessment: insulin resistance and beta-cell function from fasting plasma glucose and insulin concentrations in man," *Diabetologia*, vol. 28, no. 7, pp. 412–419, Jul. 1985, doi: 10.1007/BF00280883.

[121] "Fiji app for ImageJ." https://imagej.net/software/fiji/

[122] I. F. F. Benzie and J. J. Strain, "The Ferric Reducing Ability of Plasma (FRAP) as a Measure of '"Antioxidant Power"': The FRAP Assay," 1996.

[123] A. Chadt and H. Al-Hasani, "Glucose transporters in adipose tissue, liver, and skeletal muscle in metabolic health and disease," *Pflugers Archiv*, vol. 472, no. 9, p. 1273, Sep. 2020, doi: 10.1007/S00424-020-02417-X.

[124] V. F. Monteiro-Cardoso, A. M. Silva, M. M. Oliveira, F. Peixoto, and R. A. Videira, "Membrane lipid profile alterations are associated with the metabolic adaptation of the Caco-2 cells to aglycemic nutritional condition," *J Bioenerg Biomembr*, vol. 46, no. 1, pp. 45–57, Feb. 2014, doi: 10.1007/s10863-013-9531-y.

[125] N. R. Prabhakar and G. L. Semenza, "Adaptive and maladaptive cardiorespiratory responses to continuous and intermittent hypoxia mediated by hypoxia-inducible factors 1 and 2," *Physiol Rev*, vol. 92, no. 3, pp. 967–1003, 2012, doi: 10.1152/PHYSREV.00030.2011/ASSET/IMAGES/LARGE/Z9J0031226260014.JPEG.

[126] N. M. Punjabi and B. A. Beamer, "Alterations in Glucose Disposal in Sleep-disordered Breathing," *https://doi.org/10.1164/rccm.200809-1392OC*, vol. 179, no. 3, pp. 235–240, Dec. 2012, doi: 10.1164/RCCM.200809-1392OC.

[127] M. Louis and N. M. Punjabi, "Effects of acute intermittent hypoxia on glucose metabolism in awake healthy volunteers," *J Appl Physiol (1985)*, vol. 106, no. 5, pp. 1538–1544, May 2009, doi: 10.1152/JAPPLPHYSIOL.91523.2008.

[128] B. F. Melo *et al.*, "Evaluating the Impact of Different Hypercaloric Diets on Weight Gain, Insulin Resistance, Glucose Intolerance, and its Comorbidities in Rats," *Nutrients 2019, Vol. 11, Page 1197*, vol. 11, no. 6, p. 1197, May 2019, doi: 10.3390/NU11061197.

[129] X. Tian *et al.*, "Palmatine ameliorates high fat diet induced impaired glucose tolerance," *Biol Res*, vol. 53, no. 1, Sep. 2020, doi: 10.1186/S40659-020-00308-0.

[130] S. V. Ivanov *et al.*, "Low molecular weight NGF mimetic GK-2 normalizes the parameters of glucose and lipid metabolism and exhibits a hepatoprotective effect on a prediabetes model in obese Wistar rats," *Clin Exp Pharmacol Physiol*, vol. 49, no. 10, pp. 1116–1125, Oct. 2022, doi: 10.1111/1440-1681.13693.

[131] J. Aron-Wisnewsky *et al.*, "Chronic intermittent hypoxia is a major trigger for non-alcoholic fatty liver disease in morbid obese," *J Hepatol*, vol. 56, no. 1, pp. 225–233, Jan. 2012, doi: 10.1016/j.jhep.2011.04.022.

[132] J. Marks, N. J. C. Carvou, E. S. Debnam, S. K. Srai, and R. J. Unwin, "Diabetes increases facilitative glucose uptake and GLUT2 expression at the rat proximal tubule brush border membrane," *J Physiol*, vol. 553, no. Pt 1, pp. 137–145, Nov. 2003, doi: 10.1113/JPHYSIOL.2003.046268.

[133] D. E. James, J. Stöckli, and M. J. Birnbaum, "The aetiology and molecular landscape of insulin resistance," *Nat Rev Mol Cell Biol*, vol. 22, no. 11, pp. 751–771, Nov. 2021, doi: 10.1038/s41580-021-00390-6.

[134] D. O. Minchenko *et al.*, "Expression of IDE and PITRM1 genes in ERN1 knockdown U87 glioma cells: Effect of hypoxia and glucose deprivation," *Endocr Regul*, vol. 54, no. 3, pp. 183–195, Jul. 2020, doi: 10.2478/enr-2020-0021.

[135] G. L. Semenza, P. H. Roth, H. M. Fang, and G. L. Wang, "Transcriptional regulation of genes encoding glycolytic enzymes by hypoxia-inducible factor 1.," *Journal of Biological*

Chemistry, vol. 269, no. 38, pp. 23757–23763, Sep. 1994, doi: 10.1016/S0021-9258(17)31580-6.

[136] O. A. Mesarwi *et al.*, "Hepatocyte HIF-1 and Intermittent Hypoxia Independently Impact Liver Fibrosis in Murine Nonalcoholic Fatty Liver Disease," *Am J Respir Cell Mol Biol*, vol. 65, no. 4, pp. 390–402, Oct. 2021, doi: 10.1165/RCMB.2020-0492OC.

[137] J. Han, Y. He, H. Zhao, and X. Xu, "Hypoxia inducible factor-1 promotes liver fibrosis in nonalcoholic fatty liver disease by activating PTEN/p65 signaling pathway," *J Cell Biochem*, vol. 120, no. 9, pp. 14735–14744, Sep. 2019, doi: 10.1002/JCB.28734.

[138] S. B. Catrina and X. Zheng, "Hypoxia and hypoxia-inducible factors in diabetes and its complications," *Diabetologia*, vol. 64, no. 4, pp. 709–716, Apr. 2021, doi: 10.1007/S00125-021-05380-Z.

[139] K. Jungermann and T. Kietzmann, "Oxygen: modulator of metabolic zonation and disease of the liver," *Hepatology*, vol. 31, no. 2, pp. 255–260, 2000, doi: 10.1002/HEP.510310201.

[140] S. Furukawa *et al.*, "Increased oxidative stress in obesity and its impact on metabolic syndrome," *J Clin Invest*, vol. 114, no. 12, pp. 1752–1761, 2004, doi: 10.1172/JCI21625.

[141] M. Quintero *et al.*, "The effects of intermittent hypoxia on redox status, NF-κB activation, and plasma lipid levels are dependent on the lowest oxygen saturation," *Free Radic Biol Med*, vol. 65, pp. 1143–1154, Dec. 2013, doi: 10.1016/J.FREERADBIOMED.2013.08.180.

[142] L. M. Simon, J. Liu, J. Theodore, and E. D. Robin, "Effect of hyperoxia, hypoxia, and maturation on superoxide dismutase activity in isolated alveolar macrophages," *Am Rev Respir Dis*, vol. 115, no. 2, pp. 279–284, 1977, doi: 10.1164/ARRD.1977.115.2.279.

[143] Q. Chen *et al.*, "High-Fat Diet-Induced Mitochondrial Dysfunction Promotes Genioglossus Injury - A Potential Mechanism for Obstructive Sleep Apnea with Obesity," *Nat Sci Sleep*, vol. 13, pp. 2203–2219, 2021, doi: 10.2147/NSS.S343721.

[144] H. S. Li *et al.*, "HIF-1α protects against oxidative stress by directly targeting mitochondria," *Redox Biol*, vol. 25, Jul. 2019, doi: 10.1016/j.redox.2019.101109.

[145] M. Munder, "Arginase: an emerging key player in the mammalian immune system," *Br J Pharmacol*, vol. 158, no. 3, pp. 638–651, Oct. 2009, doi: 10.1111/J.1476-5381.2009.00291.X.

[146] J. Tarrant, "Emerging Translatable Safety Biomarkers," in *Comprehensive Medicinal Chemistry III*, Elsevier, 2017, pp. 255–284. doi: 10.1016/B978-0-12-409547-2.12387-X.

[147] T. Liu, L. Zhang, D. Joo, and S. C. Sun, "NF-κB signaling in inflammation," *Signal Transduct Target Ther*, vol. 2, 2017, doi: 10.1038/sigtrans.2017.23.